Structural Analysis of hydroxamate based Histone Deacetylase 8 (HDAC8) Inhibitors: A multi-QSAR study to procure important structural features of HDAC8 Inhibitors

Submitted by

SUVANKAR BANERJEE

EXAM ROLL NO.: ***M4PHA19021***
CLASS ROLL NO.: ***001711402021***,
REG. NO.: ***140845*** *of* ***2017-2018***

Department of Pharmaceutical Technology
Jadavpur University
Session- ***2017-2019***

Under The Guidance Of

Prof. Tarun Jha

Natural Science Laboratory
Department of Pharmaceutical Technology
Jadavpur University, Kolkata-700032

Thesis submitted in partial fulfillment of the requirements for the Degree of Master of Pharmacy
Department of Pharmaceutical Technology
Faculty of Engineering and Technology
Jadavpur University, Kolkata

2019

Jadavpur University

Jadavpur, Kolkata-700032

CERTIFICATE OF APPROVAL

This is to certify that ***Suvankar Banerjee*** (Exam Roll No. - ***M4PHA19021***, Reg. No. - **140845** of **2017-2018**) has sincerely carried out the research work on the subject entitled "***Structural Analysis of hydroxamate based Histone Deacetylase 8 (HDAC8) Inhibitors: A multi-QSAR study to procure important structural features of HDAC8 Inhibitors***" under the supervision of **Prof. Tarun Jha,** Professor, Natural Science Laboratory, Department of Pharmaceutical Technology of Jadavpur University. He has incorporated his findings in this thesis submitted by him in partial fulfillment of the requirements for the degree of **Master in Pharmacy** (Pharmaceutical Technology) of Jadavpur University. He has carried out the research work independently and sincerely with proper care and attention to our entire satisfaction.

_____ _____

Head of the Department

Department of Pharmaceutical Technology
Jadavpur University
Kolkata-700032

Prof. Tarun Jha

Natural Science Laboratory
Department of Pharmaceutical Technology
Jadavpur University
Kolkata-700032

_____

Dean
Faculty of Engineering and Technology
Jadavpur University
Kolkata-700032

Acknowledgement

The final outcome of this dissertation required a lot of guidance and assistance from many people. I am extremely fortunate to have these all along the completion of my work. Whatever I have done is only due to such guidance and assistance and I would not forget to thank them.

I am highly obliged and like to express my deep gratitude and profoundness to my reverend mentor **Prof. Tarun Jha** of Department of Pharmaceutical Technology, Jadavpur University, Kolkata for his excellent and constant guidance and help, endless encouragement, thoughtful and freedom and stupendous co-operation throughout the dissertation till its successful completion. I am greatly indebted to his motivation, fruitful suggestions and inspirations.

I owe my deep respect to **Prof. Pulok K. Mukherjee**, Head of the Department, Pharmaceutical Technology, Jadavpur University, Kolkata for all the necessary help and encouragement. **Prof. Biswajit Mukherjee,** former Head of the Department, Pharmaceutical Technology, Jadavpur University for his continuous help and encouragement. I am thankful to all of my respected **teachers** and **non-teaching staffs** in the Department of Pharmaceutical Technology, Jadavpur University for their support and help.

I am both extremely honoured and grateful to **Mr. Nilanjan Adhikari**, **Mr. Sandip Kr. Baidya** and **Mr. Sk. Abdul Amin** for their priceless guidance and support which assisted me to gather knowledge about the different aspects of this work. I also express my sincere thanks to my laboratory colleague **Mr. Saptarshi Sanyal, Mr. Rajat Sarkar, Ms. Subha Mondal** and Natural Science Laboratory, Department of Pharmaceutical Technology Jadavpur University, Kolkata.

I would like to thank my seniors **Dr. Balaram Ghosh**, BITS-Pilani, Hyderabad and **Dr. Shovanlal Gayen**, Dr. Harisingh Gour University, Sagar, India for their continuous encouragement, necessary help and support to perform my work.

I like to acknowledge all my friends and no words can suffice my feelings of gratitude to **Mr. Prabir Roy**, **Mr. Suman Banerjee**, **Dr. Subrata Chakrabarty**, **Mr. Nilanjan**

Ghosh, **Mrs. Rituparna Chaki Ghosh**, **Mr. Sagar Sengupta**, and **Mr. Avik Kr. Saha** for their help and support.

I thankfully acknowledge my classmates, especially **Mr. Arunava Ghosh**, **Mr. Arindam Sarkar**, **Mr. Pallab Mondal**, **Mr. Arunaksh Chakravarty**, **Mr. Milan Tirtha Mete**, **Ms. Ajeya Samanta**, Ms**. Suparna Ghosh**, **Ms. Sanchari Karak**, **Ms. Mousumi Tudu**, **Mr. Suvodeep Mondal** of Department of Pharmacy, Jadavpur university, Kolkata.

I would like to convey my sincere gratitude to **AICTE** and **Jadavpur University** for their financial and equipmental support for my M. Pharm course.

Finally, I would like to express my deep respect to my Father **Late. Badal Banerjee**, my Mother **Mrs. Tulu Banerjee,** my brother **Mr. Saikat Banerjee**, my beloved **Ms. Rachana Mukherjee** and her parents **Mr. Biswajit Mukherjee** and **Mrs. Ruma Mukherjee** and also my other friends and relatives for their continuous help, love, encouragement and moral support throughout the period of my work.

.....

[SUVANKAR BANERJEE]

Date:

Place: Department of Pharmacy, Jadavpur University, Kolkata.

Declaration of Originality and Compliance of Academic Ethics

I hereby declare that this thesis contains literature survey and original research work performed by me (Suvankar Banerjee) as a part of my Master of Pharmacy studies. All the information in this document have been obtained and presented in accordance with academic rules and ethical conduct.

I also declare that, as required by these rules and conduct, I have cited and referenced the materials and results that are mot original to this work.

Name: Suvankar Banerjee
Exam Roll Number: M4PHA19021
Class Roll Number: 001711402021
Registration Number: 140845 of 2017-2018
Thesis Title: "Structural Analysis of hydroxamate based Histone Deacetylase 8 (HDAC8) Inhibitors: A multi-QSAR study to procure important structural features of HDAC8 Inhibitors".

(Suvankar Banerjee)
Signature with Date:

Dedicated To

My mother, seniors, friends and teachers

Contents

Preface

The term “Cancer” specifies a group of diseases triggers abnormal and uncontrolled cellular growth in the living organisms is one of the substantial to the mankind in our modern era. Cancer is also one of the major causes of death in this era and the size of human population suffering from cancer is increasing rapidly. Also, the treatment of the patients suffering from cancer is both critical and expensive which can take us toward social and economical crisis.

There are numerous internal and external factors related to cancer which helps in cancer occurrence and progression. Apart from the internal factors like genetic mutation, abnormal hormonal regulation etc. several external factors like pollution, malnutrition, radiation, lifestyle, etc are associated with the alteration of the biological system and induces cancer progression. Hence, controlling these factors can be a way to prevent this deadly disease. Aside this, there are other approaches are present to prevent the cancer progression and death from cancer. These treatments include chemotherapy, radiation therapy, vaccination, etc.

It is seen that, inside our biological system there are a variety of proteins those are associated with the cancer occurrence and progression. Amidst these proteins, metalloenzymes are a special group of metal containing enzymes associated with cancer and influences occurrence and progression of cancer inside the biological systems. Human histone deacetylase enzymes are a group of zinc dependent metalloenzymes which regulates the genetic transcription by deacetylation of the nuclear histone proteins also provides significant influences in cancer and tumor progression and many other diseases.

Histone deacetylase 8 (HDAC8) is one significant members of the HDAC family contributes towards many epigenetic disorders, viral and parasitic diseases including a large group of cancers namely colon, lung, breast and pancreatic cancers as well as leukaemia. Also, though holding numerous HDAC8 inhibitors lack of selective HDAC8 inhibitors as effective anticancer agent is a major disadvantage for the in treatment of cancers and diseases associated with HDAC8.

Preface

There are three crucial structure factors to develop an effective HDAC8 inhibitor are the presence of a cap group, a linker moiety and a zinc binding group whereas the hydroxamic acid moiety has proven itself as a better zinc binding group for HDAC8 inhibitors.

Also, the Quantitative structure-activity relationship (QSAR) is a widely used technique to correlate the biological activity of the molecules with their molecular structure and identification of important structural factors for the activity of these compounds. Hence in this study, a multi-QSAR approach is performed on a large and diverse group of HDAC8 inhibitors containing the hydroxamate group as the zinc binding motif while possessing a wide range of HDAC8 inhibitory activity. The purpose of this study is to identify the crucial structural features present in the cap and the linker moiety important for regulating the HDAC8 inhibitory activity for the HDAC8 inhibitors. This study was able to identify several crucial structural and molecular factors for the HDAC8 inhibitors influencing the activity of these compounds which may be helpful and encourage designing of effective and HDAC8 selective HDAC8 inhibitors to aid the treatment against cancers related with HDAC8 enzymatic activity.

Chapter 1: *Introduction*

Chapter 1: *Introduction*

1.1. Histone deacetylases Enzymes

Among various factors responsible for the regulation of the numerous biological mechanisms, acetylation and deacetylation of the *N*-terminal lysine residue of the nuclear histone proteins play crucial roles in the modulation of different epigenetic functions including occurrence and progression of cancer and tumor conditions [Amin et al. 2017a, 2017b, 2018a, Chakrabarty et al. 2015, Adhikari et al. 2018].

These eraser enzymes are known as the histone deacetylases. These are a group of either Zn^{2+} or nicotinamide adenine dinucleotide (NAD^{+}) containing metalloenzymes generally involved in the deacetylation of the histone proteins. They are also involved in chromatin condensation and transcriptional regulation via eliminating the terminal acetate group from the acetylated amino acid residue of the histone proteins [Amin et al. 2017a, 2017b, 2018]. Hence, this process of acetate group elimination from acetylated ε-amino acid residue of histone lysine is familiar as the "deacetylation of the histone proteins" (***Figure 1.1***). Due to this process, the HDACs are also well-reputed as the KDACs or "Lysin Deacetylase" or [Amin et al. 2018a].

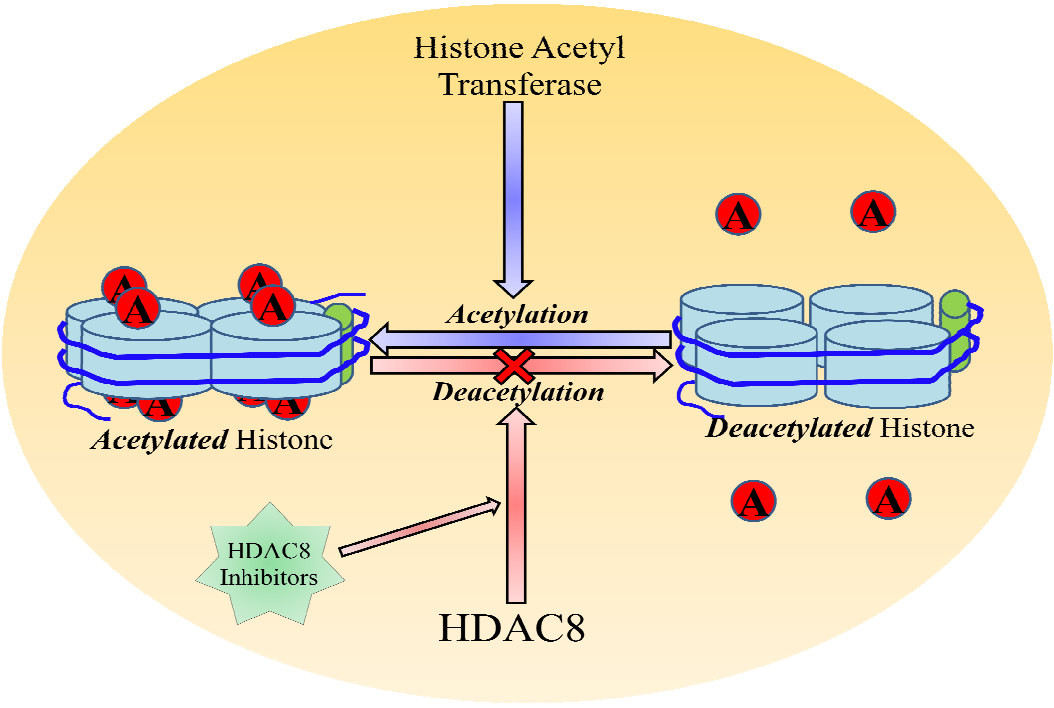

Figure 1.1. Acetylation and Deacetylation of Histone proteins by HDAC enzymes

Because of the deacetylation ability, the HDAC enzymes are connected with numerous significant biological pathways while modulating and/or regulating them. Though maintaining different normal physiological processes HDACs are also involved in the progression of numbers of diseases, pathophysiological conditions and cancers [Chakrabarty et al. 2015]. These diseases such as inflammation, neurodegenerative disorders, metabolic dysfunctions, and autoimmune diseases can also be correlated with the activities of the HDAC isoforms [Chakrabarty et al. 2015]. For these contributions in the pathophysiology of the histone deacetylase enzymes, they have become a significant target for the treatment of the diseases especially cancers and tumors related to these enzymes [Nian et al. 2009, Adhikari et al. 2018]. Generally, the abnormal expression of HDAC enzymes or the abnormal activity of HDAC8 can lead to different abnormal cellular functions and can cause progression and occurrence of various disease conditions. Because of this, the histone deacetylase enzymes are in the spotlight for the prevention of the abnormal epigenetic diseases and pathophysiological conditions and progression of cancers which are related to them [Amin et al. 2017a, 2017b, 2018a, 2018b, Chakrabarty et al. 2015, Chakrabarty et al. 2016, Halder et al. 2015].

1.2. The HDAC family and its classification

Histone deacetylases are the group of enzymes comprised of either Zn^{2+} or NAD^{+} in their structure [Halder et al. 2015]. In the family of histone deacetylase enzymes till date, a total number of 18 different HDAC isoforms are discovered ***Table 1.1***. Among these, most of the isoforms are Zn^{2+}-dependent metalloenzymes in nature while the rest of the members of the HDAC family are NAD^{+}-dependent isoforms known as the Sirtuins (SIRTs) [Amin et al. 2017a, 2017b, Chakrabarty et al. 2016, Banerjee et al. 2019a].

As on the basis of the structural and functional characteristics, the enzymes of HDAC family can be classified into four classes namely class I, class II, class III and class IV. The class I and class II enzymes including the class IV HDAC isoforms are the Zn^{2+}-dependant metalloenzymes in nature whereas the seven NAD^{+}-dependent Sirtuins (SIRT 1-7) are come under the class-III of the HDAC family [Amin et al. 2017b,

Gregoretti et al. 2004, Trivedi et al. 2018]. Among the Zn^{2+}-dependant HDACs, class I HDACs bears structural similarity with yeast RPD3 whereas class II HDAC isoforms have a structural resemblance to yeast Hda I enzyme [Chakrabarty et al. 2015, Bertrand 2010, Xu et al. 2007]. The class IV of the HDAC metalloenzymes contains only HDAC11 which is the shortest HDAC isoform and can be differentiated from the other classes of Zn^{2+}-dependant HDACs. Moreover, though the catalytic region/domain of each isoform of the class I and class II HDACs bears resemblance to each other, the HDAC isoforms also possess structural differences due to their amino acid sequences [Mottamal et al. 2015, Bertrand 2010].

Table 1.1. List of the isoforms belongs to the HDAC family of deacetylase enzymes

Class	Dependency	Sub class	Isoform	Cellular localization	Non-histone substrates
I	Zn^{2+}	IA	HDAC1	Nucleus	SHP,p53,MyoD,E2F1, STAT3, NF-$_k$B,CtIP,AMPK, RB1
			HDAC2	Nucleus	GCCR,BCL6,STAT3, YY1
		IB	HDAC3	Nucleus	SHP, YY1, GATA1, p65, STAT3, MEF2D
		IC	HDAC8	Nucleus	SMC3, actin
II		IIA	HDAC4	Nucleus/Cytoplasm	GATA1, HP1
			HDAC5	Nucleus/Cytoplasm	SMAD7, HP1
			HDAC7	Nucleus/Cytoplasm	PLAG1, PLAG2
			HDAC9	Nucleus/Cytoplasm	----------
		IIB	HDAC6	Mostly Cytoplasm	α-tubulin, HSP90, SHP, SMAD
			HDAC10	Nucleus/Cytoplasm	——
III	NAD^+	----	SIRTs	Nucleus/Cytoplasm/	Not given

				Mitochondria	
IV	Zn^{2+}	----	HDAC11	Nucleus/Cytoplasm	——

Among the HDAC family, the class I and class II are the most important classes which are also known as the classical HDACs. These classical HDACs generally possess a conserved deacetylase domain which supervises the deacetylation of the N-terminal residue of the histone lysine in presence of the Zn^{2+} ion [Li et al. 2014].

Concerning the classes and the isoforms of the HDAC family, the class I and class II HDACs can be further sub-divided into several sub-classes. The class I of HDAC family contains the HDACs namely HDAC1-3 and HDAC8 which are sub-classified on their phylogenic data. Class IA isoforms contain HDAC1 and HDAC2, the class IB containing HDAC3 whereas class IC containing isoform HDAC8. Similarly, class II of HDAC family can be also sub-classified as class IIA containing HDAC4-5, HDAC7 and HDAC9 whereas class IIB containing only HDAC6 and HDAC10 [Amin et al. 2017a, 2017b, 2018a, 2018b, Mottamal et al. 2015, Bertrand 2010, Banerjee et al. 2019a]. Additionally, it is also seen that the protein kinase A (PKA) regulates the HDAC8 whereas the regulation of class IA isoforms are dependent on the casein kinase 2 [Chakrabarty et al. 2015]. It has also seen that the HDAC isoforms of class I catalyzes numerous non-histone and histone substrates which includes various transcriptional elements [Bertrand 2010].

The cellular localization of the HDAC isoforms is also seemed to be similar for each class of HDACs. The HDACs of class I such as HDAC1-3 and HDAC8 are generally found in the nucleus. The class II and class IV HDAC isoforms are localized either in the cytoplasm or in the nucleus. Fascinatingly, the only special case is the, found mostly in cytoplasm. Also, the class III HDACs or the SIRTs are found in the nucleus and cytoplasm as well as in the mitochondria [Bertrand 2010].

1.4. An outlook on the structural aspects of HDAC8

Since the first exploration of the crystal structure of HDAC8 in the year 2004, numerous structural analysis and exploration of newer crystal structures of the HDAC8 enzymes are done till date [Somoza et al. 2004]. From the structural analysis, it is clearly seen that in

case of human HDAC8 the carbonyl moiety of the acetylated-L-lysine substrate forms coordination with the Zn^{2+} present in the HDAC8 and succeeded by interacting with catalytic tyrosine (Y306) via hydrogen bond formation [Dowling et al. 2008, Vannini et al. 2007, Porter et al. 2016, Estiu et al. 2010]. Besides that, a histidine pair (H142 and H143) also provides a crucial role in the HDAC8 transition state. These two amino acid residues in which the H142 and H143 act as the general base catalyst and general acid-base catalyst to stabilize the HDAC8 during the transition state [Porter et al. 2016, Gantt et al. 2016]. In this case, histidine deprotonates the metal-bound water molecule which interacts with the carbonyl moiety of the acetylated lysine and forms an intermediated tetrahedral form (***Figure 1.2***). The other histidine residue protonates the acetylated lysine amino-leaving group and forms products of the lysine and acetate [Amin et al. 2017a, Gantt et al. 2016].

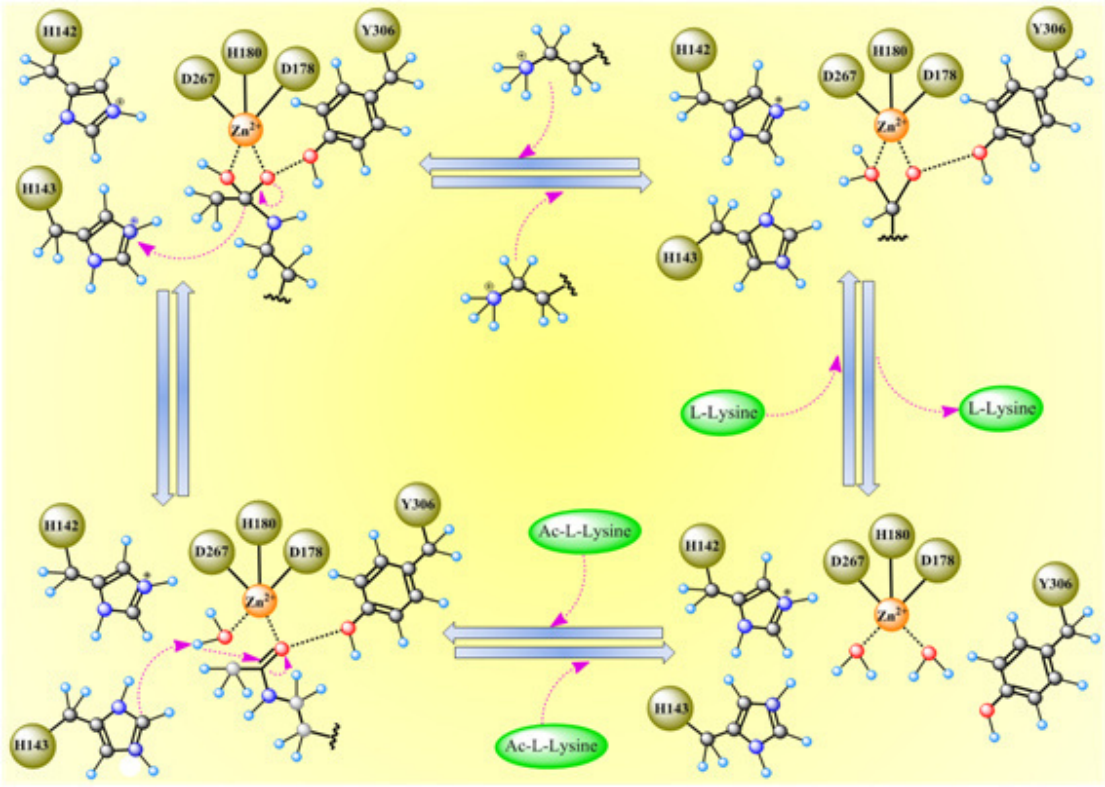

Figure 1.2. *M*echanism of the HDAC8 enzyme.

Though HDAC8 is from class I of HDAC family, a number of structural and functional differentiations can be done for HDAC8 with the other members of class I as well as

members of other classes of HDAC family. From the structural aspects, the nuclear localization sequence of the HDAC 8 is present between the catalytic domains of its structure while containing a serine binding motif at the terminal position of its catalytic domain. Also, the phosphorylation of S39 via the cAMP-dependent PKA phosphorylation causes negative modulation of the catalytic activities of HDAC8 [Wilson et al. 2010].

The HDAC8 of humans is an X-linked protein and provides any co-complex independent activity [Buggy et al. 2000, Van den Wyngaert et al. 2000]. In the case of HDAC8, loop 1 is proximal to its active site and is highly flexible in nature. The loop is able to undergo certain conformational changes which are specific to the substrates. Also, HDAC8 do not contain any the C-terminal domain for protein binding which is present in other isoforms of class-I [Somoza et al. 2004].

For HDAC8 the loop1 and loop 6 and the catalytic tyrosine creates a specific pocket for HDAC8 which only allows inhibitors with an "L" shaped structure to bind with HDAC8 selectively. On the other hand, these two loops of the other HDAC isoforms cause hindrance for the binding with these isoforms [Marek et al. 2018].

HDAC8 is also can be differentiated with the other class I HDACs on the basis of its N-terminal L1 loop. The L1 loop present at the N-terminal of HDAC8 forms a major part in one side of its active site and is expanded to the surface of the protein [Chakrabarty et al. 2015, Lombardi et al. 2011]. HDAC8, in association with other non-histone proteins namely, ERR- α, cohesin can control energy homeostasis, microtubular integrity, chromatid separation and muscle contraction [Wilson et al. 2010, Li et al. 2014]. In case of the active site, the pocket of HDAC8 is almost similar to the other class I HDAC isoforms whereas, the HDAC8 possess a methionine in place of leucine of the other class I HDACs [Somoza et al. 2004].

In the recent studies, the functional and structural significance of the G302GGGY, a conserved glycine-rich loop in the HDAC8 active site is explored [Porter et al. 2016] which seemed to be that this catalytic loop is crucial because in that loop of HDAC8, nonsense and missense mutations can produce multiple congenital diseases like Cornelia de Lange Syndrome (CdLS) [Liu & Krantz 2009]. The G302GGGY loop was signified as

an important part for maintaining the Y306 amino acid residue by Porter et al [Porter et al. 2016]. A molecular dynamics (MD simulation) simulation study revealed that the flexibility of this G302GGGY segment, maintained by the G304 and G305 glycine amino acid residues, is an important factor that helps in the conformations of Y306 during the transition which the HDAC8 inhibitors may be able to modulate [Porter et al. 2016].

The catalytic domain of HDAC8 contains seven loops in which the Zn^{2+} ion resides between the loop 4 and loop 7 where it is conserved by a sequence of D(A,V,L,F)$Hx_{\sim 100}$D and ligated with D178, H180 and D267 amino acid residues [Somoza et al. 2004, Tabackman et al. 2016, Lombardi et al. 2011].

The study of HDAC8 showed that the active site of HDAC8 enzyme consists of a narrow and long tunnel of hydrophobic nature. Walls of this long tunnel of the active site is formed by the amino acid residues namely G151, H180, F152, Y306, M274 and F208 where the catalytic Zn^{2+} resides at the very end of the tunnel (***Figure 1.3***) [Somoza et al. 2004, Tabackman et al. 2016].

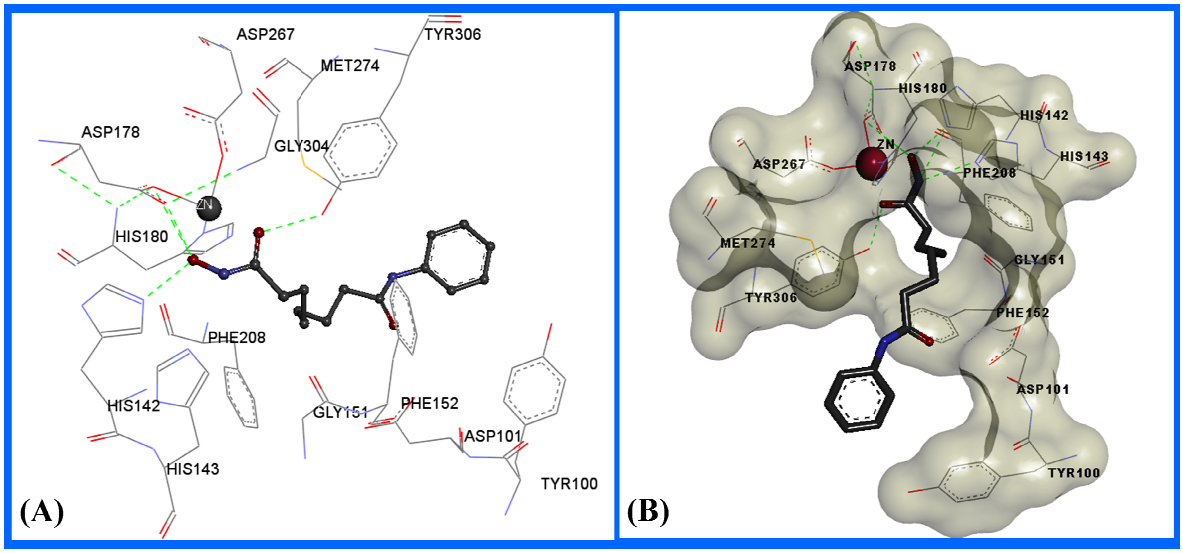

Figure 1.3 Contours of the ligand binding site of HDAC8 isoform including the catalytic Zn^{2+} ion and the important amino acid residues for ligand binding. ***(A)- (B)*** Ligand (SAHA) bound crystal structure of HDAC8 active site (PDB: 1T69)

In the case of class I HDACs, these amino acid residues are generally conserved and hydrophobic in nature which helps in the binding of inhibitors containing hydrophobic

linker moiety. The catalytic Zn^{2+} ion of the HDAC8 resides at the very end of this narrow hydrophobic tunnel, bound to the heterocyclic nitrogen atom of H180, and the oxygen atoms carboxylate group of D178 and D267 amino acid residues. The crystal structure of the HDAC8 catalytic domain containing SAHA (PDB ID-1T69) depicted that the Zinc-binding hydroxamate group of SAHA entered to the long and narrow tunnel of HDAC8 and chalets with the Zn^{2+} ion residing at the very end of the tunnel. In the mean time, the phenyl cap group of SAHA fits inside the hydrophobic pocket of HDAC8. Additionally, a list of HDAC8 crystal structures [Research Collaboratory for Structural Bioinformatics (RCSB) Protein Data Bank (PDB). www.rcsb.org, 2018 (accessed 14 November 2018)] is given in ***Table 1.2***.

Table 1.2. List of available ligand/substrate bound crystal structures of HDAC8

PDB	*Organism*	*Ligand*	*Substrate*	*Resid.*	*Res. (Å)*	*Year*
1T64	*H. sapiens*	TSA	--	754	1.90	2004
1T67	*H. sapiens*	M344	--	377	2.31	2004
1T69	*H. sapiens*	SAHA	--	377	2.91	2004
1VKG	*H. sapiens*	CRA 19156	--	754	2.20	2004
1W22	*H. sapiens*	PSTB-Hydroxamate	--	754	2.50	2004
2V5W	*H. sapiens*	--	Acetylpeptide	791	2.00	2007
2V5X	*H. sapiens*	Hydroxamate	--	776	2.25	2007
3EW8	*H. sapiens*	M344	--	388	1.80	2008
3EWF	*H. sapiens*	--	Acetylpeptide	1572	2.50	2008
3EZP	*H. sapiens*	M344	--	776	2.65	2008
3EZT	*H. sapiens*	M344	--	776	2.85	2008
3FO6	*H. sapiens*	M344	--	776	2.55	2008
3F07	*H. sapiens*	APHA	--	1164	3.30	2008
3F0R	*H. sapiens*	TSA	--	1164	2.54	2008
3MZ3	*H. sapiens*	M344	--	778	3.20	2010
3MZ4	*H. sapiens*	M344	--	778	1.85	2010
3MZ6	*H. sapiens*	M344	--	389	2.00	2010
3MZ7	*H. sapiens*	M344	--	389	1.90	2010
3SFF	*H. sapiens*	Amino acid derivative	--	378	2.00	2011
3SFH	*H. sapiens*	Amino acid derivative	--	378	2.70	2011
3RQD	*H. sapiens*	Largazole thiol	--	788	2.14	2011
4BZ5	*S. mansoni*	--	Acetylpeptide	1784	1.78	2013
4BZ6	*S. mansoni*	SAHA	--	1784	2.00	2013
4BZ7	*S. mansoni*	M344	--	1784	1.65	2013
4BZ8	*S. mansoni*	J1038	--	1784	2.21	2013
4BZ9	*S. mansoni*	J1075	--	1784	2.00	2013
4CQF	*S. mansoni*	Marcapto acetamide	--	1784	2.30	2014
4QA0	*H. sapiens*	SAHA	--	778	2.24	2014
4QA1	*H. sapiens*	M344	--	1156	1.92	2014
4QA2	*H. sapiens*	SAHA	--	778	2.38	2014
4QA3	*H. sapiens*	TSA	--	778	2.88	2014
4QA4	*H. sapiens*	M344	--	389	1.98	2014

4QA5	*H. sapiens*	--	Acetylpeptide	788	1.76	2014
4QA6	*H. sapiens*	--	Acetylpeptide	788	2.05	2014
4QA7	*H. sapiens*	--	Acetylpeptide	394	2.31	2014
4RN0	*H. sapiens*	Largazole analog	--	778	1.76	2015
4RN1	*H. sapiens*	Largazole analog	--	778	2.18	2015
4RN2	*H. sapiens*	Largazole analog	--	778	2.39	2015
5D1B	*H. sapiens*	TSA	--	778	2.90	2015
5D1C	*H. sapiens*	--	Tetrapeptide	790	1.42	2015
5D1D	*H. sapiens*	--	Tetrapeptide	790	2.01	2015
5DC5	*H. sapiens*	M344	--	778	1.94	2016
5DC6	*H. sapiens*	--	Tetrapeptide	790	1.55	2016
5DC7	*H. sapiens*	--	Tetrapeptide	790	2.30	2016
5DC8	*H. sapiens*	--	Tetrapeptide	790	1.30	2016
5FUE	*S. mansoni*	3- benzamidobenzo hydroxamate	--	1784	2.19	2016
5BWZ	*H. sapiens*	Droxinostat	--	778	1.59	2016
5FCW	*H. sapiens*	Hydroxamic Acid	--	766	1.97	2016
5THS	*H. sapiens*	M344	--	778	1.90	2016
5THT	*H. sapiens*	M344	--	1556	2.40	2016
5THU	*H. sapiens*	M344	--	778	1.95	2016
5THV	*H. sapiens*	M344	--	778	1.86	2016
6HQY	*S. mansoni*	PCI-34051	--	1788	2.50	2018
6HRQ	*S. mansoni*	NCC-149	--	1788	1.85	2018
6HSF	*S. mansoni*	PCI-34051	--	1788	1.90	2018
6HSG	*S. mansoni*	NCC-149	--	1788	1.85	2018
6HSH	*S. mansoni*	Quisinostat	--	1788	1.54	2018
6HSK	*H. sapiens*	Quisinostat	--	160	2.10	2018
6HSZ	*S. mansoni*	Benzohydroxamate inhibitor 2	--	1788	2.37	2018
6HT8	*S. mansoni*	Benzohydroxamate inhibitor 3	--	1788	2.50	2018
6HTG	*S. mansoni*	Benzohydroxamate inhibitor 4	--	1788	1.94	2018
6HTH	*S. mansoni*	Benzohydroxamate inhibitor 5	--	1788	1.95	2018
6HTI	*S. mansoni*	Benzohydroxamate inhibitor 6	--	1788	1.69	2018
6HTT	*S. mansoni*	Benzohydroxamate inhibitor 7	--	1788	1.75	2018
6HTZ	*S. mansoni*	Benzohydroxamate inhibitor 8	--	1788	1.84	2018
6HU0	*S. mansoni*	Benzohydroxamate inhibitor 9	--	1788	1.75	2018
6HU1	*S. mansoni*	Benzohydroxamate inhibitor 10	--	1788	2.00	2018
6HU2	*S. mansoni*	Benzohydroxamate inhibitor 11	--	1788	1.99	2018
6HU3	*S. mansoni*	Triazole hydroxamate inhibitor	--	1788	1.65	2018

Chapter 2: *Literature Review*

Chapter 2: *Literature Review*

In the modern medical and pharmaceutical fields, the enzyme HDAC8 has come into the spotlight and becoming a target for the treatment of different pathophysiological conditions related to it [Amin et al. 2017a, 2017b, 2018a, 2018b]. As because there are no HDAC8 specific inhibitors are present in the market, designing of selective and potent inhibitors for HDAC8 inhibition has become an utmost task to combat such diseases.

Also, a few compounds have appeared as a pioneering medium to modify and designing of potent and isoform-selective HDAC inhibitors. Some of these pan-HDAC inhibitors such as vorinostat/SAHA (**FDA-01**), Romidepsin (**FDA-02**), Belinostat (**FDA-03**), Panobinostat (**FDA-04**) and Pracinostat/SB-939 (**FDA-05**) already approved by the United States Food and Drug Administration (US-FDA) and are used for the treatment of a few cancer conditions (cutaneous T-cell lymphoma, relapsed multiple myeloma, acute myeloid leukemia (***Figure 2.1***) [Amin et al. 2017a, 2017b, Banerjee et al. 2019a]. Chidamide/HBI-8000 (**FDA-06**) is the sole pan-HDAC inhibitor present in the market which is approved by the Chinese Food and Drug Administration (CFDA) for relapsed peripheral T-cell lymphoma [Amin et al. 2017a, 2017b, Mottamal et al. 2015] [***Figure 2.1***].

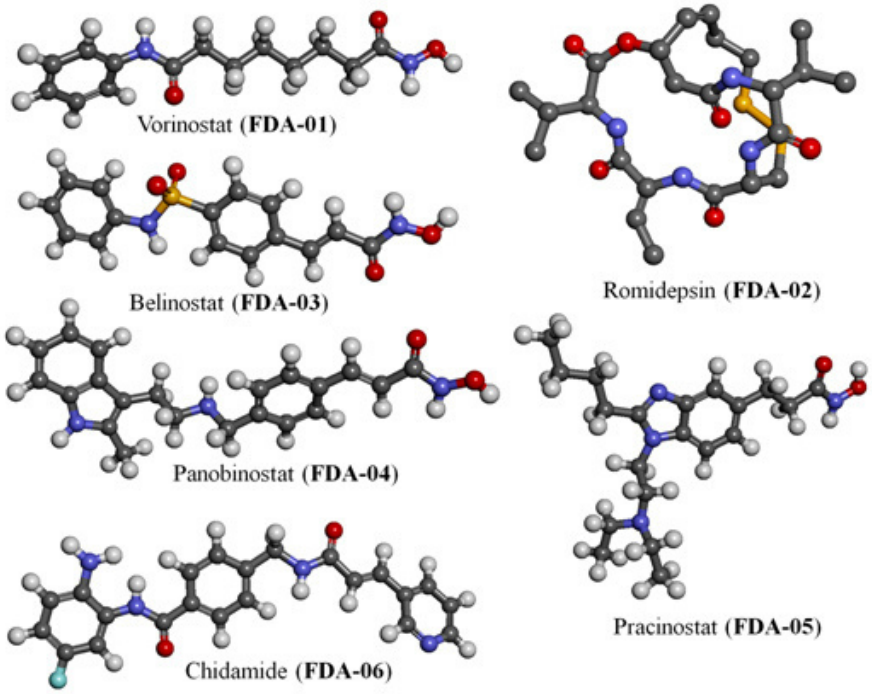

Figure 2.1. FDA approved pan-HDAC inhibitors.

Moreover, besides the synthetic approaches, several computational methods have been performed on existing HDAC8 inhibitors for the identification of the important molecular properties for better HDAC8 inhibition and to design more potent and isoform-selective HDAC8 inhibitors [Amin et al. 2017a, 2017b]. The studies disclosed that the basic diagrammatic structure of an HDAC8 inhibitor must contain three principal pharmacophoric features such as a hydrophobic CAP group as the surface recognition factor, a linker motif including a zinc-binding group (ZBG) for Zn^{2+} chelation. Department of pharmaceutical technology, Javapur university also proposed that a modified fish-like structure of the HDAC inhibitors should be more effective than the usual fish-like structure of the pan-HDAC inhibitors [Amin et al. 2017a, 2017b].

2.1 An overview of the reported HDAC8 inhibitors

The basic structure of HDAC8 inhibitors generally contains three common features such as a cap group (surface recognition group), a linker region and a zinc-binding motif (ZBG). Among these, the cap moiety of these inhibitors may be responsible for the isoform specificity via surface recognition and forming interactions at the binding site of HDAC8 because of its hydrophobic nature. As for the ZBG, they are is required to interact inside the HDAC8 active site by chelating with the catalytic zinc ion present deep inside the HDAC8 active site. Commonly amidst numerous ZBG group, the hydroxamic acid group is preferred as the ZBG for higher HDAC8 inhibition because of its strong zinc binding property [Amin et al. 2017a]. Frequently it is seen that the compounds containing a hydroxamate group as the zinc binding group provides better HDAC8 inhibition than the compounds containing other ZBGs. But at the same time, higher zinc binding capability of the hydroxamate group-containing groups leads toward the non-specific/non-selective HDAC inhibition and can also interact and inhibit other zinc-dependent metalloproteinases namely matrix metalloproteinases enzymes (MMPs) and aminopeptidase N (APN/CD13), etc. Additionally, these hydroxamate derivated inhibitors can be able to lower the in vivo absorption of the molecules, hence affecting the efficacy of the inhibitors. In order to avoid such situations, using the non-hydroxamate ZBG containing HDAC inhibitors have been designed in order to search the proper ZBG to provide an effective HDAC8 inhibition and selectivity [Amin et al.

2018b]. A number of various groups and moieties such as oximes, hydroxy-pyridine-2-thiones, ketones, thiols, trifluoromethyl derivatives, β-lactams, boronic acids and carboxylic acid groups (***Figure 2.2.***) has been used non-hydroxamate ZBG group to replace the hydroxamate groups of the HDAC8 inhibitors which eas also able to provide convincing and fruitful HDAC8 inhibition.

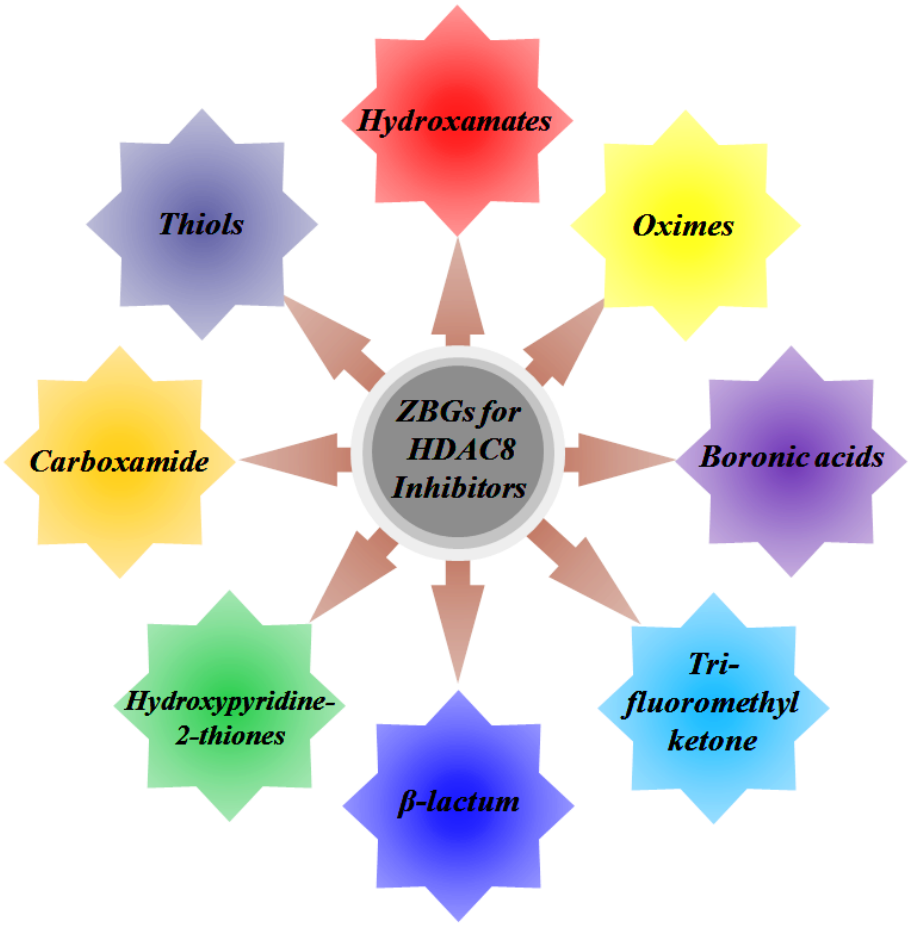

Figure 2.2. Various reported ZBGs used to develop potent HDAC8 inhibitors.

In this chapter, different promising HDAC8 inhibitors with hydroxamate and non-hydroxamate ZBGs are studied while highlighting their selectivity and non-selectivity (***Table 2.1***) [Banerjee et al. 2019a].

In the year 2002, Furumai and his co-workers studied on a group of cyclic hydroxamic acid containing peptide derivatives (CHAPs) [Furumai et al 2002]. These compounds seemed to have detrimental effects on the HeLa cell growth at the S phase of the cell

cycle. Among these compounds, CHAP31 (Compound **1,** HDAC IC_{50} = 3.32 nM) [***Figure 2.3***], displayed a very good and effective HDAC8 inhibition.

Table 2.1. List of hydroxamate and non-hydroxamate ZBGs containing potential HDAC8 inhibitors.

Sl No.	*Scaffold*	*Most active isoform*	*HDAC8 activity*		*References*
			Cpd No.	*IC_{50} (nM)*	
1	Peptide containing cyclic hydroxamic acid derivative	--	1	3.32	Furumai et al 2002
2	Trifluoro methyl and tetrafluoro ethyl ketone based cyclic tetrapeptide derivative	HDAC1, HDAC8	2	230	Jose et al. 2004
3	Mercapto acetamide based hydroxamate	HDAC6	3	1,050	Kozikowski et al. 2007
4	Amino phenyl benzamide based hydroxamate	HDAC1, HDAC2	4	400	Moradei et al. 2007
5	5-pyrimidinyl based hydroxamate	HDAC1	5	23	Arts et al. 2007
6	4-napthyl-phenyl based linkerless hydroxamate	HDAC8	6	300	Krennhrubec et al. 2007
7	Triazolyl based hydroxamate	HDAC6	7	406	Chen et al. 2008
8	Phenyl iso-oxazole based hydroxamate	HDAC6	8	938	Kozikowski et al. 2008
9	Aryl hydroxamate derivative	HDAC8	9	10	Balasubramanian et al. 2008
10	Amide derivative	Pan HDAC	10	779	Andrianov et al. 2009
11	Pyrimidyl hydroxamate	HDAC1, HDAC2	11	4.26	Arts et al. 2009
12	3,4-dihydroquinoxaline-2-(1H) one derivative	HDAC6	12	210	Smil et al. 2009
13	Piperazine-2,5-dione aryl hydroxamate	HDAC6	12	210	Smil et al. 2009
14	N-hydroxy-(4-oxime)-cinnamate based hydroxamate	HDAC8	13	70	Giannini et al. 2009
15	2-morpholinyl ethyl	HDAC8	14	235	Giannini et al.

	hydroxamate				2009
16	1,2,3-triazole based NLSP hydroxamate	HDAC1, HDAC2	15	1,243	Canzoneri et al. 2009
17	Non peptide macrocyclic derivative	HDAC1, HDAC6	16	994	Oyelere et al. 2009
18	Cyclic α/β tetra peptide derivative	HDAC8	17	120	Montero et al. 2009
19	Benzyloxy phenyl carbamoyl hydroxamate	HDAC-8	18	2,710	He et al. 2009
20	Boronic acid-based derivative	HDAC6	19	6,600	Suzuki et al. 2009
21	2-piperazinyl-5-pyrimidyl hydroxamate	Pan HDAC	20	--	Angibaud et al. 2010
22	Acetyl urea based hydroxamate	HDAC1	21	270	Wang et al. 2010
23	Triazole-4-yl phenyl based hydroxamate	Pan HDAC	22	1,190	He et al. 2010
24	Tricyclic ketolide based hydroxamate	HDAC8	23	544.6	Mwakwari et al. 2010
25	Cyclo peptide based hydroxamate	HDAC1, HDAC2, HDAC8	24	23,000	Terracciano et al. 2010
26	Tetrahydro isoquinoline based hydroxamate	HDAC8	25	580	Zhang et al. 2010
27	Tetrahydro isoquinoline based hydroxamate	HDAC6	26	47	Zhang et al. 2011a
28	Tetrahydro isoquinoline based hydroxamate	HDAC6	27	146	Zhang et al. 2011b
29	Benzohydroxamate derivative	HDAC8	28	23	Tang et al. 2011
30	Oxime amide derivative	Pan HDAC	29	22,600	Botta et al. 2011
31	Gamma lactym derivative	HDAC6	30	119.7	Choi et al. 2011
32	Gamma and del-lactum based hydroxamate	HDAC3	31	17	Neelarapu et al. 2011
33	1,4-dithia-7-aza spiro[4.4] nonane-8-carboxylate based derivatives	HDAC8	32	21	Zhang et al. 2011c

34	Short chained(phenyl butyryl) based hydroxamate	HDAC1	33	4,000	Fass et al. 2011
35	SAHA derivative with osthole derived CAP region	HDAC1	34	267.85	Huang et al. 2011
36	Ferrocinyl based JAHA derivative	Pan HDAC	35	2	Spencer et al. 2011
37	Amino acid derivative	HDAC1, HDAC2	36	90	Whitehead et al. 2011
38	SAHA derivative	HDAC6	37	220	Guerrant et al. 2012
39	2,2,3,3,4,4,5,5,6,6,7,7-dodecafluoro-N-hydroxy octane di-amide derivative	HDAC1	38	1,400[a]	Henkes et al. 2012
40	Tetrapeptide derivatives without ZBG	HDAC8	39	28,000	Vaidya et al. 2012
41	Cu(I) catalyzed azide alkyne cyclo addition library of HDAC8 inhibitors	HDAC8	40	70	Suzuki et al. 2012
42	Alkoxamide linked hydroxamate	HDAC4, HDAC5, HDAC6	41	893	Marek et al. 2013
43	Phenyl glycin based hydroxamate	HDAC8	42	967	Zhang et al. 2014
44	Quinazoline-4-one derivative	HDAC6	43	420	Yu et al. 2013
45	3‑Hydroxypyridin-2-thione derivative	HDAC6	44	800	Patil et al. 2013
46	N-Methylpyrrole (Py)-N-methylimidazole (Im) polyamides (pips) derivative	HDAC1, HDAC2, HDAC8	45	130	Saha et al. 2013
47	Amide-linked p-substituted phenyl hydroxamate	HDAC6	46	689	Wagner et al. 2013
48	Carrbostyril derivative	Pan HDAC	47	6	Tashima et al. 2014
49	Triazole derivative	HDAC8	48	53	Suzuki et al. 2014
50	Aminotetralin derivative	HDAC6, HDAC8	49	30	Tang et al. 2014

51	1,2,4-oxadiazole containing 2-amino benzamide derivative	HDAC1, HDAC2	50	200	Cai et al. 2015
52	Benzohydroxamate derivative	HDAC6	51	3	Shen et al. 2016
53	Pteroate hydroxamide derivative	HDAC6	52	581	Sodji et al. 2015
54	Benzothiophene based hydroxamate derivative	HDAC6	53	1,400	De Vreese et al. 2015
55	Benzohydroxamate derivative	HDAC6	54	376	Lee et al. 2015
56	Suberonyl hydroxamate derivative	HDAC8	55	119	Zhang et al. 2015
57	Glutamic acid derivative	HDAC8, MMP-2	56	2,890	Halder et al. 2015
58	Aminopyrrolidinone derivative	HDAC6	57	80	Lin et al. 2015
59	1-hydroxypyridine-2-thione derivative	HDAC8	58	980	Muthyala et al. 2015
60	2,5-Disubstituted-1,3,4-oxadiazole derivative	HDAC8	59	98	Pidugu et al. 2016
61	Triazole analogue	HDAC8	60	0.8	Ingham et al. 2016
62	Tetrahydro isoquinoline based hydroxamate	HDAC1, HDAC3	61	44	Taha et al. 2017
63	N^1-hydroxy tetrapthalamide based derivative	HDAC8	62	5,500	Wang et al. 2017
64	Propargylamine derivative	HDAC6	63	417	Wünsch et al. 2017
65	Meta-sulfamoyl N-hydroxybenzamide derivative	HDAC8	64	50	Zhao et al. 2018
66	*iso*-Combretastatin based derivatives	HDAC8	65	60	Lamaa et al. 2018

[a] = HDAC8 K_d value

A pool of cyclic tetrapeptide derivated compounds with trifluoromethyl and pentafluoroethyl ketone zinc binding groups were synthesized by Jose and his co-worker [Jose et al. 2004]. The activity of these compounds was evaluated in p21 promoter assay and against different HDAC isoforms. Among these compounds, compound 2 (***Figure***

2.3), possessing a thioether linker moiety and a trifluoromethyl ketone group as ZBG showed good HDAC8 inhibition of IC_{50} = 230 nM. Oh et al. reported a group of β-lactam containing HDAC inhibitors which exhibited higher inhibition against HDAC than the sodium butyrate [Oh et al. 2007]. These compounds seemed to provide cytotoxicity while modulating the HDAC8 inhibitory potency via activating NF-κB mediated pathway. A group of mercaptoacetamide and hydroxamate-based HDAC inhibitors have been reported by Kozikowski et al. in 2007 [Kozikowski et al. 2007]. Among these compounds, the molecules containing the hydroxamate group (Compound **3**, IC_{50} = 1,050 nM) (***Figure 2.3***) seemed to be providing better HDAC inhibition than the thiol and the carbonyl functions. This may because of the higher binding ability of the hydroxamate moiety with the catalytic zinc of the enzyme which again signifies the preference of hydroxamic acid moiety for higher HDAC8 inhibition and better Zn^{2+} chelation.

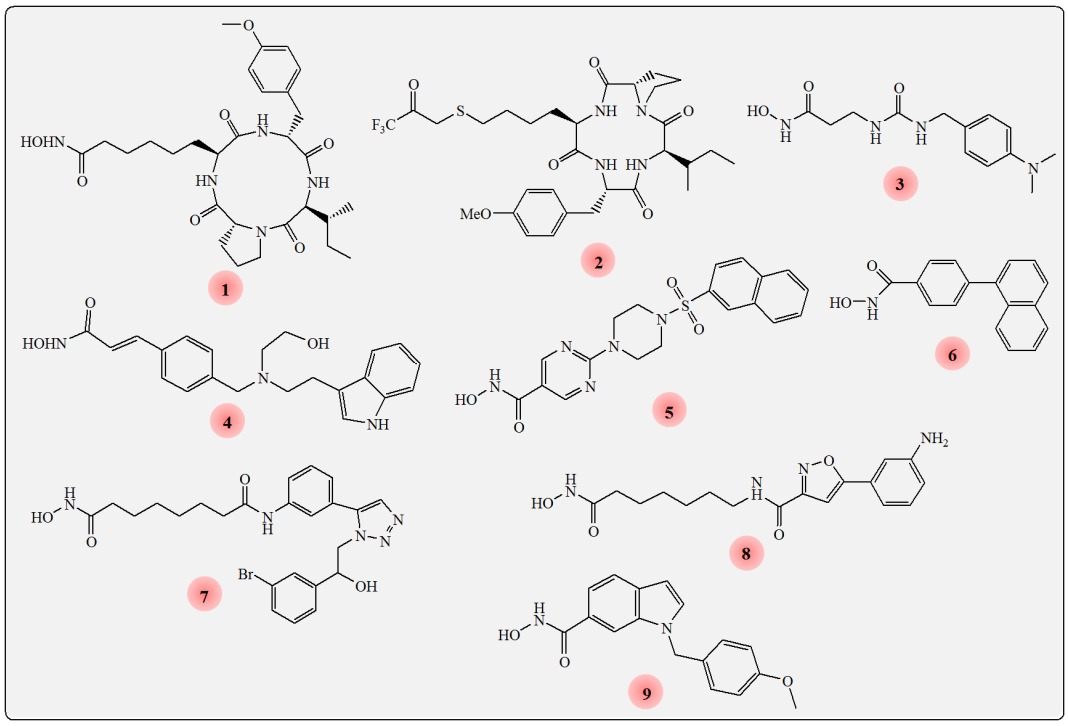

Figure 2.3. HDAC8 inhibitors **1-9**

Some bis-(aryl) like potent HDAC inhibitors has been reported by Moradei and his co-researchers [Moradei et al. 2007]. Amidst these HDAC inhibitors, LAQ-824 (Compound **4**) (***Figure 2.3***) delivered good inhibition against HDAC1 and HDAC2 along with an

HDAC8 inhibition of IC_{50} = 400 nM. A group of 5-pyrimidinyl hydroxamate derivated HDAC inhibitors was developed by Arts et al. in which, compound R306465 (Compound **5**) (***Figure 2.3***) was able to deliver excellent HDAC8 inhibition (IC_{50} = 23 nM) along with good inhibition against the activity of other HDAC isoforms of class I [Arts et al. 2007]. After studying the different crystal structures of HDAC8 enzyme, KrennHrubec et al. developed a few linker-less HDAC8 inhibitors containing the cap and the ZBG groups [Krennhrubec et al. 2007]. These compounds seemed to possess better selectivity for HDAC8 than the class I isoforms like HDAC1 and class II isoforms like HDAC6. The compound **6**, (HDAC8 IC_{50} = 300 nM) (***Figure 2.3***) was observed to have better fitting inside the HDAC8 pocket which may lead the compounds toward more sufficient and stronger binding with HDAC8. Chen et al. synthesized a group of triazolylphenyl derivated HDAC8 inhibitors with a significantly modified cap group in their structure [Chen et al. 2008]. Though many of these compounds exhibited poor HDAC8 inhibition and showed selectivity toward HDAC6, compounds **7** (***Figure 2.3***) was able to deliver HDAC8 inhibition in the nanomolar range (HDAC8 IC_{50} = 406 nM). A series of hydroxamate derivated HDAC inhibitors containing a phenylisoxazole moiety was developed by Kozikowski and his co-workers] with greater selectivity for HDAC6 than HDAC8 [Kozikowski et al. 2008. In this series of compounds, compound **8** (HDAC8 IC_{50} = 938 nM) (***Figure 2.3***) was able to provide the best HDAC8 inhibition. PCI-34051 (Compound **9**) (***Figure 2.3***) is one of the most potent and selective HDAC8 inhibitors reported by Balasubramanian et al. provided an excellent inhibition against HDAC8 activity of IC_{50} = 10 nM [Balasubramanian et al. 2008].

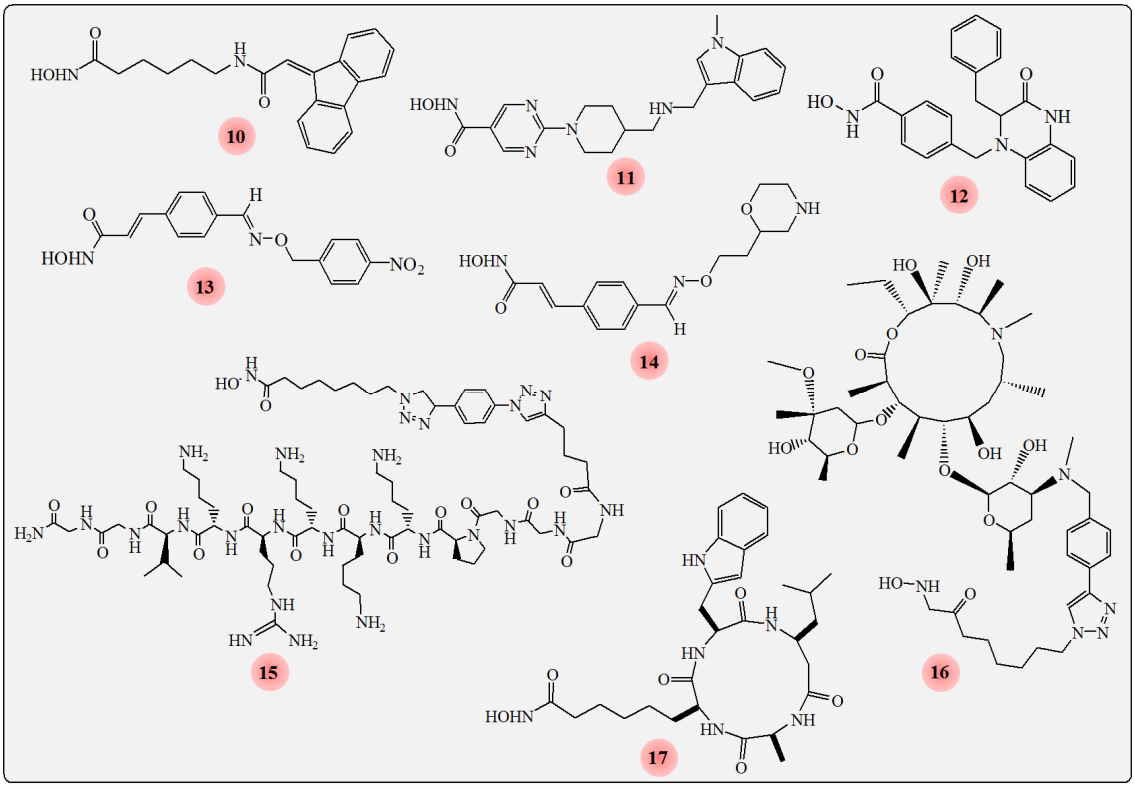

Figure 2.4. HDAC8 inhibitors **10-17**

Among the hydroxamate derivated HDAC inhibitors synthesized by Andrianov et al., compound **10** (***Figure 2.4***) was able to provide an HDAC8 inhibition of IC_{50} = 779 nM and was also potent against HDAC6 and HDAC1 isoforms [Andrianov et al. 2009].

While conducting an in vivo pharmacodynamics study on a group of pyrimidyl hydroxamate derivated compounds, Arts et al. reported a compounds JNJ-26481585 (Compound **11**) (***Figure 2.4***) having a good HDAC8 inhibitory activity of IC_{50} = 486 nM [Arts et al. 2009]. The compound was much more selective toward HDAC8 than the class I HDACs like HDAC1 and HDAC2. Reports of a group of 3, 4-dihydroquinoxaline-2-(1H)-one and piperazine-2,5-dione aryl hydroxamate derivated HDAC8 inhibitors has been done by Smil and his co-workers [Smil et al. 2009]. Though these compounds were mostly selective to HDAC6 isoform, Compound **12** (***Figure 2.4***), a piperazine-2,5-dione aryl group containing hydroxamate derivative was able to exhibit good nanomolar activity against HDAC8 (IC_{50} = 210 nM). These compounds also provide information

that the chiral compounds can also be useful to design potent and selective HDAC8 inhibitors.

A pool of N-hydroxy-(4-oxime)-cinnamate containing compounds were developed by Giannini et al. as a cytotoxic agent and HDAC8 inhibitor [Giannini et al. 2009]. Compounds with bulky group substitutions such as aryl group substituted oxime moiety, *para*-substituted cinnamic acid and heteroaryl moiety can deliver higher HDAC8 inhibition. Compound **14** (IC_{50} = 235 nM) **[*Figure 2.4*]** containing a *para*-nitrobenzyl moiety in its structure showed at least 2-fold selectivity toward HDAC8 than the other tested HDAC isoforms.

Canzoneri and his co-workers discovered a group of nuclear localization signal peptide (NLS)-derivatives containing 1, 2, 3-triazole and hydroxamate group as potent HDAC inhibitors [Canzoneri et al. 2009] where these compounds indicated the significance of the length of the linker moiety present in these compounds. Among the compounds present in this series, compounds **15** (***Figure 2.4***) showed an HDAC8 inhibition of IC_{50} = 1,243 nM).

In the year 2009, a newer group of non-peptide derivated HDAC inhibitors has been discovered by Oyelere et al. [Oyelere et al. 2009]. The macrocyclic structure of these compounds was inspired by the macrocyclic structure of the macrolide class of antibiotics. Compound **16** (***Figure 2.4***) of this class of HDAC inhibitors, though having better response toward HDAC1 and HDAC2 isoforms, exhibited inhibitory potency of IC_{50} = 994 nM against HDAC8 enzymatic activity.

Some β-amino acid derivated containing structural resemblance with cyclic tetrapeptide were reported by Montero et al. [Montero et al. 2009]. These compounds were designed through h several changes like positional alteration of the catalytic zinc chelating amino acid moiety, chirality, β-3-amino acid position including amide nitrogen alkylation of the macrocyclic backbone. Compound **17** (***Figure 2.4***) is the compound among these compounds provided promising HDAC8 inhibition of IC_{50} = 120 nM.

A pool of aryl derivated cap containing 4-triazolyl hydroxamate compounds was synthesized by He and his co-researchers as HDAC inhibitors [He et al. 2009]. Instead of having pan-HDAC activity for the most active compounds and some of these compounds

had nanomolar activity against other HDACs like HDAC6, HDAC1, and HDAC3, compound **18** (***Figure 2.5***) showed HDAC8 inhibition of IC_{50} = 2,710 nM.

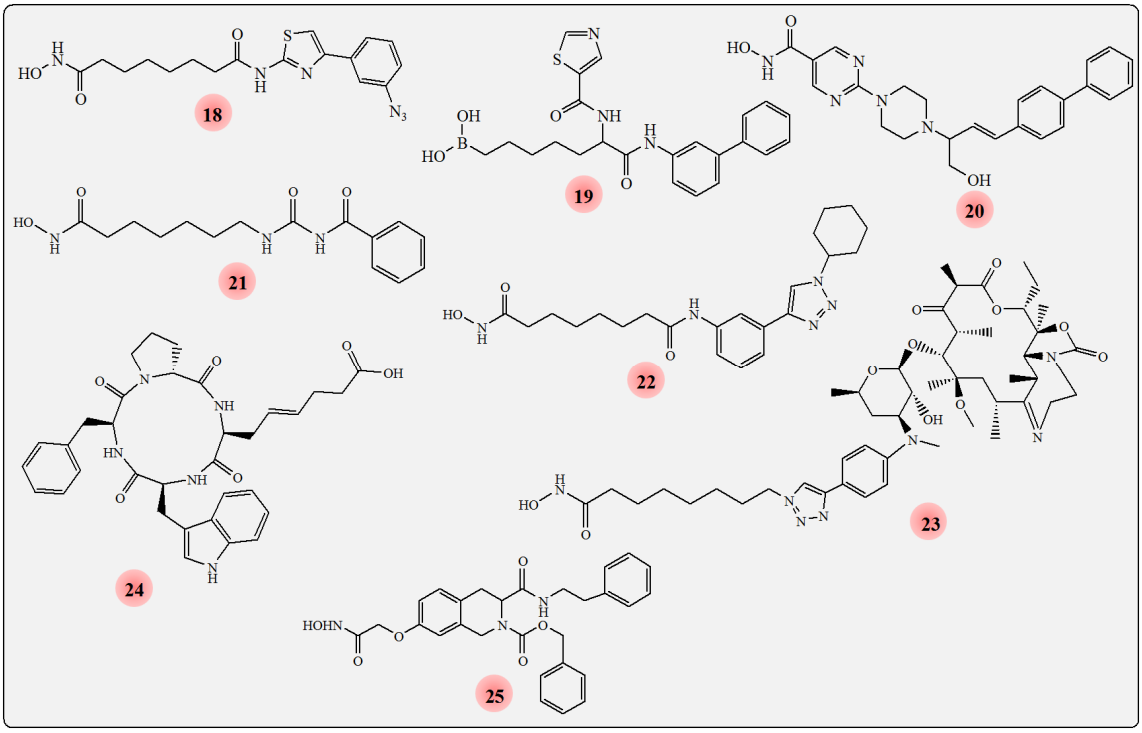

Figure 2.5. HDAC8 inhibitors **18-25**

Using the Boronic acid moiety as a zinc-binding motif for HDAC inhibitors, Suzuki et al. reported a group of HDAC inhibitors and tested against different HDAC enzyme activity [Suzuki et al. 2009]. Authors suggested that, among these inhibitors, the compounds with (*S*)-conformation provided a significant role in their HDAC inhibitory activity and were more active against HDAC6 than other HDAC isoforms. Though having lower HDAC8 inhibition compound **19** (***Figure 2.5***)showed HDAC8 IC_{50} of 6,600 nM.

A set of 2-piperazinyl-5-pyrimidy group containing hydroxamate derivatives was developed as HDAC inhibitors by Angibaud et al. [Angibaud et al. 2010]. Among these 2-piperazinyl-5-pyrimidy derivated compounds with biphenyl group substitution (Compound **20**) [***Figure 2.5***]exhibited an excellent HDAC8 inhibition in sub-nanomolar concentration IC_{50} = 0.9 nM. Wang et al. reported a group of compounds as good HDAC inhibitors containing acyl urea containing linear chain hydroxamic acid group [Wang et al. 2010]. From these compounds, it can be observed that the compound with n-pentyl

liner provides better HDAC1 (IC_{50} = 53 nM) inhibition than HDAC8 (IC_{50} = 608 nM) whereas the n-hexyl analog (Compound **21**, HDAC8 IC_{50} = 270 nM) [***Figure 2.5***] delivered higher HDAC8 inhibitory potency.

He et al. in the year 2010 synthesized a pool of 4-triazolyl hydroxamate derivated HDAC inhibitors with poor HDAC8 inhibitory potency [He et al. 2010]. Though these compounds having more affinity toward HDAC6 and HDAC3, Compound **22** (***Figure 2.5***), containing a cyclohexyl moiety provided weaker HDAC8 inhibitory potency (IC_{50} of 1,190 nM). Some tricyclic ketolide derivated HDAC inhibitors similar to the macrocyclic peptide backbone structure were introduced by Mwakwari et al. [Mwakwari et al. 2010]. Though showing better selectivity toward the HDAC1 and HDAC2 isoforms by these inhibitors, compound **23** (HDAC8 IC_{50} = 544.6 nM) was able to provide HDAC8 inhibitory potency in nanomolar concentration (***Figure 2.5***). Terracciano et al. reported an FR235222 derivated cyclopeptide compound (Compound **24**, HDAC8 IC_{50} = 23,000 nM) (***Figure 2.5***) as a promising inhibitor HDAC8 HDAC8 activity [Terracciano et al. 2010].

A series of tetrahydroisoquinoline moiety containing hydroxamate derivative was reported by Zhang et al. [Zhang et al. 2010] as potent and selective HDAC8 inhibitors. Among the compounds of this series, Compound **25** (***Figure 2.5***) provided good HDAC8 inhibition of IC_{50} = 580 nM. Additionally, in another study, these authors used the tetrahydroisoquinoline moiety as a linker motif and synthesized a group of tetrahydroisoquinoline group containing hydroxamate derivatives [Zhang et al. 2011a]. The 4-methoxyphenyl moiety along with the *t*-butoxycarbonyl (Boc) substituted compound (Compound **26**, HDAC8 IC_{50} = 47 nM) (***Figure 2.6***) seemed to have a significant influence on the HDAC8 inhibition of these compounds. Further optimization of the tetrahydroisoquinoline derivatives led the author's design ZYJ-34c (Compound **27**) (***Figure 2.6***), an HDAC8 inhibitor with greater potency and orally active than Vorinostat (**FDA-01**) (***Figure 2.1***). This compound was also exhibited good antitumor activity in an MDA-MD-231 xenograft model for human breast cancer [Zhang et al. 2011b].

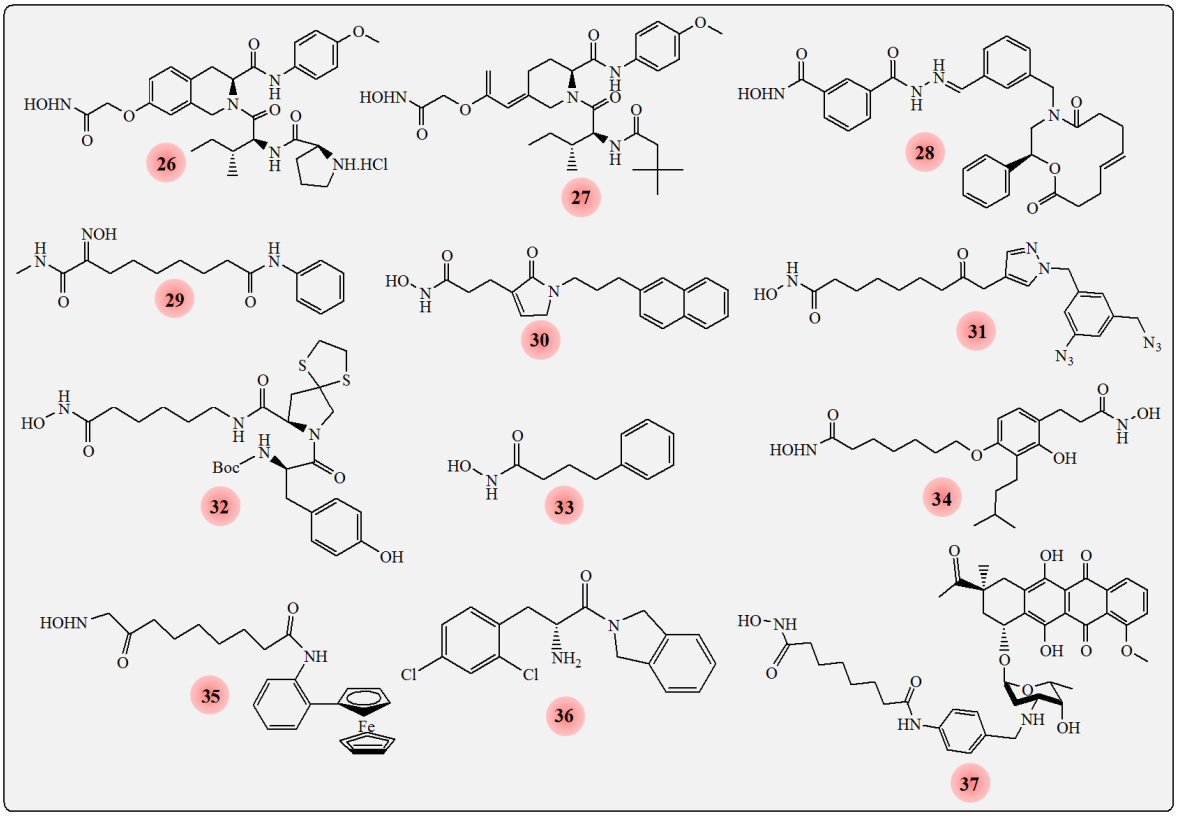

Figure 2.6. HDAC8 inhibitors **26-37**

Using a bi-step protocol to design and synthesize a pool of benzohydroxamate derivatives Tang et al. designed a group of potent HDAC8 inhibitors [Tang et al. 2011]. The synthesized compounds were excellently active against HDAC8 enzymatic activity and provided nanomolar range activity against HDAC8. The compound **28** (***Figure 2.6***) was the most active compound against HDAC8 activity and was able to show an excellent activity of IC_{50} = 23 nM) against HDAC8 enzymatic activity where it was 15-65 fold more selective for HDAC8 than HDAC2 and HDAC3 isoforms.

Compound **29** (***Figure 2.6***), containing an oxime group as the ZBG was synthesized by Botta et al. [Botta et al. 2011]. The compound though having a poor HDAC8 inhibitory potency (IC_{50} = 22,600 nM), it was observed that, at the active site of HDAC8, the α-oxime moiety adapted perfectly in order to coordinate with the catalytic Zn^{2+} of the enzyme.

Choi et al. synthesized and evaluated a group of γ-lactam derivated HDAC inhibitors for promising inhibition of the major HDAC classes [Choi et al. 2011]. Though these

compounds were intended to provide better class I and class II HADC inhibition, these molecules tended to be more effective against the HDAC6 isoform. Among these molecules, the compound **30 (*Figure 2.6*)** exhibited good HDAC8 inhibitory activity of IC_{50} = 119.7 nM along with an excellent HDAC6 inhibitory activity of IC_{50} = 0.8 nM.

A class of pyrazole or iso-oxazole derivated diazide containing compounds were synthesized by Neelarapu and co-workers [Neelarapu et al. 2011]. Between the iso-oxazole and pyrazole derivatives, the pyrazole moiety eas better effective for both HDAC8 and HDAC3 isoforms whereas the compound **31** (***Figure 2.6***) showed an excellent HDAC8 inhibition of 17 nM (IC_{50} = 17 nM).

A group of tripeptidomimetics derivated compounds as potent HDAC inhibitors have been synthesized by Zhang and his co-workers [Zhang et al. 2011c]. From this series, the compound **32** (HDAC8 IC_{50} = 21 nM) [***Figure 2.6***] was the most potent HDAC8 inhibitor which contained a 1, 4-dithia-7-azaspiro-[4, 4]-nonane-8-carboxylate moiety as the surface recognition group and a 6-amino hexanoic acid moiety as the linker function.

In an attempt to develop potent HDAC8 inhibitors Fass et al. synthesized some short chain containing hydroxamate derivated compounds [Fass et al. 2011] among which the compound **33** (HDAC8 IC_{50} = 4,000 nM) [***Figure 2.6***], containing a phenyl cap moiety provided the highest HDAC8 inhibition.

A newer class of SAHA linked osthole containing hydroxamic acid compounds were reported by Huang et al. [Huang et al. 2011]. Compound **34** [***Figure 2.6***] was able to provide better HDAC8 inhibition than SAHA (**FDA-01**) [***Figure 2.1***] and was the most active compound in the series providing an IC_{50} = 267.85 nM activity against HDAC8.

A group of organometallic SAHA analogs with a ferrocenyl group named as Jay Amin hydroxamic acid (JAHA) was synthesized by Spencer et al. [Spencer et al. 2011]. Among these JAHA derivatives, compound **35** (HDAC8 IC_{50} = 2 nM) (***Figure 2.6***) exhibited excellent HADC8 inhibition.

Whitehead et al. in the year 2011, derived some potent α-amino-ketone containing HDAC inhibitors. Among these compounds, compound **36** (***Figure 2.6***), containing a dichlorophenyl moiety in its structure at least 20-fold selectivity for HDAC8 the other

HDAC isoforms such as HDAC6, HDAc1, and HDAC2. Compound **36** was also excellent active against HDAC8 *in vitro* enzymatic activity (IC_{50} = 90 nM) [Whitehead et al. 2011].

In order to obtain HDAC-topoisomerase-II dual inhibitors, Guerrant et al. tried to combine chemotherapeutic agents like anthracycline derivatives and SAHA which resulted in a group of compounds [Guerrant et al. 2012]. Some of these compounds exhibited moderate to poor activity against HDAC8 where compound **37** (***Figure 2.6***) provided good HDAC8 inhibition of HDAC8 = 220 nM.

Through the modification of the linker moiety of the SAHA (***Figure 2.1***), Henkes et al. derivated a group of HDAC inhibitors in order to conserve the significance of the liker motif of these molecules [Henkes et al. 2012]. The compound **38** (***Figure 2.7***), with HDAC8 K_d value of 1,400 nM, containing an anthracene ring was showed twice the potency against HDAC8 than SAHA **[**Henkes et al. 2012].

The task of development and evaluation of a group of tetrapeptide derivated compounds as potent HDAC inhibitors were performed by Vaidya et al. in the year 2012 [Vaidya et al. 2012]. Through the study, it was seen that the compounds the hydroxamic acid moiety as the ZBG group signified its importance toward the activity for these compounds. Though having poor potency against HDAC8, compound **39** (***Figure 2.7***) was able to show an HDAC8 inhibitory activity of IC_{50} = 28,000 nM.

A pool of potent HDAC8 inhibitors was able to develop by Suzuki and co-workers through a click-chemistry mediated Cu (I)-catalyzed-azide-alkyne cycloaddition process [Suzuki et al. 2012]. In this library of compounds, compound **40** (***Figure 2.7***) showed promising potency of IC_{50} = 70 nM against HDAC8 along with the selectivity toward that specific isoform.

The synthesis and evaluation of a class of alkoxamide containing hydroxamate derivatives were performed and reported by Marek et al. in the year 2013 [Marek et al. 2013]. Although these synthesized compounds were moderately potent against HDAC8 the compound **41** (***Figure 2.7***) provided effective HDAC8 inhibition (HDAC8 IC_{50} = 893 nM).

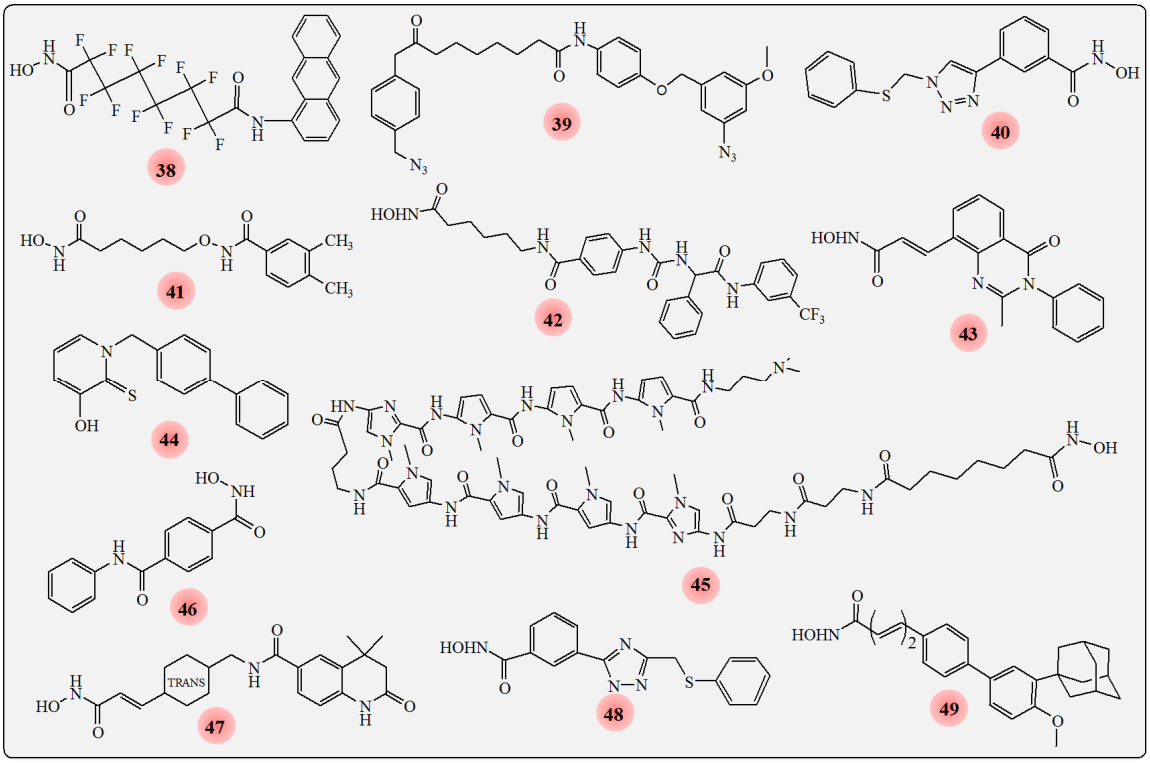

Figure 2.7. HDAC8 inhibitors **38-49**

A class of potent arylhydroxamic acid derivated compounds was synthesized by Zhang et al. [Zhang et al. 2014]. For these compounds, it was noticed that the substitution at the *para*- and *ortho*- positions of the phenyl ring of these compounds is detrimental for the activity of these compounds whereas, the meta-trifluoromethylphenyl derivated analog (Compound 42) **[*Figure 2.7*]**possessed highest HDAC8 inhibition (IC_{50} = 967 nM).

In order to aid the treatment of Alzheimer's disease via the development of potent HDAC inhibitory compounds, Yu et al. developed and reported a group of quinazoline-4-one derivatives as potent HDAC inhibitors having a higher selectivity for HDAC6 isoform [Yu et al. 2013]. Compound **43** (***Figure 2.7***) was the most potent inhibitor among this class of inhibitors while testing against HDAC8 enzymatic activity of IC_{50} = 420 nM almost similar to its HDAC6 inhibitory potency.

With the help of Suzuki cross-coupling reaction, Patil and co-workers] synthesized a newer class of HDAC inhibitors containing 3-hydroxy-pyridine-2-thione (3-HPT) moiety as the ZBG of these compounds [Patil et al. 2013. Among these inhibitors, compound **44**

(***Figure 2.7***), a *para*-methyl biphenyl derivated compound showed the highest potency against HDAC8 enzyme activity.

In the year 2013, a group of PIP (pyrrole-imidazole polyamides) containing JAHA derivated compounds were synthesized by Saha et al. [Saha et al. 2013]. Among these JAHA derivatives, PIP-δ complexed compound **45** (JAHA-PIP-δ) (***Figure 2.7***), exhibited an excellent HDAC8 inhibitory activity of IC_{50} = 130 nM.

A set of para-phenyl substituted amide-linked hydroxamate derivated compounds was reported by Wagner et al. [Wagner et al. 2013]. The evaluation of these compounds against different HDAC isoforms. The study revealed that reduction in the chain length from phenethyl moiety increases the activity against HDAC8 whereas the ethylene-piperazine moiety showed its detrimental effects as the cap group on the activity of the compounds. The compound **46** (***Figure 2.7***) of this series showed moderate HDAC8 inhibition (IC_{50} = 689 nM).

Some 15 carbostyril derivated compounds were reported by Tashima et al. [Tashima et al. 2014] as the potent HDAc inhibitors. It is seen that, for these compounds, the 1-carboxamino linker moiety (1-CONH) and the 1-aminocarbonyl linker moiety (1-NHCO) present between the zinc binding group and the cap moiety plays an important part while the interactions of these compounds with the HDAC isoforms. Also, compound **47** (***Figure 2.7***) showed an excellent HADC8 inhibitory potency of IC_{50} = 6 nM among these molecules.

A group of α- and β-tropolone derivated compounds were reported by Ononye et al. in 2013 as effective HDAC inhibitors which provided superior selectivity toward HDAC2 isoform than HDAC4-6 of class II and HDAC8 and HDAC1 of class I including promising HDAC8 inhibition [Ononye et al. 2013].

From further modification of the compound NCC-149 (Compound **40**) [***Figure 2.7***], in order to enhance the HDAC8 inhibitory activity of the compound **40**, through the modification of the linker and scaffold, Suzuki et al. reported a compound (Compound **48**) [***Figure 2.7***] with altered orientation of the triazole moiety as more potent HDAC8 inhibitor [Suzuki et al. 2014]. The compound **48** expressed a small enhancement of its HADC8 inhibitory activity (IC_{50} = 53 nM) than compound **40** (IC_{50} = 70 nM).

Cincinelli and his co-workers were able to develop a group of biphenylacrylohydroxamic acid derivated compounds as potent HDAC inhibitors [Cincinelli et al. 2014]. Fascinatingly, the evaluation of these compounds against HDAC8 enzymatic activity showed the detrimental effects of the adamantly moiety toward their HDAC8 inhibition. As it is seen that bulky features in the cap region of the HDAC8 inhibitors facilitate their HDAC8 inhibition, it seemed to be that the adamantly moiety is an exception of this suggestion for these compounds. A newer series of aminotetralin containing compounds were suggested as promising HDAC8-HDAC6 dual inhibitors by Tang et al. Among these dual HDAC inhibitors, compound **49** (***Figure 2.7***) expressed the highest HDAC8 inhibition of IC_{50} = 30 nM [Tang et al. 2014].

Two series of compounds containing the 2-aminobenzamide moiety and the hydroxamic acid moiety were derivated by Cai et al. [Cai et al. 2015]. The *in vitro* evaluations of these series of compounds exhibited a good anti-proliferative property against a number of cancer cell lines namely U937, A549, NCI-H661, HCT-116, and MDAMB-231. The hydroxamate derivatives as usually showed better HDAC8 inhibition than the 2-aminobenzamide derivatives and were also expressed its selective for HDAC8 thanHDAC1 and HDAC2 enzymes. Amidst these hydroxamates, compound **50** (***Figure 2.8***) with a phenyl cap group showed good HDAC8 inhibition of IC_{50} = 200 nM.

Through effective attempt for enhancement of the activity of the HDAC6 inhibitors, Shen and his co-workers designed and synthesized several benzohydroxamate derivated compounds with bi-cyclic cap moiety which expressed higher selectivity to HDAC6 enzymatic activity [Shen et al. 2016]. Though having superior activity against HDAC6, the compound **51** (HADC8IC_{50} = 176 nm) [***Figure 2.8***] of this series of HDAC6 inhibitors exhibited a good HDAC8 inhibition also.

Two different hydroxamates derivated compounds one containing folic acid where the other containing a pteroic acid were synthesized and evaluated by Sodji and co-workers in 2015 [Sodji et al. 2015]. The folic acid derivated compound (Compound **52**) was proved itself as the more effective HDAC8 inhibitor than the pteroic acid derived compound (HDAC8 IC_{50} = 581 nM) but also having higher selectivity toward the HDAC6 isoform [***Figure 2.8***].

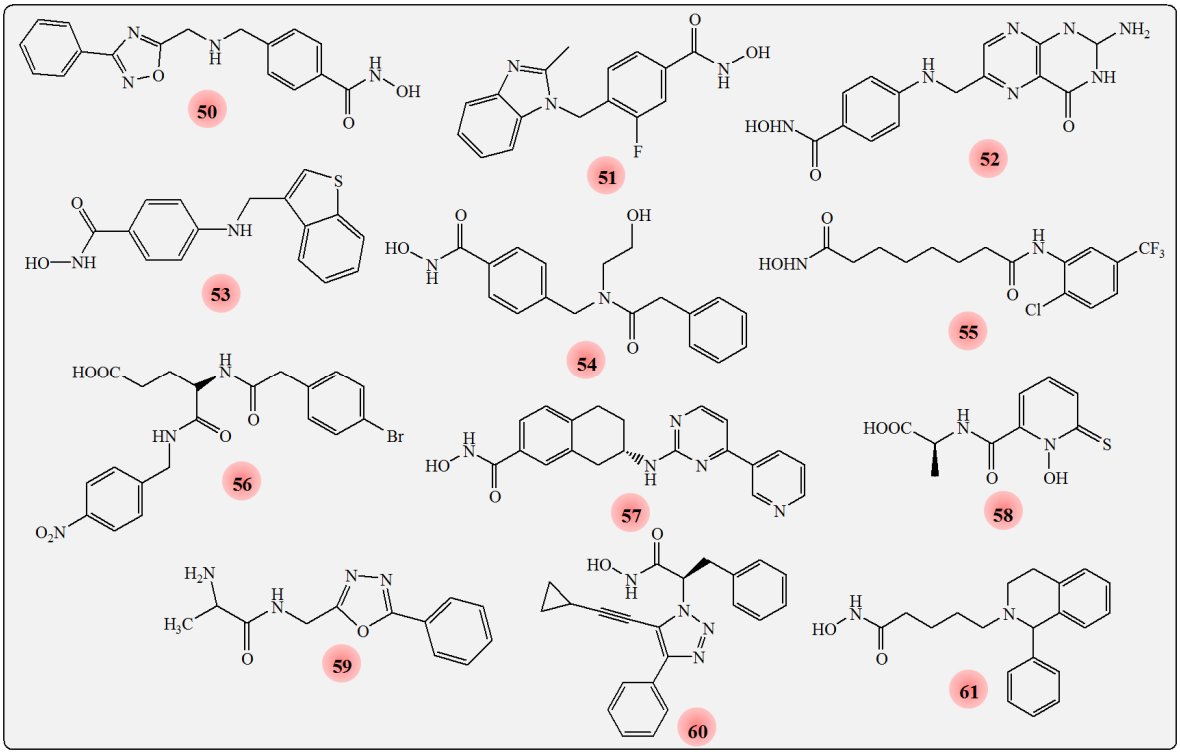

Figure 2.8 HDAC8 inhibitors **50-61**

Among the numerous HDAC inhibitors with various cap groups, a group of hydroxamate derivated compounds having benzothiophene group as the cap moiety were synthesized by De Vreese et al. in order to procure HDAC inhibitors with higher potency [De Vreese et al. 2015]. The compounds suggested the unfavorability of the *para*-bromo group substitution in their fused benzothiophene phenyl cap moiety and preferred the unsubstituted analog as better HDAc inhibitor. Between these molecules, compound **53** (***Figure 2.8***) was able to deliver moderate activity of 1,400 nM as the HDAC8 inhibitory activity of the compound.

Lee et al. reported a benzohydroxamate compound named as HPB (Compound **54**) [***Figure 2.8***] as a selective and potent HDAC6 inhibitor [Lee et al. 2015]. Apart from expressing its effectiveness against HDAC6 compound 54 also provided induction of the cellular apoptosis for the cancer cells without effecting the normal healthy cells and possessed good HDSAC8 inhibition of IC_{50} = 376 nM also [Lee et al. 2015].

Several HDAC8 inhibitors with a better binding affinity toward HDAC8 isoform, Zhang et al. designed a group of analogous compounds of SAHA [Zhang et al. 2015]. Among

these, the compound **55** (***Figure 2.8***) with chlorine at the sixth and a trifluoromethyl function in the third position of its phenyl ring moiety delivered good HDAC8 inhibition.

A group of carboxylate-containing isoglutamine derivated compounds was reported by Halder and his co-workers in order to provide dual inhibition for HDAC8 and MMP-2 metalloenzymes [Halder et al. 2015]. Amidst these *iso*-glutamate derivatives, compound **56** (***Figure 2.8***) exhibited anti-invasive and anti-migratory activity in A549 lung cancer cell line along with an in vitro HDAC8 inhibition of IC_{50} = 2,890 nM.

To develop orally active and bioavailable inhibitors for HDAC6 enzyme, Lin and his co-workers [Lin et al. 2015] developed several aminopyrrolidinone derivated potent HDAC6 inhibitors, in which the compound **57** (***Figure 2.8***) delivered a very good HDAC8 inhibitory (IC_{50} = 80 nM) potency along with excellent inhibition against HDAC6 isoform.

Several potent HDAC inhibitors containing a 1-hydroxypyridine-2-thione (1-HPT) moiety as the zinc binding motif was reported by Muthyala et al. in the year 2015 [Muthyala et al. 2015]. Interestingly, these compounds during the coordination with the catalytic zinc of HDAC8 isoform were seemed to form a special octahedral like structure in which, compound 58 showed moderate HDAC8 inhibition of IC_{50} = 980 nM (***Figure 2.8***).

A pool of oxadiazole containing alanine/glycine linked HDAC inhibitors were developed by Pidugu et al. for the inhibition of class I HDAC isoforms [Pidugu et al. 2016]. The compound 59 of this series, provided antiproliferative activity in breast cancer cell line (MDA-MB-23) and provided an HDAC8 inhibitory potency of IC_{50} = 98 nM for *in vitro* HDAC8 inhibition.

Till now, the most potent and selective, HDAC8 inhibitor, OJI-I (Compound **60**) [***Figure 2.8***] via a database screening of the various sets of compounds and was reported by Ingham et al. in 2016 [Ingham et al. 2016]. This triazole derivated compound (Compound **60**) exhibited s sub-nanomolar activity of IC_{50} = 0.8 nM against HDAC8 *in vitro* enzymatic activity.

As the tetrahydroisoquinoline derivated compounds were reported as potent HDAC8 inhibitors, Taha and co-workers designed and synthesized a group of 1-substituted

tetrahydroisoquinoline N-alkyl hydroxamate derivated compounds as potent HDAC8 inhibitors [Taha et al. 2017]. As expected, these compounds provided an excellent iHDAC8 inhibition while indicating the importance of the *n*-alkyl linker chain length for the activity of these compounds along with substitution in the tetrahydroisoquinoline based cap moiety of these compounds. The tetrahydroisoquinoline derivated compound **61** exhibited (***Figure 2.8***) an IC_{50} value of 44 nM against HDAC8.

By fusing the scaffolds of quisinostat (JNJ-26481585, **11**) [***Figure 2.4***] and panobinostat (**FDA-04,** ***Figure 2.1***) Wang et al. reported a group of N1-hydroxytetrephthalamide derivated compounds with indole moiety as the cap group as potent HDAC inhibitors [Wang et al. 2017]. Among these indole derivatives, compound **62** (***Figure 2.9***) with an HDAC IC_{50} of 74 nM showed good inhibition against HDAC isoforms.

Wünsch et al. [Wünsch et al. 2017], in order to inhibit the HDAC isoforms containing a catalytic zinc ion in their structure developed a group of propargylamine derivated HDAC6 inhibitors, in which the compound **63** (***Figure 2.9***) (HDAC8 IC_{50} = 417 nM) delivered a moderated but the best inhibition against HDAC8 than the other inhibitors of this series. Among the group of *meta*-sulfamoyl *N*-hydroxybenzamide derivated HDAC inhibitors, designed as potent HDAC inhibitors by Zhao et al. [Zhao et al. 2018], the compound 64 (***Figure 2.9***) exhibited an excellent HDAC8 inhibitory potency in vitro.

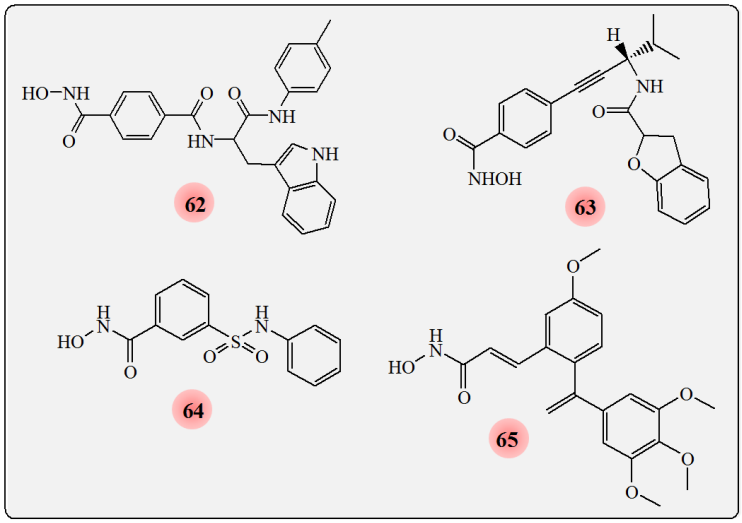

Figure 2.9. HDAC8 inhibitors **62-65**

A set of Laama *iso*-combretastatin based HDAC inhibitors were reported by Laama and his co-workers in 2018 [Lamaa et al. 2018]. The in vitro evaluations of these compounds expressed there higher selective nature against the HDAC8 isoform over the HDAC11 and HDAC6 enzymes. Among these benzamide derivatives, the compound 65 was able to provide an IC_{50} of 60 nM against *in vitro* activity of HDAC8 enzyme and was able to show antiproliferative activity in a number of cell lines namely, A549, HCT 116, K562, U87, PC3, MiaPaca2 and MCF-7 cell lines [Lamaa et al. 2018].

2.2 Overviewing the QSAR Studies performed on HDAC8 inhibitors

For, the purpose of screening, identification and designing of potential biologically active molecules, the different molecular modelling studies like Quantitative structure-activity relationship (QSAR) study, molecular dynamics (MD Simulation) simulation, molecular docking study are an acceptable, effective and widely applied technique used to screen, identify and design newer molecules with potent and promising biological activity.

A variety of computational approaches has been also applied for a decade to identify, screen and design potent, selective and promising HDAC8 inhibitors for effective and selective HDAC8 inhibition [Banerjee et al. 2019a]. The different QSAR studies conducted in search of the potent HDAC8 inhibitors are also given in ***Table 2.2*** and discussed in brief below.

Table 2.2. Different QSAR studies conducted on a diverse set of HDAC8 inhibitors

No.	*Scaffold*	*QSAR Technique*	*Reference*
01	Diverse Hyderoxamates	Docking-based 3D QSAR	Ortore et al. 2009
02	Diverse molecules	Pharmacophore-based 3D QSAR	Thangapandian et al. 2010
03	Diverse molecules	3D QSAR Pharmacophore mapping	Debnath et al. 2014
04	Diverse molecules	Lazy learning-based classification QSAR	Cao et al. 2015
05	Diverse compounds	Pharmacophore-based 3D QSAR	Halder et al. 2015
06	Diverse compounds	Regression-based 2D QSAR, Pharmacophore-based 3D QSAR	Noor et al. 2015
07	Diverse molecules	SVC and SVM-based 2D QSAR	Cao et al.

			2016
08	SAHA derivative	MLR based 2D-QSAR, Gaussian kernel based non-linear SVM 2D QSAR	Praseetha et al. 2016
09	N-hydroxyfurylacrylamidederivatives	DFT based MLR and ANN 2D QSAR	Tassine & Elhallaoui 2016
10	Aryl valproic acids	MLR 2D QSAR, Feed forward ANN 2D QSAR	Martínez-Pacheco et al. 2017
11	Diverse hydroxamates	Pharmacophore-based 3D QSAR	Manal et al. 2017
12	Diverse molecules	DFT based pharmacophore dependant 3D QSAR	Kim et al. 2018
13	Diverse compounds	Fragment-based Bayesian classification QSAR	Amin et al. 2018a

A docking mediated 3D-QSAR study was performed by 2009, Ortore et al. [Ortore et al. 2009] on a diverse set of molecules containing 48 hydroxamic acid derivatives in order to identify potent HDAC8 and HDAC1 inhibitors. Authors reported several factors after conducting this study that, the potency of the HDAC1 and HDAC8 inhibitors may depend on the different capabilities of the compounds such as the capability of forming polar interaction of the compounds with amino acid residues of the HDAC8 and the hydrogen bond formation between the enzyme and the compound where the interaction of between the phenylalanine amino acid residue and the aromatic moiety of the compounds may cause the selectivity toward the HDAC1 or HDAC8. Authors also suggested the favorability of compounds with more aromatic rings or having short indole ring containing linker can be effective for HDAC8 selectivity.

In 2010, Thangapandian and his co-workers [Thangapandian et al. 2010] employed the pharmacophore-based 3D QSAR analysis in order to design several molecules for HDAC8 inhibition. From this study, it was observed that different pharmacophoric features namely, pharmacophore models were hydrogen bond donor (HBD), hydrogen bond acceptor (HBA), hydrophobic features including a metal binding motif were used to construct the pharmacophore hypothesis which suggested the significance of six pharmacophoric features for better HDAC8 interaction of the molecules [Thangapandian

et al. 2010]. The hydrophobic feature was suggested as good surface recognition factor (cap) by the first model, suggesting the hydrogen bond donor and acceptor moieties as the ZBG group features. On the other hand, the other model displayed two hydrophobic features acting as a cap and the linker moiety.

In the year 2014, Debnath et al. [Debnath et al. 2014] applied a 3D QSAR pharmacophore based analysis on 20 diverse set compounds possessing HDAC8 inhibitory potency. The best-constructed pharmacophore model delivered a regression coefficient value of R^2 = 0.982 and a Leave-One-out R^2 value of 73.14%. This pharmacophore model was constructed using three features such as ring aromatic (RA), hydrogen bond donor and acceptor features (HBD and HBA). The selected features indicated toward the favorability of the better HDAC8 interactions of the compounds. It is possible that the compound **66** (***Figure 2.10***), a compound with a hydroxamate ZBG, indolyl ethyl cap group and two RA linker features may deliver good HDAC8 inhibitory activity.

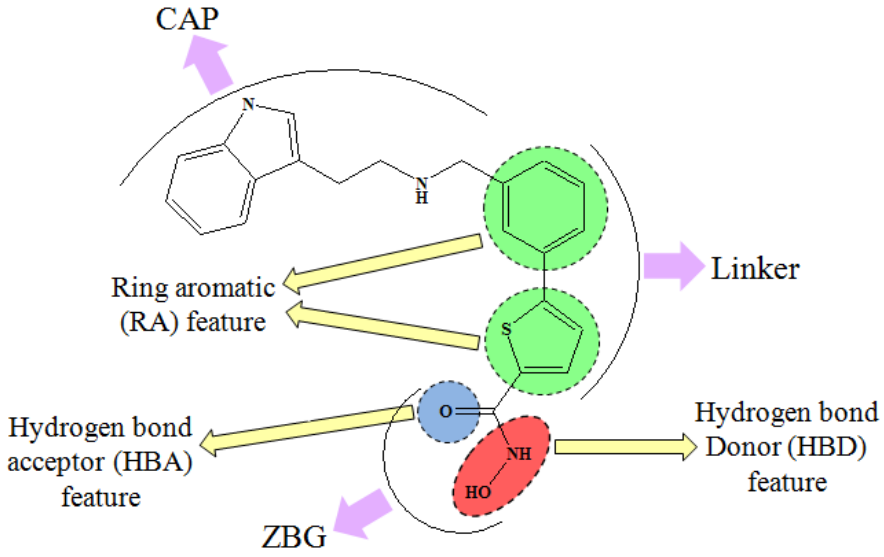

Figure 2.10. The pharmacophoric features of the compound **66**

Authors also suggested that proximal location of the HBD to the indole nitrogen atom can facilitate HDAC8 inhibition through a 3D-QSAR study where they also suggested the favorability of the hydrophobicity near the cap and linker phenyl group and presence of

electron withdrawing group near the zinc binding group and nitrogen atoms can benefit the HDAC8 inhibition for the compounds [Debnath et al. 2014].

A diverse group of molecules containing 37 non-HDAC inhibitor and 38 HDAC8 inhibitor compounds was used to construct a classification based QSAR study via lazy-learning technique to screen and identify HDAC8 inhibitory lead molecules by Cao et al. [Cao et al. 2015]. After conducting the study, the authors identified and reported five promising compounds namely compound **67** (AW00409), compound **68** (HTS03338), compound **69** (JFD03558), compound **70** (KM00731) and compound **71** (KM02921) [***Figure 2.11***] as lead HDAC8 inhibitors.

In the year 2015, A structure and ligand-based pharmacophore analysis study, on a set of diverse molecules was performed by Halder and his co-workers [Halder et al. 2015] with the purpose to design MMP2-HDAC8 dual inhibitors. The most statistically significant model constructed through this study, a few pharmacophoric features were identified as a significant factor for designing potent HDAC8-MMP-2 dual inhibitors which are, hydrophobic feature (HY), HBA-Lipid feature (HBAL) and an HBA feature. These features were also seemed helpful to the author for designing several glutamate-based HDAC8-MMP-2 dual inhibitor molecules [Halder et al. 2015].

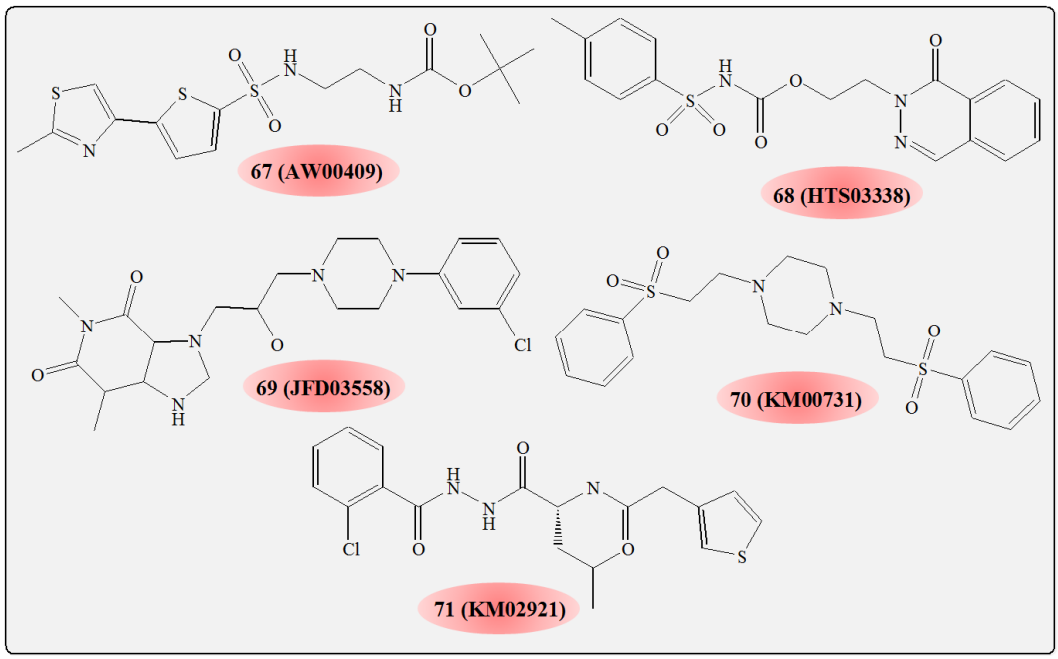

Figure 2.11. Compounds **67-71** screened as lead HDAC8 inhibitors.

Noor et al. [Noor et al. 2015] in 2015, conducted a 2D- regression-based and a 3D-pharmacophore based QSAR analysis on a group of 16 class I HDAC inhibitors possessing HDAC8 inhibitory potency. The reported 2D-QSAR model constructed using 5 molecular descriptors delivered an R^2 value of 0.980 including an standard error of 0.240 and also suggested that the increase in the polarizability of these compounds can reduce their potency. This study also identified and positively correlated different molecular features such as the topological polar surface area of these compounds (TPSA), lipophilicity (*logP*) with the HDAC8 inhibition of these molecules while negatively correlating the number of HBA groups with the activity. Aside from suggesting the significant features, authors also were able to screen 10 lead molecules (Compounds **72-81**) [***Figure 2.12***] as potent HDAC inhibitors.

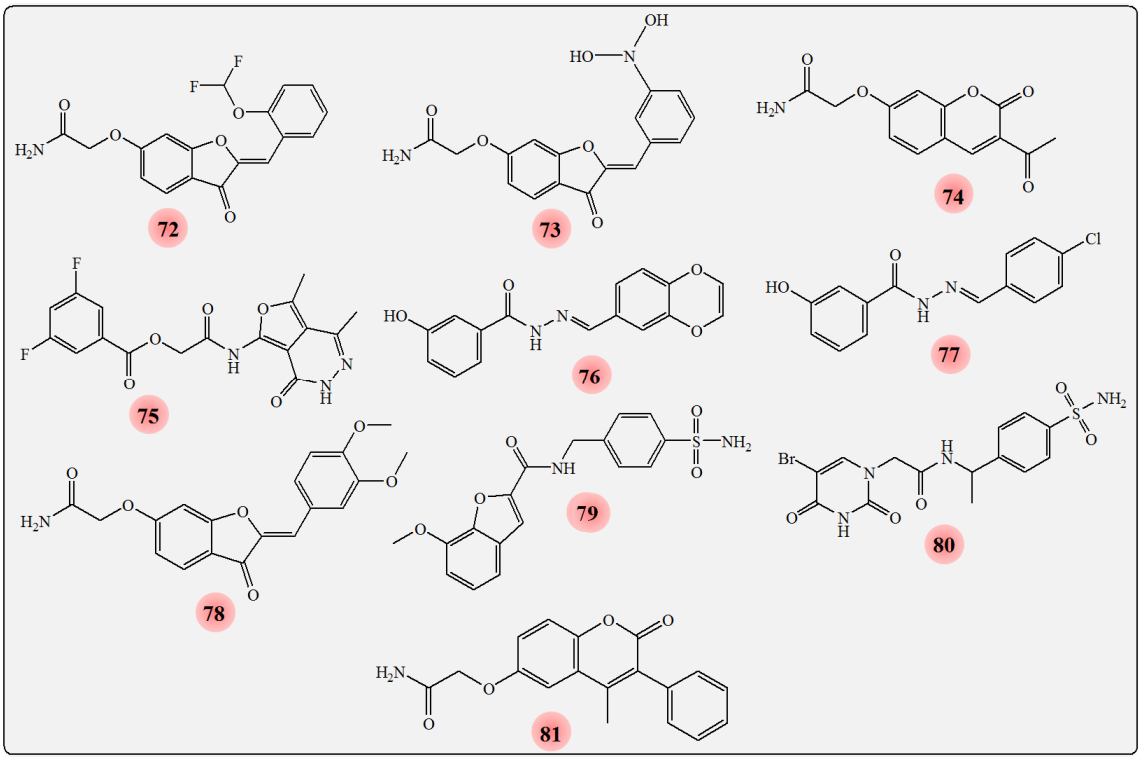

Figure 2.12. Compounds **72-81** screened as lead HDAC8 inhibitors

Cao and his co-workers in 2016, implemented a classification based 2D-QSAR technique and MD simulation study on a group of 80 HDAC8 inhibitors of diverse structure. The support vector machine (SVM) based classification study delivered a support vector component (SVC) shoed accuracy of 93.33% along with a false positive rate (FPR) and

true positive rate (TPR) of 13.33% and 100% respectively for the training set. The model also delivered a regression coefficient value of 74%. This QSAR study was able to identify several significant molecular properties of these compounds such as *TPSA, Span, H_Don, XlogP, Inertia Z* and *N_Atoms* which may have a significant influence on the HDAC8 inhibitory activity of these compounds Cao et al. 2016]. Through the screening of a total 59,652 molecules, the authors reported two lead compounds which might provide effectiveness as hit molecules against HDAC8 activity Cao et al. 2016].

A multi-QSAR study containing the Gaussian kernel based SVM study and multiple linear regression (MLR) study on a group of SAHA derivatives containing 1, 2, 4-oxadiazole moiety was performed by Praseetha et al. [Praseetha et al. 2016]. The4 MLR model constructed by the authors contained 5 different molecular descriptors delivered a cross-validated R^2 of R^2_{CV} = 0.905, the R^2 value of 0.945 whereas the SVM model also contained 5 molecular descriptors showed an R^2 value of 0.990 and a cross-validated R^2 of R^2_{CV} = 0.923. Interestingly, it was observed that both the MLR and the SVM model signified different 3D MoRSE descriptors namely *Mor09u* and *Mor32e* of these SAHA analogs as important factors for their HDAC8 inhibition where the MLR model positively correlated the *Mor32e* (electronegativity) of these molecules with their activity. Additionally, other molecular properties such as *JGI7*, *L3s* and $R53^+$ were negatively correlated with the HDAC8 inhibitory potency of these study suggesting their detrimental effect on the activity of these SAHA analogs [Praseetha et al. 2016].

A DFT (Density Function Theory) based 2D-QSAR study was performed on a group of N-hydroxyfurylamide derivated HDAC8 inhibitors by Tassine and Elhallaoui in 2016 [Tassine & Elhallaoui 2016]. Two different QSAR techniques such as an MLR and artificial neural networking (ANN) study was conducted by the authors in which the MLR model delivered a correlation coefficient of 0.800 along with a standard deviation value of 0.288. On the other hand, the outcomes of the ANN model showed a correlation coefficient value of 0.980. Five different descriptors were used to build the MLR model which indicated detrimental effects of the total energy of these compounds toward their potency whereas the hardness of these compounds was seemed to have a beneficial effect on their activity. Aside from that, this study also indicated the negative influence of the

melting point, greater electron affinity and lower ionization potential of these compounds for their HDAC8 inhibitory potency.

Since aryl-valproic acid is a very interesting and promising molecule for HDAC inhibition, Martinez-pacheco et al. [Martínez-Pacheco et al. 2017] conducted a QSAR study on a group of aryl valproic acid derivated compounds as HDAC8 inhibitors through a 2D-MLR and 2D- ANN based QSAR techniques. Authors developed the 2D-QSAR models on a set of 40 hydroxamic acid-based compounds, using them as the training set compounds while validating these models on a group of 500 aryl valproic acid derivated compounds containing a linker, a ZBG along with a hydrophobic tail in their structure. The authors also used a docking study of these compounds using Autodock 4.2 software and HDAC8 crystal structure with the purpose of screening these molecules. In order to develop the QSAR models 1194 molecular descriptors containing Dragon molecular descriptors, descriptors produced by docking study and quantum descriptors were used for this study. Also, through this study, the authors identified an aryl-valproate derivative Compound **82** (**DAVP042**) [***Figure 2.13*(C)**] was reported as a lead molecules. Biological evaluation of this compound (Compound **82**) showed very good activity in A549 and HCT-116 cell lines while delivering good/moderate antiproliferative activity in U937 and MCF-7 cell lines [Martínez-Pacheco et al. 2017].

A group of hydroxamate-based HDAC8 inhibitors was used by Manal et al. [Manal et al. 2017] to construct a 3D-QSAR pharmacophore analysis study. The pharmacophore model provided an R^2 value of 0.850 for the training set along with an internally cross-validated R^2 of 0.890 for the external validation set. The constructed model was built using different features namely ring aromatic (RA), hydrogen bond acceptor and donor (HBA and HBD) suggesting their significance in their activity. The model generated contours of the most and the least active compounds (Compound **83-84**) [***Figure 2.13* (A)**] suggested proximity of the HBD feature near the nitrogen atom of the hydroxamate function can favor HDAC8 inhibition for the most active compound. Also, the contours suggested the bulky hydrophobic group substitution proximal to the thiazole moiety (RA feature) might have a positive influence on the activity whereas the RA feature, near the methoxyphenyl group of the least active compound (Compound **84**) indicated negative

influence on the HDAC8 inhibitory activity [Manal et al. 2017]. Additionally, for the most active molecule of that series (Compound **83**), the thiazole group was indicated as the positive influencer of the activity because of its electron withdrawing property while depicting the carboxylate moiety as the negative influencer towards its activity for its electron-withdrawing the property.

Through this study, the author also reported two promising lead HDAC8 inhibitors namely, Compound **85** (DB08732) and Compound **86** (15602) [***Figure 2.13*** **(B)**] using the pharmacophore analysis. Moreover, similarity was observed on the basis of conducted DFT based study, Highest occupied molecular orbital (HOMO) and Lowest occupied molecular orbital (LOMO) analysis including the ADMET study of compounds **85-86**, with FDA approved HDAC inhibitor SAHA (**FDA-01**) which may justify the compounds **85-86** as promising lead molecules for HDAC inhibition including the HDAC8.

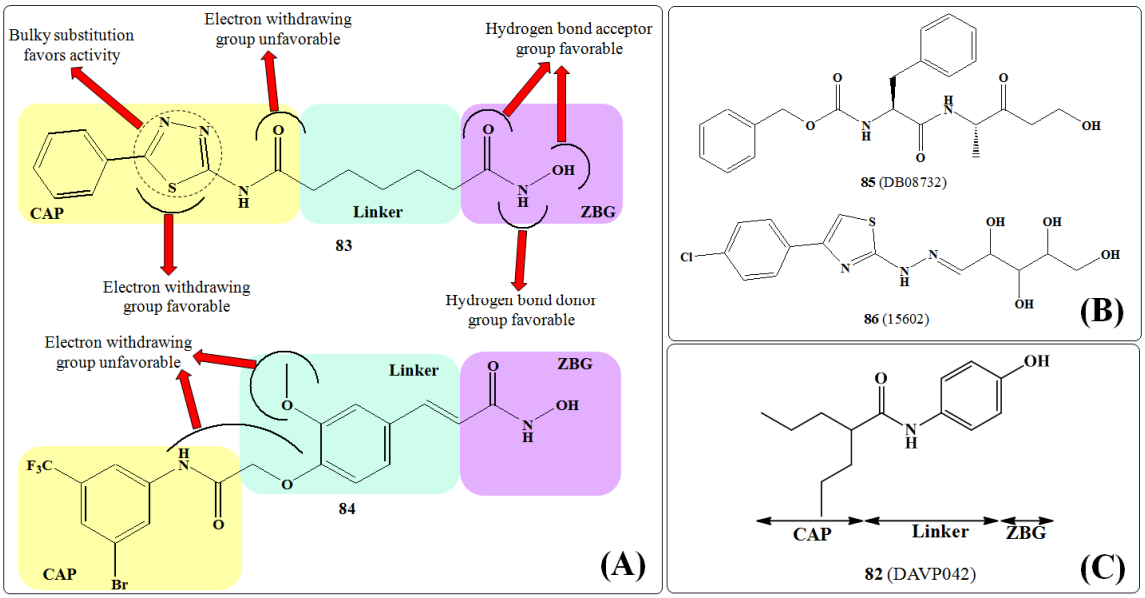

Figure 2.13. (A) Schematic representation of the 3D-QSAR study of the most active compound **83** and the least active compound **84** (B) Identified lead molecules (Compounds **85-86**) reported in the study. (C) Structure of valproic acid derivated compound **82** (DAVP042) identified as a lead molecule.

In the year 2018, Kim and his co-workers [Kim et al. 2018] used various combinations of pharmacophoric features on the 16 training set compounds possessing HDAC8 inhibitory

potency for development of pharmacophore based 3D-QSAR model. Authors used this study in order to screen promising lead molecules for HDAC8 inhibition form a diverse set of compounds. Among the constructed models, the pharmacophore model displayed best statistical results consisted with two RA features and an HBD features, along with the most active molecule (Compound **87**) in the series is given in ***Figure 2.14***.

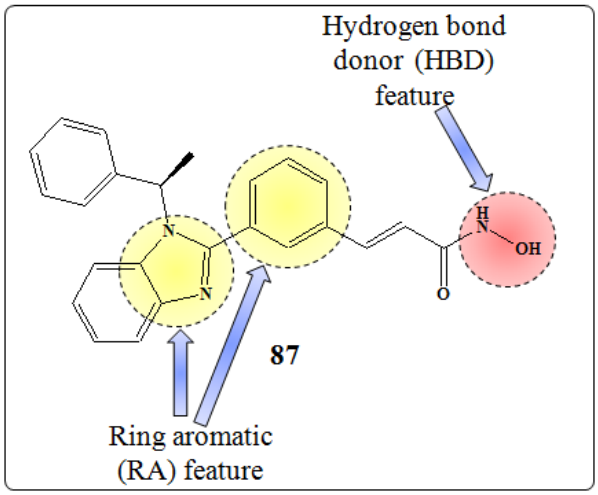

Figure 2.14. Compound **87** and its pharmacophore features generated from 3D-QSAR pharmacophore study.

Also, in a virtual screening process of screening potent HDAC8 inhibitors, authors screened 193 molecules by the ADMET study and the constructed pharmacophore model from 1,10,000 molecules, which eas again filtered using a docking study, procuring 11 molecules. In the final stage, through a HOMO-LOMO based analysis authors identified and reported three lead compounds such as Compound **88** (KM055296), Compound **89** (HTS10917) and Compound **90** (SPB02579) [***Figure 2.15***] as promising leads for HDAC8 inhibition [Kim et al. 2018].

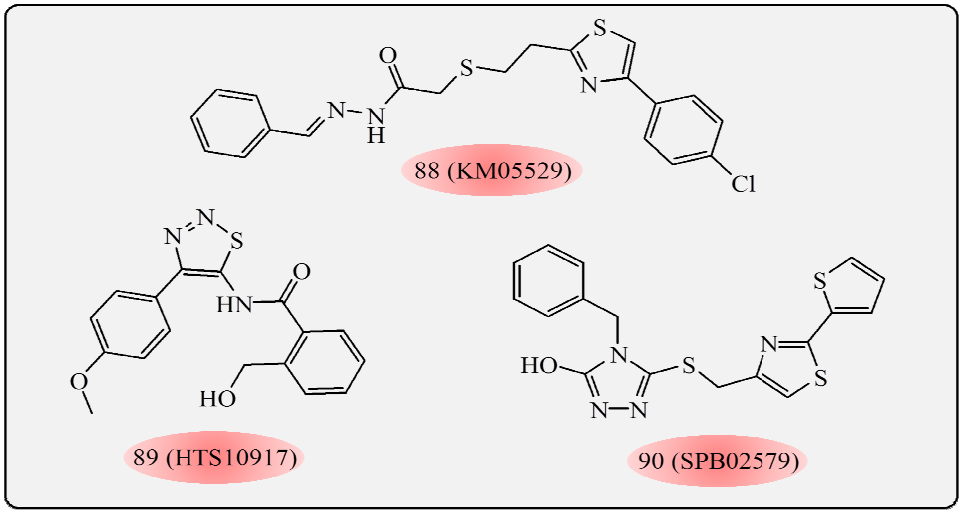

Figure 2.15. Compounds **88-90** screened as lead molecules for potent HDAC8 inhibition.

As because the Bayesian classification study is a very useful and widely used technique for identification of molecular fingerprints important for the biological, potency regulation of the compounds Amin et al. [Amin et al. 2018a] used a Bayesian classification based 2D-QSAR analysis on a group HDAC8 inhibitory compounds to procure and identify the molecular fragments of these compounds with positive and negative influence on the HDAC8 inhibition of these compounds. From a pool of 1,266 compounds, through the duplicate removal and using the Veber's and Lipinski's rule [Veber et al. 2002; Lipinski et al. 2001] authors procured 852 molecules which they used to conduct the Bayesian classification study. Authors divided the compounds into a training set containing 588 compounds and a test/external validation set containing 264 compounds along with different molecular properties and *ECFP_6* fingerprint descriptors as the independent property for construct the model [Amin et al. 2018a]. Through the observations of the results, the authors reported the favorability of either the carboxamide or the hydroxamate group as the ZBG to enhance the HDAC8 inhibition of the compounds rather than other groups like benzamide, etc. Additionally, larger, bulky and hydrophobic aromatic groups like phenyl imidazole or biphenyl moiety was suggested as better surface recognition group (cap moiety) can favor better interactions with HDAC8 and increase the potency of the compounds.

Chapter 3: *Rationale behind the work*

Chapter 3: *Rationale behind the work*

Through years of research on the HDAC8 isoform, similar to the other HDAC isoforms different contributions of the HDAC8 isoforms in different epigenetic abnormalities and pathophysiology has been observed. The abnormal expression and enzymatic activity of the HDAC8 enzyme are also observed in a diverse group of diseases, epigenetic disorders, and cancers **(*Figure 3.1*)**.

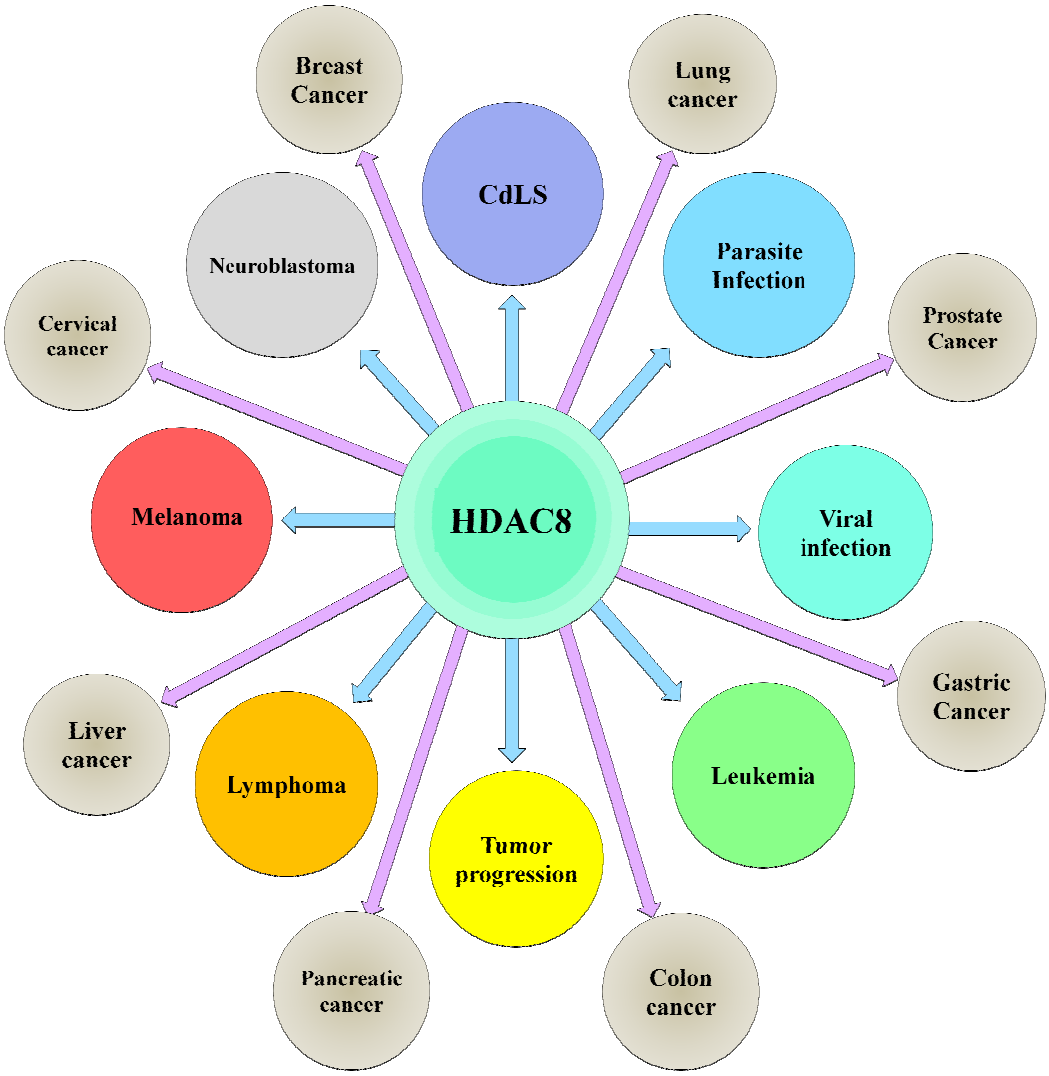

Figure 3.1. Contributions of HDAC8 in different pathophysiological conditions and diseases.

Though the expression of the HDAC8 isoform in the cancer cells and the normal healthy tissues are alike, the tendency of increase HDAC8 expression has been observed in the cancer cells [Nakagawa et al. 2007, Wu et al. 2013]. It is reported that

the SRY-box 4 (SOX 4/sex determining region Y), a transcription factor is responsible for the activation of HDAC8 promoter and causes HDAC expression in cancer cells [Schilham et al. 1996, Potzner et al. 2010, Bergsland et al. 2006, Higuchi et al. 2013]. The RNAi mediated HDAC 8 knockdown is also seemed to be beneficial for restraining the proliferation of different human cancers (colon, cervical and lung cancer) whereas the up-regulation of HDAC8 prevents cellular apoptosis and causes proliferation in hepatocellular cancer [Haberland et al. 2009, Gurard-Levin et al. 2009]. HDAC8 upregulation causes overexpression of HDAC1 and HDAC6 which promotes invasion in the invasive breast cancer cells. The overexpression of matrix metalloproteinase-9 (MMP-9) in MCF-7 breast cancer cell lines has been seen due to the over expression of HDAC8 [Park et al. 2011].

In associated with different co-repressors and inv (16) protein, HDAC8 is also responsible for the activation of acute myeloid leukaemia-I (AML-I) regulating genes which causes the abnormal haematopoetic cellular proliferation [Durst et al. 2003, Lutterbach, & Hiebert 2000]. Regulating the expression of Tap73 HDAC8 causes reduction of the tumor suppressor expressions and in myeloproliferative neoplasm, HDAC8 inhibition restrains Cytokine Signalling 1/3 mediated cellular proliferation and suppresses the activity of haematopoetic cell [Marek et al. 2013, Chen et al. 2013, Gao et al. 2013]. The regulation of Bcl-2 Modifying Factor (BMF) through HDAC8-STAT3 plays an important part in cellular proliferation and apoptosis whereas the BMF plays a significant role in methyl selenopyruvate-mediated cellular apoptosis [Nian et al. 2009, Adhikari et al. 2018]. Also, the decrease in the HDAC8 activity influences the cell proliferation of tumor cells with p53 mutation, suggesting the direct relationship of HDAC8 with the tumor adjuvants bearing p53 mutation [Chakrabarty et al. 2015]. HDAC8 also reported being an important factor for cancer sensitive genetic expression by aiding to mold platform, carrying cytokines to the nucleus and via acting on a specific DNA locus [Chakrabarty et al. 2015].

Besides all these, significant HDAC8 expression is noticed in cancers such as lung, colon, breast, pancreatic and gastric cancers, including acute myeloid leukaemia (AML), acute lymphocytic leukaemia (ALL) and childhood neuroblastoma [Adhikari et al. 2018, Nakagawa et al. 2007, Chen et al. 2013, Gao et al. 2013, Gao et al. 2009].

Chapter 3: *Rationale behind the work*

The HDAC8 up-regulation is found to be obstructing the cellular apoptosis and hence inducing hepatocellular proliferation and proliferation in gastric carcinoma cell line [Nakagawa et al. 2007]. In association with the HDAC8, the inv (16) fusion protein causes repression of AML-I regulated genetic transcription whereas, the HDAC8 knockdown represses HoxA5 which in terms causes a reduction of HoxA5 mediated expression of wild type mutant p53 and abnormal expression of HDAC8 increases transcription of p53 [Chakrabarty et al. 2015, Vannini et al. 2004, Whitehead et al. 2011].
Apart from the connection of HDAC8 with cancer and tumors, there also lie important relationships of HDAC8 with different viral and parasitic diseases. An important contribution of HDAC8 is noticed in schistosomiasis, a parasitic disease caused by a flatworm named *Schistosoma mansoni* [Chakravarty et al. 2016]. Several effects of the HDAC8 deacetylation activity are evidenced for influenza A and Uukuniemi virus infections, in which the studies depicted HDAC8 dependent penetration, acidification, and endocytosis of viruses like Uukuniemi and Influenza A [Yamauchi et al. 2011].
In the congenital malformations, the role of HDAC8 is also discovered as an important enzyme for SMC3 deacetylation related to the Cornelia de Lange Syndrome (CdLS) [Deardorff et al. 2012] whereas the HDAC8 expression is also correlated with the cranial neural crest cell formation in mice.

From all these studies the role of the enzymatic activity of the HDAC8 isoform is correlated with a large group of cancer and other pathophysiological disorders. After considering all these contributions of the HDAC8 in the human pathophysiology, the designing of HDAC8 selective inhibitors for effective HDAC8 inhibition is a major concern for the treatment of cancer and pathophysiological conditions which can be correlated with the activity of HDAC8.
Through different studies conducted on HDAC8 and its inhibitors it is observed that the three pharmacophoric features are necessary to design potent HDAC8 inhibitors namely a surface recognition cap group, should be hydrophobic in nature in order to interact inside the active site of the HDAC8; a ZBG, which is essential to interact

with the catalytic Zn^{2+} ion resides deep inside the tunnel-like pocket of the HDAC8 and a linker moiety is also necessary to provide an optimal distance between the cap and the ZBG to interact properly inside the HDAC8 active site whereas the compounds resembling a modified fish like structure can provide HDAC8 selectivity [Amin et al. 2017a].

Although the hydroxamate moiety has proven itself as the most effective ZBG for the HDAC8 inhibitors, aside from the ZBG there are several structural factors such as the moieties present in the cap and the linker region of the HDAC8 inhibitors affecting the activity of HDAC8 inhibitors. Hence, this study is conducted with the purpose of identification of the factors present in the cap and the linker moieties of the HDAC8 inhibitors influencing their potency against HDAC8 enzymatic activity.

Chapter 4: *Materials and Methods*

Chapter 4: *Materials and Methods*

4.1. Preliminary structural analysis of small dataset of tetrahydroisoquinoline derivatives In the recent observations of HDAC8 inhibitors, among the numerous scaffolds and compounds, the tetrahydroisoquinoline scaffold emerged as a potential tool for designing potent and selective HDAC8 inhibitors. The tetrahydroisoquinoline derivatives which were designed in the past few years as potent HDAC inhibitors have provides potent and selective HDAC8 inhibition in against of *in vitro* enzymatic activity of HDAC8 [Zhang et al. 2010, Zhang et al. 2011a, Zhang et al. 2011b, Taha et al. 2017]. Also, it is evidenced that the tetrahydroisoquinoline moiety is used as a tool to design potent inhibitors for other important metalloenzymes such as the MMPs [Matter et al. 2002]. This might indicate the significance of the tetrahydroisoquinoline moiety as an important tool to produce potent HDAC8 as well as other metalloproteinase inhibitors [Banerjee et al. 2019a].

Therefore, a preliminary study on the structural analysis on a group of tetrahydroisoquinoline derivated compounds with HDAC8 inhibitory potency has been performed via multi-QSAR study in order to analyze and identify the structural importance of these derivatives for HDAC8 inhibitory activity.

4.1.1. Preparation of Dataset

In this preliminary study, 81 hydroxamate group containing tetrahydroisoquinoline derivated compounds with HDAC8 inhibitory activity has been procured from the studies (***Table 4.1***) [Zhang et al. 2010, Zhang et al. 2011a, Zhang et al. 2011b, Taha et al. 2017] as the dataset in order to perform the multi-QSAR study **(*Figure 4.1*)**. The structures of the molecules used in this preliminary study along with their activity are given in ***Table 4.1***.

Prior to conduct the study, the compound structures were drew and saved into suitable format using the ChemDraw ultra 5.0 software (Cambridge Soft Corporation, U.S.A.) and the HDAC8 inhibitory activity [IC_{50} (μM)] of these compounds were converted into their logarithmic (pIC_{50}) values using the ***Equation 4.1*** [Amin et al. 2019] for the study.

$$pIC_{50} = -Log\ (IC_{50} * 10^{-6}) \qquad \textbf{Equation 4.1}$$

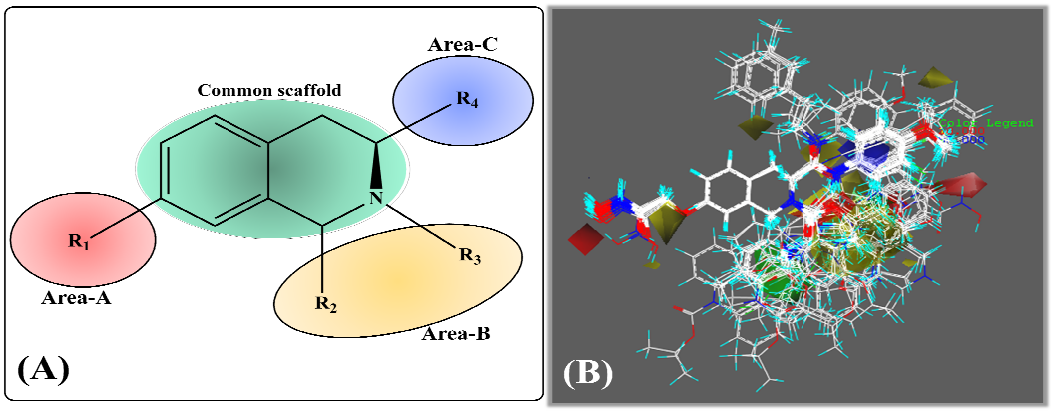

Figure 4.1. (A) Tetrahydroisoquinoline scaffold along with the substitution positions. (B) Molecular alignment of the tetrahydroisoquinoline derivatives on the tetrahydroisoquinoline scaffold.

In order to extract the molecular features of these compounds, the 2D molecular features in term of the molecular descriptors were calculated using "PaDEL-descriptor" software [Yap 2011] while a dataset pretreatment process was performed to eliminate the highly correlated molecular descriptors. Additionally, through a random division of compounds, the 81 molecules (**T-1** to **T-81**) [***Table 4.1***] are divided into the training and the test set. While keeping the most and the least active compounds into the training set a ratio of 3:1 of the compounds was maintained for the training set and the test set [Banerjee et al. 2019b].

Table 4.1. Compound table of tetrahydroisoquinoline derivatives used for the preliminary study

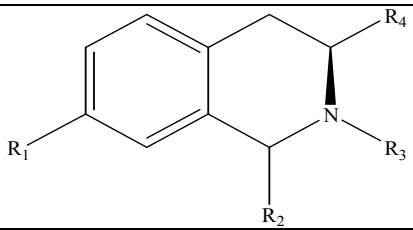

Cpd.	R1	R2	R3	R4	pIC50
T-1	$OCH_2CONHOH$	H	Boc	(*S*)-CONHPh	5.889
T-2	$OCH_2CONHOH$	H	H	(*S*)-CONHPh	5.086
T-3	$OCH_2CONHOH$	H	Boc	(*S*)-CONHBnz	5.467
T-4	$OCH_2CONHOH$	H	H	(*S*)-CONHBnz	5.292
T-5	$OCH_2CONHOH$	H	Boc	(*S*)-CONHPhenethyl	5.573
T-6	$OCH_2CONHOH$	H	H	(*S*)-CONHPhenethyl	5.390

T-7	$OCH_2CONHOH$	H	Boc	(*S*)-CONH4-OMePh	6.000
T-8	$OCH_2CONHOH$	H	H	(*S*)-CONH4-OMePh	5.254
T-9	$OCH_2CONHOH$	H	Boc	(*S*)- (*S*)-CONH*p*-Tolyl	5.783
T-10	$OCH_2CONHOH$	H	H	(*S*)-CONH*p*-Tolyl	5.418
T-11	$OCH_2CONHOH$	H	Boc	(*S*)-CONH(2-MePh)	5.398
T-12	$OCH_2CONHOH$	H	H	(*S*)-CONH(2-MePh)	5.384
T-13	$OCH_2CONHOH$	H	Boc	(*S*)-CONH(3-MePh)	5.752
T-14	$OCH_2CONHOH$	H	H	(*S*)-CONH(3-MePh)	5.441
T-15	$OCH_2CONHOH$	H	Boc	(*S*)-CONH(4-FPh)	5.592
T-16	$OCH_2CONHOH$	H	H	(*S*)-CONH(4-FPh)	5.491
T-17	$OCH_2CONHOH$	H	Boc	(*S*)-CONH(3-ClPh)	5.932
T-18	$OCH_2CONHOH$	H	H	(*S*)-CONH(3-ClPh)	5.495
T-19	$OCH_2CONHOH$	H	Boc	(*S*)-CONH(2,4-diMePh)	5.423
T-20	$OCH_2CONHOH$	H	H	(*S*)-CONH(2,4-diMePh)	5.470
T-21	$OCH_2CONHOH$	H	Boc	(*S*)-CONH(3-Cl,4-FPh)	5.810
T-22	$OCH_2CONHOH$	H	H	(*S*)-CONH(3-Cl,4-FPh)	5.476
T-23	$OCH_2CONHOH$	H	Boc	(*S*)-CONH(1-Naphthyl)	5.372
T-24	$OCH_2CONHOH$	H	H	(*S*)-CONH(1-Naphthyl)	5.975
T-25	$OCH_2CONHOH$	H	Boc	(*S*)-CONHBiphenyl	5.703
T-26	$OCH_2CONHOH$	H	H	(*S*)-CONHBiphenyl	5.656
T-27	$OCH_2CONHOH$	H	Boc	(*S*)-CONH*n*-Pentyl	5.520
T-28	$OCH_2CONHOH$	H	H	(*S*)-CONH*n*-Pentyl	5.451
T-29	$OCH_2CONHOH$	H	Boc	(*S*)-CONH*n*-Hexyl	5.355
T-30	$OCH_2CONHOH$	H	H	(*S*)-CONH*n*-Hexyl	5.239
T-31	$OCH_2CONHOH$	H	Boc	(*S*)-CONH*t*-Butyl	5.339
T-32	$OCH_2CONHOH$	H	H	(*S*)-CONH*t*-Butyl	4.915
T-33	$OCH_2CONHOH$	H	$COCH_2OPh$	(*S*)-CONHPhenethyl	6.237
T-34	$OCH_2CONHOH$	H	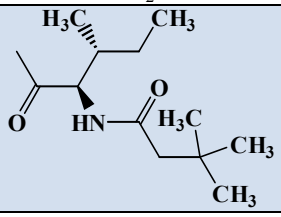	(*S*)-CONH(4-MePh)	7.284
T-35	$OCH_2CONHOH$	H	$CO(CH_2)_2Ph$	(*S*)-CONH(4-MePh)	6.299
T-36	$OCH_2CONHOH$	H	$CO(CH_2)_2Ph$	(*S*)-CONHPhenethyl	6.160
T-37	$OCH_2CONHOH$	H	$CO(CH_2)_2Ph$	(*S*)-Ph	6.120
T-38	$OCH_2CONHOH$	H	$COCH_2NHBoc$	(*S*)-CONH(4-MePh)	6.289
T-39	$OCH_2CONHOH$	H	$COCH_2NH_2$	(*S*)-CONH(4-MePh)	5.670
T-40	$OCH_2CONHOH$	H	(*S*)-COCH(Bnz)NHBoc	(*S*)-CONH(4-MePh)	6.987
T-41	$OCH_2CONHOH$	H	(*S*)-COCH(NH_2)Bnz	(*S*)-CONH(4-MePh)	6.434
T-42	$OCH_2CONHOH$	H	(*S*)-COCH(*p*-OH-nz)NHBoc	(*S*)-CONH(4-MePh)	6.757
T-43	$OCH_2CONHOH$	H	(*S*)-COCH(p-OH-Bnz)NH_2	(*S*)-CONH(4-MePh)	6.198

T-44	$OCH_2CONHOH$	H	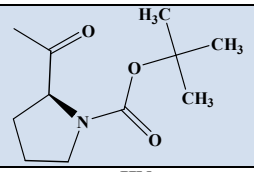	(*S*)-CONH(4-MePh)	6.674
T-45	$OCH_2CONHOH$	H	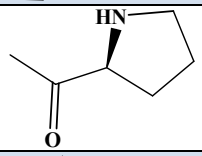	(*S*)-CONH(4-MePh)	6.318
T-46	$OCH_2CONHOH$	H	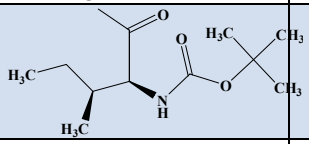	(*S*)-CONH(4-MePh)	6.857
T-47	$OCH_2CONHOH$	H	(*S*)-$COCH(NH_2)CH(Me)Et$	(*S*)-CONH(4-MePh)	5.983
T-48	$OCH_2CONHOH$	H	(*S*)-COCH(*i*-But)NHBoc	(*S*)-CONH(4-MePh)	6.788
T-49	$OCH_2CONHOH$	H	(*S*)-COCH(*i*-But)NH_2	(*S*)-CONH(4-MePh)	6.171
T-50	$OCH_2CONHOH$	H	(*S*)-COCH(Me)NHBoc	(*S*)-CONH(4-MePh)	6.740
T-51	$OCH_2CONHOH$	H	(*S*)-COCH(Me)NH_2	(*S*)-CONH(4-MePh)	5.893
T-52	$OCH_2CONHOH$	H	(*S*)-COCH(*i*-Pr)NHBoc	(*S*)-CONH(4-MePh)	6.983
T-53	$OCH_2CONHOH$	H	(*S*)-COCH(*i*-Pr)NH_2	(*S*)-CONH(4-MePh)	5.991
T-54	$OCH_2CONHOH$	H	COBnz	(*S*)-CONH(4-MePh)	6.851
T-55	$OCH_2CONHOH$	H	Phenethyl	(*S*)-CONH(4-MePh)	5.991
T-56	$OCH_2CONHOH$	H	COPh	(*S*)-CONH(4-MePh)	6.785
T-57	$OCH_2CONHOH$	H	Bnz	(*S*)-CONH(4-MePh)	5.717
T-58	$OCH_2CONHOH$	H	$CO(CH_2)_3Ph$	(*S*)-CONH(4-MePh)	6.943
T-59	$OCH_2CONHOH$	H	$(CH_2)_3Ph$	(*S*)-CONH(4-MePh)	5.764
T-60	H	H	$(CH_2)_6CONHOH$	H	5.721
T-61	H	H	$(CH_2)_2CONHOH$	H	4.721
T-62	H	(*S*)-Ph	$(CH_2)_4CONHOH$	H	7.357
T-63	H	(*S*)-Ph	$(CH_2)_2CONHOH$	H	6.022
T-64	H	(*S*)-Ph	$(CH_2)_1CONHOH$	H	4.721
T-65	H	(*S*)-3-MePh	$(CH_2)_2CONHOH$	H	6.959
T-66	H	(*S*)-4-MePh	$(CH_2)_2CONHOH$	H	7.086
T-67	H	(*S*)-4-OEtPh	$(CH_2)_2CONHOH$	H	6.678
T-68	H	(*S*)-3-CF_3Ph	$(CH_2)_2CONHOH$	H	6.469
T-69	H	(*S*)-4-CF_3Ph	$(CH_2)_2CONHOH$	H	6.721
T-70	H	(*S*)-*c*-Hex	$(CH_2)_2CONHOH$	H	5.174
T-71	H	(*S*)-4-(*t*-butyl)Ph	$(CH_2)_2CONHOH$	H	6.319
T-72	H	(*S*)-2-aphthyl	$(CH_2)_2CONHOH$	H	6.409
T-73	H	(*S*)-Biphenyl	$(CH_2)_2CONHOH$	H	7.260
T-74	$OCH_2CONHOH$	H	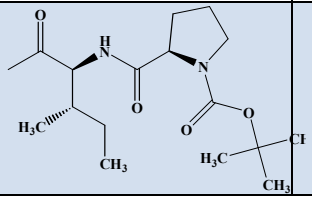	(*S*)-CONH(4-MePh)	6.717

T-75	$OCH_2CONHOH$	H	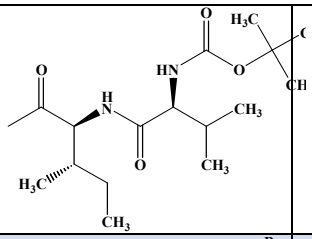	(*S*)-CONH(4-MePh)	6.697
T-76	$OCH_2CONHOH$	H	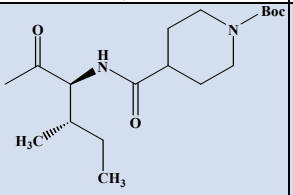	(*S*)-CONH(4-MePh)	6.833
T-77	$OCH_2CONHOH$	H	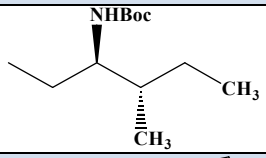	(*S*)-CONH(4-MePh)	6.580
T-78	$OCH_2CONHOH$	H	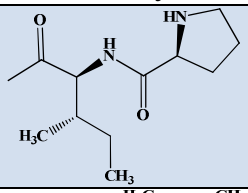	(*S*)-CONH(4-MePh)	7.328
T-79	$OCH_2CONHOH$	H	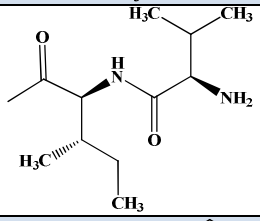	(*S*)-CONH(4-MePh)	7.167
T-80	$OCH_2CONHOH$	H	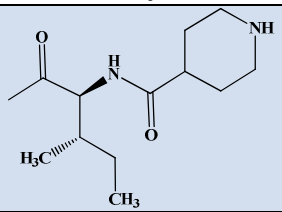	(*S*)-CONH(4-MePh)	5.842
T-81	$OCH_2CONHOH$	H	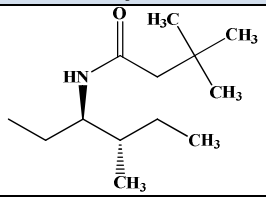	(*S*)-CONH(4-MePh)	6.478

4.1.2. 2D QSAR study

4.1.2.1. Multiple Linear Regression (MLR) Study

Multiple linear regression (MLR) is a the fundamental, simple and frequently applied 2D QSAR technique used to form a linear regression between the biological activity and the molecular features (molecular descriptors) of the compounds while considering the

biological activity of the compounds as the function of their molecular descriptors [Amin et al. 2017c, Mandi et al. 2012].

In this study, by employing the stepwise-MLR (SMLR) method an MLR based 2D-QSAR model is constructed with 8 molecular descriptors as the independent variable and the dependent variable on the training set and was externally validated on the test set. In order to validate the reliability of the constructed model, different statistical parameters namely correlation coefficient (R), leave one out R^2 (Q^2), squared correlation coefficient (R^2), adjusted correlation coefficient (R^2_{adj}), standard error of estimate (SEE) etc. were calculated and analyzed [Amin et al. 2017c, Banerjee et al. 2019b].

$$R^2 = 1 - \frac{\sum(Y_{obs} - Y_{calc})^2}{\sum(Y_{obs} - \bar{Y}_{obs})^2} \qquad \textbf{Equation 4.2}$$

The ***Equation 4.2*** reveals about the squared correlation coefficient (R^2) calculated using the observed biological activity (Y_{obs}) of the molecules and the 2D QSAR model predicted biological activity by the (Y_{calc}) including the mean value of the observed biological activity of these compounds. The ***Equation 4.3*** containing a number of compounds present in the training set (N), number of descriptors in the constructed MLR model (P) and the R^2 is used to calculate the adjusted squared correlation coefficient (R^2_{adj}) for the training set. In this case, the value of N and P are 61 and 8 respectively suggesting the number of compound in the training set and the 8 descriptors used to construct the MLR model.

$$R^2_{adj} = \frac{\{(N-1)*R^2\}-P}{N-P-1} \qquad \textbf{Equation 4.3}$$

The standard error of the model is calculated using ***Equation 4.4*** which was used to calculate the standard error of estimate (SEE) of the model.

$$SEE = \sqrt{\frac{\sum(Y_{obs} - Y_{calc})^2}{N-P-1}} \qquad \textbf{Equation 4.4}$$

Internal cross-validation for this model was also performed in the form of the Leave-One-Out cross-validation Q^2 calculated using the equation. Besides that, the MLR model was also externally validated using ***Equation 4.5***. In ***Equation 4.5***, the Y_{pred} and Y_{obs} indicate

the model predicted and observed the biological activity of the test set compounds respectively.

$$R^2{}_{pred} = 1 - \frac{\sum(Y_{obs} - Y_{pred})^2}{\sum(Y_{obs} - \bar{Y}_{obs})^2} \qquad \textbf{Equation 4.5}$$

Additionally, the r_m^2 metrics for the training set and the test set has been calculated to examine the closeness of the observed and model predicted values for the compounds of the training and the test set. The equation for the calculation of r_m^2 value of the test set is provided in ***Equation 4.6*** in which the r^2 and r_0^2 of signified the squared correlation values between the observed or experimented activity values and the predicted activity values for the test set molecules.

$$r_m{}^2{}_{(test)} = r^2 * (1 - \sqrt{r^2 - r_0{}^2}) \qquad \textbf{Equation 4.6}$$

The Y randomization test (cR_p^2) is calculated using ***Equation 4.7*** and R_r^2 where t R_r^2 denotes the R^2 of the randomized model for the training set molecules.

$$cR_p{}^2 = R * (\sqrt{R^2 - R_r{}^2}) \qquad \textbf{Equation 4.7}$$

4.1.2.2. Classification based 2D QSAR study

The Bayesian classification study is a classification based QSAR study established on the Bayes theorem and is an effective technique for the identification of the important molecular sub-structures having a notable correlation with the biological activity of the compounds [Amin et al. 2018a].

The Bayesian classification based study of these tetrahydroisoquinoline derivatives was conducted using the Discovery studio 3.0 software [Accelrys Software Inc., San Diego, California, USA]. A variety of structural and physicochemical descriptors of these compounds with extended-connectivity fingerprints descriptors (*ECFPs*) [David & Mathew 2010, Liu et al. 2014] were employed to construct the model. For this study, the compounds having the observed biological activity less than the pIC_{50} value of 6.055 were marked as "0" and considered as inactive molecules whereas the compounds with pIC_{50} equal to 6.055 or more were marked as "1" and denoted as active molecules. Besides the statistical outcomes, this study was able to provide 40 molecular fingerprints

with significant correlation with the biological activity of these tetrahydroisoquinoline derivatives.

4.1.3. 3D QSAR Study

4.1.3.1. Molecular alignment

As Molecular alignment of the compounds is an important task to perform before performing a 3D QSAR study, a molecular alignment process was performed for these tetrahydroisoquinoline derivatives using the SYBYL-X 2.0 software [Certara USA, Inc., USA]. Prior the alignment, these compounds were individually charged by Gasteiger-Marsili algorithm [Gasteiger & Marsili 1980] and the energy of the compounds was minimized by the "*Distill-rigid*" alignment feature of the SYBYL-X 2.0 software [Vyas et al. 2017] molecular component common to the structures of these tetrahydroisoquinoline derivatives. The molecular alignment for these tetrahydroisoquinoline derivatives on their common tetrahydroisoquinoline scaffold is shown in ***Figure 4.1***.

4.1.3.1. Comparative Molecular Field Analysis (CoMFA) study

The Comparative Molecular Field Analysis (CoMFA) is one of the frequently applied 3D-QSAR technique generally used to understand the effects of different properties such as the molecular steric and electrostatic fields on the biological activity of the molecules (Zhao et al. 2011). For these tetrahydroisoquinoline derivatives, a CoMFA study was used to analyze the influences of the electrostatic and steric fields of these molecules on their biological activity. To validate the model a statistical analysis of the statistical parameters of the CoMFA model was also performed on the constructed CoMFA Model [Banerjee et al. 2019b].

4.1.4. Hologram based QSAR (H-QSAR) study

For any drug substances, the study of the importance of the molecular fragments for their biological activity is not only important but an undeniable fact also. Hence, the identification of the molecular fragments with good or bad influence of the compounds is a beneficial factor for design newer molecules and for the improvement of their selectivity and biological activity. A hologram based QSAR study was conducted for the

better understanding of the correlations of the sub-molecular fragments with their HDAC8 inhibitory potency of these tetrahydroisoquinoline derivated HDAC8 inhibitors in the preliminary studies [Amin et al. 2017c, Gaikwad et al., 2017, Banerjee et al. 2019b]. The HQSAR analysis is performed via a partial least square (PLS) analysis, conducted using multiple combinations of molecular parameters namely atomic connections (C), chirality (Ch), atomic number (A), hydrogen (H), bond type (B), and electron donor-acceptor groups (DA) present in these tetrahydroisoquinoline based HDAC8 inhibitors in the SYBYL-X 2.0 [Yu et al., 2015]. As usually, the validated and cross-validated statistical parameters like cross-validated R^2, R^2_{cv}, standard error (*SE*) and R^2_{pred} for the test set were also calculated for the constructed H-QSAR model [Banerjee et al. 2019b].

4.2. Structural analysis of hydroxamate containing HDAC8 inhibitors

From the various studies conducted on the HDAC8 inhibitors, it is well known that any HDAC8 inhibitor has to contain three specific pharmacophoric features namely a hydrophobic cap group, a zinc-binding motif for coordination with the catalytic Zn^{2+} of the HDAC8 and a cap-ZBG connecting linker motif in its structure to bind inside the HDAC8 pocket to provide effective inhibition against the HDAC enzymatic activity. The recent studies clarified that that, the hydroxamate group, in comparison with the other Zn^{2+} binding groups such as the benzamide group, carboxamide group, etc. is more effective for the coordination with the catalytic zinc of the HDAC8. Hence, in this current study, a structural analysis is performed to identify important structural features suitable for cap and linker moiety to provide better HDAC8 inhibition.

4.2.1. Preparation of Dataset

For this study, a pool of 1,324 small molecules belongs to the class of HDAC8 inhibitors with a broad range of HDAC8 inhibitory activity in nanomolar concentration was retrieved from Binding database [https://www.bindingdb.org/bind/index.jsp (Accessed on 28 January 2019)]. In the first dataset processing, initially, 178 duplicate compounds were deleted. Then, the rest of the 1146 compounds were filtered again using the Lipinski and Veber's rule [Veber et al. 2002, Lipinski et al. 2001]. From this process, only the 870 compounds following the Lipinski and Veber's rule are taken for the next step. In the

next step, among the 870 HDAC8 inhibitors, the 600 compounds containing a hydroxamate group [-CONHOH] in their structures are taken for another duplicate removal process which finally yielded a dataset of 593 HDAC8 inhibitors covering a wide range of HDAC8 inhibitory study is taken for the study (***Table 4.2***).

Moreover, the in order to construct the classification based QSAR studies like the Bayesian classification study and the Recursive Partitioning (RP) study, the HDAC8 inhibitory potency (IC_{50}) values of these molecules are converted into binary form. The average biological activity of this hydroxamate-based dataset was calculated used as the threshold value. The compounds of this dataset possessing an HDAC8 inhibitory activity superior to the threshold are marked as '1' (active molecules) and the compounds possessing HDAC8 inhibitory activity equals to or inferior to the threshold are marked as '0' (inactive molecules).

Table 4.2. Smile format of the Hydroxamate based compounds used to conduct the study.

Cpd.	*SMILES*	*Cl.*
H-1	c1cc(ccc1C(=O)/C(=C/[C@@H](C)/C=C/C(=O)NO)/C)N(C)C	1
H-2	c1ccc(cc1)/C=C/c1scc(n1)CCCC(=O)NO	1
H-3	ONC(=O)/C=C/C(=C/[C@H](C(=O)c1ccc(N(C)C)cc1)C)/C	1
H-4	c1cc(ccc1/C=C/C(=O)NO)CN(CCO)CCc1c[nH]c2c1cccc2	1
H-5	O=C(NO)/C=C/c1ccc(CNCCc2c3c([nH]c2C)cccc3)cc1	1
H-6	c1(c(cc2c(c1)c(ncn2)Nc1c(cc(cc1)Cl)Cl)OC)OCCCCCC(=O)NO	1
H-7	c1ccccc1NC(=O)CCCCCCC(=O)NO	1
H-8	[C@@H]1(CNC(=O)c2cc3C(CC(=O)Nc3cc2)(C)C)CC[C@H](CC1)/C=C/C(=O)NO	1
H-9	c1c(cc2c(c1)ccn2Cc1ccc(cc1)OC)C(=O)NO	1
H-10	n1(c(c(nc1c1cccc(c1)/C=C/C(=O)NO)Cc1ccccc1)C)CCc1ccccc1	1
H-11	c1ccccc1[C@@H](n1c2ccccc2nc1c1cccc(c1)/C=C/C(=O)NO)C	1
H-12	n1(c(c(nc1c1cccc(c1)/C=C/C(=O)NO)C)Cc1ccccc1)CCc1ccccc1	1
H-13	c1ccccc1[C@H](n1c2ccccc2nc1c1cccc(c1)/C=C/C(=O)NO)C	1
H-14	n1(c(c(nc1c1cccc(c1)/C=C/C(=O)NO)c1ccccc1)C)CCc1ccccc1	1
H-15	O=S(=O)(c1c(ccc(c1)C(=O)NO)OC)Nc1ccc(cc1)C	1
H-16	[C@@H]1(CNC(=O)c2cc3C(CC(=O)Nc3cc2)(C)C)CC[C@@H](CC1)/C=C/C(=O)NO	1
H-17	c1c(cc(cc1)C(=O)N/N=C/c1cccc(c1)CN1C[C@H](OC(=O)CCC=CCCC1=O)c1ccccc1)C(=O)NO	1
H-18	[C@@H]1(CNC(=O)c2cc3C(CC(=O)Nc3cc2)(C)C)CC[C@@H](CC1)CCC(=O)NO	1
H-19	c1(c(cc(cc1)C(=O)NO)OCc1ccccc1)OC	1
H-20	c1(ccccc1)CCn1c2ccccc2nc1c1cccc(c1)/C=C/C(=O)NO	1
H-21	c1ccccc1CCCn1c2ccccc2nc1c1cccc(c1)/C=C/C(=O)NO	1
H-22	n1(c(c(nc1c1cccc(c1)/C=C/C(=O)NO)C)c1ccccc1)CCc1ccccc1	1

H-23	c1(c(cc(cc1)C(=O)NO)NC(=O)c1ccc(cc1)c1ccccc1)OC	1
H-24	c1cc2c(cc1S(=O)(=O)N1CCN(CC1)c1ncc(cn1)C(=O)NO)cccc2	1
H-25	[C@@H]1(CNC(=O)c2cc3C(CC(=O)Nc3cc2)(C)C)CC[C@H](CC1)CCC(=O)NO	1
H-26	c1(c(cc(cc1)C(=O)NO)NC(=O)c1ccccc1)OC(C)C	1
H-27	c1c(cc(cc1)C(=O)N/N=C/c1ccc(cc1)OCC#C)C(=O)NO	1
H-28	[C@H](N1CCN(CC1)c1ncc(cn1)C(=O)NO)(/C=C/c1ccc(cc1)F)CO	1
H-29	c1(c(cc(cc1)C(=O)NO)NC(=O)c1ccc2c(n1)cccc2)C	1
H-30	c1(ccc2c(c1)CN(CC2)Cc1ccc(o1)c1cccc(c1)[N+](=O)[O-])C(=O)NO	1
H-31	n1(c(c(nc1c1cccc(c1)/C=C/C(=O)NO)C)C)CCc1ccccc1	1
H-32	C1[C@@H](CCCN1C(C)C)n1c(c(nc1c1cccc(c1)/C=C/C(=O)NO)c1ccccc1)C	1
H-33	C1[C@@H](CCCN1CC)n1c(c(nc1c1cccc(c1)/C=C/C(=O)NO)c1ccccc1)C	1
H-34	c1ccc2c(c1)cc([nH]2)C(=O)c1cc(ccc1)/C=C/C(=O)NO	1
H-35	C(=O)(CCCCCCC(=O)Nc1cc2C(CC(=O)Nc2cc1)(C)C)NO	1
H-36	C(C(=O)Nc1scc(n1)c1ccc(s1)CC(=O)NO)Oc1ccccc1	1
H-37	c1ccc2c(c1)nc(n2C(C)C)c1cccc(c1)/C=C/C(=O)NO	1
H-38	n1([C@@H]2CCCN(C2)C(C)C)c(c(nc1c1cccc(c1)/C=C/C(=O)NO)C)c1ccccc1	1
H-39	c1ccccc1Cn1c2ccccc2nc1c1cccc(c1)/C=C/C(=O)NO	1
H-40	c1ccc(cc1)CC(=O)Nc1scc(n1)c1ccc(s1)CC(=O)NO	1
H-41	C(=O)(CCCCCCC(=O)Nc1cc2ccc(=O)[nH]c2cc1)NO	1
H-42	C(=C\C(=O)NO)/c1ccc(CNC(=O)c2cc3C(CC(=O)Nc3cc2)(C)C)cc1	1
H-43	c1ccc2c(c1)nc(n2C1CCCCC1)c1cccc(c1)/C=C/C(=O)NO	1
H-44	c1(ccccc1)n1c2ccccc2nc1c1cccc(c1)/C=C/C(=O)NO	1
H-45	c1(ccc(cc1)Cl)n1c2ccccc2nc1c1cccc(c1)/C=C/C(=O)NO	1
H-46	n1(c(c(nc1c1cccc(c1)/C=C/C(=O)NO)Cc1ccccc1)C)[C@@H]1CCCN(C1)CC	1
H-47	C1[C@@H](CCCN1C)n1c(c(nc1c1cccc(c1)/C=C/C(=O)NO)c1ccccc1)C	1
H-48	n1([C@@H]2CCCN(C2)CC)c(c(nc1c1cccc(c1)/C=C/C(=O)NO)C)c1ccccc1	1
H-49	n1(c(c(nc1c1cccc(c1)/C=C/C(=O)NO)Cc1ccccc1)C)CCN1CCOCC1	1
H-50	n1(c(nc(c1c1cccc(c1)/C=C/C(=O)NO)C)c1ccccc1)CCc1ccccc1	1
H-51	c1cc(cc(c1)NC(=O)[C@H](CCCCCC(=O)NO)NC(=O)[C@@H]1NC(=O)CC1)C	1
H-52	c1c(cc(cc1)C(=O)N/N=C/c1ccccc1)C(=O)NO	1
H-53	C(=O)(CCCCCCNC(=O)c1cc2CCC(=O)Nc2cc1)NO	1
H-54	CN(C)c1ccc(C(=O)N(C)/N=C(\C)/c2ccc(C(=O)NO)cc2)cc1	1
H-55	C(=O)(CCCCCCNC(=O)c1cc2C(CC(=O)Nc2cc1)(C)C)NO	1
H-56	C(=O)(CCCCCCNC(=O)c1cc2C(CC(=O)N(c2cc1)C)(C)C)NO	1
H-57	c1ccc2c(c1)nc([nH]2)c1cccc(c1)/C=C/C(=O)NO	1
H-58	c1ccc2c(c1)nc(n2CCN(CC)CC)c1cccc(c1)/C=C/C(=O)NO	1
H-59	n1(c(c(nc1c1cccc(c1)/C=C/C(=O)NO)C)Cc1ccccc1)CCN1CCOCC1	1
H-60	c1(ccc(cc1)OC)n1c2ccccc2nc1c1cccc(c1)/C=C/C(=O)NO	1
H-61	c1(ccccc1)Cc1n(c(c(n1)C)c1cccc(c1)/C=C/C(=O)NO)CCc1ccccc1	1
H-62	c1ccc2c(c1)nc(n2CCN1CCCC1)c1cccc(c1)/C=C/C(=O)NO	1
H-63	c1c(c([nH]c1c1ccc(cc1)O)C(=O)NCc1ccc(cc1)C(=O)NO)c1ccsc1	1

H-64	c1c(cccc1c1cn(nn1)CSc1ccccc1)C(=O)NO	1
H-65	c1(ccc(cc1)/C=C/C(=O)NO)c1ccc(cc1)OC	1
H-66	c1c(cc(cc1)C(=O)NO)N(C)C	1
H-67	c1c(ccc(c1)/C=C/C(=O)NO)/C=N/OCc1ccc(cc1)[N+](=O)[O-]	1
H-68	C(=O)(CCCCCCNC(=O)c1cc2ccc(=O)n(c2cc1)C)NO	1
H-69	C(=O)(CCCCCCNC(=O)c1cc2ccc(=O)[nH]c2cc1)NO	1
H-70	[nH]1c(c(cc1c1ccc(cc1)O)c1cocc1)C(=O)NCc1ccc(cc1)C(=O)NO	1
H-71	c1c(ccc(c1)N[C@@]1(CCN(C1=O)c1cc2c(cc1)nccc2)C)C(=O)NO	1
H-72	C(CCCCCC(=O)NO)C(=O)Nc1cnn(c1)Cc1ccccc1	1
H-73	c1(c(cc(cc1)C(=O)NO)NC(=O)c1ccc(cc1)OC)OC	1
H-74	n1(c(c(nc1c1cccc(c1)/C=C/C(=O)NO)c1ccccc1)C)CCN1CCOCC1	1
H-75	c1ccc2c(c1)cc(o2)C(=O)c1cc(ccc1)/C=C/C(=O)NO	1
H-76	n1(c(c(nc1c1cccc(c1)/C=C/C(=O)NO)Cc1ccccc1)C)[C@@H]1CCCN(C1)C	1
H-77	n1(c(c(nc1c1cccc(c1)/C=C/C(=O)NO)C)c1ccccc1)CCN1CCOCC1	1
H-78	c1(ccc2c(c1)C[C@@H](CC2)Nc1nccc(n1)c1ccccnc1)C(=O)NO	1
H-79	C(=O)(CCCCCCNC(=O)c1cc2ccc(nc2cc1)OC)NO	1
H-80	C(=O)(c1c(cccc1)OC)N[C@H](COc1cc(ccc1)/C=C/C(=O)NO)Cc1c[nH]c2c1cccc2	1
H-81	C(=O)(N[C@@H](Cc1ccc(cc1)OCC(=O)NO)C(=O)Nc1ccc(cc1)OC)c1ccccc1	1
H-82	c1(c(cc(cc1)C(=O)NO)NC(=O)c1ccccc1)OC	1
H-83	c1(cc2cc(c1)CCCO[C@@H](C(=O)Nc1c(OC2)cccc1)CCCCCC(=O)NO)OC	1
H-84	c1cccc(c1)NC(=O)[C@H](CCCCCC(=O)NO)NC(=O)[C@H]1NC(=O)CC1	1
H-85	C(=O)(CCCCCCC(=O)Nc1cc2CCC(=O)Nc2cc1)NO	1
H-86	n1([C@@H]2CCCN(C2)C)c(c(nc1c1cccc(c1)/C=C/C(=O)NO)C)c1ccccc1	1
H-87	n1(c(nc(c1c1cccc(c1)/C=C/C(=O)NO)C)C)CCc1ccccc1	1
H-88	c1ccc2c(c1)nc(n2CCN1CCCCC1)c1cccc(c1)/C=C/C(=O)NO	1
H-89	c1ccc2c(c1)nc(n2C)c1cccc(c1)/C=C/C(=O)NO	1
H-90	c1(ccccc1)Cc1n(c(c(n1)C)c1cccc(c1)/C=C/C(=O)NO)[C@@H]1CCCN(C1)CC	1
H-91	n1(c(c(nc1c1cccc(c1)/C=C/C(=O)NO)C)C)[C@@H]1CCCN(C1)CC	1
H-92	c1c(cccc1c1cn(nn1)CCc1cscc1)C(=O)NO	1
H-93	c1(c(cc(cc1)C(=O)NO)NC1CCCCC1)C	1
H-94	CN(C)c1ccc(C(=O)N/N=C(\C)/c2ccc(C(=O)NO)cc2)cc1	1
H-95	c1(cccc(c1)CN1C[C@@H](OC(=O)CCC=CCCC1=O)c1ccccc1)/C=N/NC(=O)c1cccc(c1)C(=O)NO	1
H-96	c1c(ccc(c1)N[C@@H]1CCN(C1=O)c1ccc(cc1)C(F)(F)F)C(=O)NO	1
H-97	c1c(cc2c(c1)C[C@H](N(C(=O)CCCc1ccccc1)C2)C(=O)Nc1ccc(cc1)OC)OCC(=O)NO	1
H-98	c1(cc2cc(c1)/C=C\CO[C@@H](C(=O)Nc1c(OC2)cccc1)CCCCCC(=O)NO)OC	1
H-99	c1cc(cc2c1n(c(n2)C[C@H](c1ccccc1)C)CCCO)/C=C/C(=O)NO	1
H-100	c1(c(cc(cc1)C(=O)NO)NC(=O)c1ccccc1)Cl	1
H-101	O=S(=O)(c1ccc(N2CC[C@@H](Nc3ccc(cc3)C(=O)NO)C2=O)cc1)C	1
H-102	c1c(ccc(c1)N[C@H]1CCN(C1=O)c1ccc(cc1)Cl)C(=O)NO	1
H-103	n1(c2ccccc2nc1c1cccc(c1)/C=C/C(=O)NO)[C@@H]1CCCN(C1)CC	1

H-104	n1(c2ccccc2nc1c1cccc(c1)/C=C/C(=O)NO)[C@@H]1CCCNC1	1
H-105	n1(c2ccccc2nc1c1cccc(c1)/C=C/C(=O)NO)[C@H]1CCCNC1	1
H-106	n1(c2ccccc2nc1c1cccc(c1)/C=C/C(=O)NO)[C@H]1CCCN(C1)CC	1
H-107	[nH]1c(c(cc1c1cocc1)c1ccc(cc1)F)C(=O)NCc1ccc(cc1)C(=O)NO	1
H-108	c1(cc(on1)CN1CCOCC1)c1ccc(cc1)/C=C/C(=O)NO	1
H-109	CN(C)c1ccc(C(=O)N(C)/N=C/c2ccc(C(=O)NO)cc2)cc1	1
H-110	O=S(=O)(c1cc(/C=C/C(=O)NO)ccc1)c1nc2c(cc1)cccc2	1
H-111	c1(cc2cc(c1)CCCO[C@H](C(=O)Nc1c(OC2)cccc1)CCCCCC(=O)NO)OC	1
H-112	c1cccc(c1)NC(=O)[C@H](CCCCCC(=O)NO)NC(=O)[C@H]1NC(=O)C1	1
H-113	c1ccc2c(c1)cc([nH]2)CCN(Cc1ccc(cc1)/C=C/C(=O)NO)CCO	1
H-114	c1c(cc2c(c1)C[C@H](N(C(=O)Cc1ccccc1)C2)C(=O)Nc1ccc(cc1)OC)OCC(=O)NO	1
H-115	c1(c2nc3c(n2CCCO)ccc(c3)/C=C/C(=O)NO)ccccn1	1
H-116	c1c(cc(cc1)C(=O)NO)NCc1ccccc1	1
H-117	c1cc(cc2c1n(c(n2)COCc1ccccc1)CCCO)/C=C/C(=O)NO	1
H-118	C(c1nc2c(n1C)ccc(c2)/C=C/C(=O)NO)Cc1ccccc1	1
H-119	c1c(c([nH]c1c1ccc(cc1)OC)C(=O)NCc1ccc(cc1)C(=O)NO)c1ccoc1	1
H-120	c1(c(cc(cc1)C(=O)NO)NC(=O)c1ccc(cc1)c1ccccc1)OCC	1
H-121	c1c(ccc(c1)N[C@H]1CCN(C1=O)c1ccccc1Cl)C(=O)NO	1
H-122	c1c(ccc(c1)N[C@H]1CCN(C1=O)c1ccc(cc1)C#N)C(=O)NO	1
H-123	c1(ccc(cc1)/C=C/C(=O)NO)c1ccc(cc1)O	1
H-124	c1c(ccc(c1)N[C@@H]1CCN(C1=O)c1ccc(c(c1)Cl)Cl)C(=O)NO	1
H-125	n1(c2ccccc2nc1c1cccc(c1)/C=C/C(=O)NO)[C@H]1CCCN(C1)C	1
H-126	c1ccc2c(c1)nc(n2CCN(C)C)c1cccc(c1)/C=C/C(=O)NO	1
H-127	c1(ccc2c(c1)C[C@@H](CC2)NS(=O)(=O)c1cc(ccc1)Cl)C(=O)NO	1
H-128	c1(c2nc3c(n2CCCO)ccc(c3)/C=C/C(=O)NO)ccncc1	1
H-129	c1c(cc2c(c1)C[C@H](N(C(=O)c1ccccc1)C2)C(=O)Nc1ccc(cc1)OC)OCC(=O)NO	1
H-130	c1(c(cc(cc1)C(=O)NO)NC(=O)c1ccccc1)OCC	1
H-131	c1ccc2c(c1)n(cc2CCN1CCN(CC1)C)CC1=CC[C@@H](C=C1)C(=O)NO	1
H-132	C1CC[C@H]2[C@H](C1)[C@H](C[C@@H]2CCN1CCN(CC1)C)c1ccc(cc1)C(=O)NO	1
H-133	c1c(c([nH]c1c1ccc(cc1)OC)C(=O)NCc1ccc(cc1)C(=O)NO)c1ccsc1	1
H-134	C(=O)(CCCCC[C@@H](c1c[nH]c2c1cccc2OC)c1c[nH]c2c1cccc2OC)NO	1
H-135	c1c(ccc(c1)N[C@]1(CCN(C1=O)c1ccc(cc1)Cl)C)C(=O)NO	1
H-136	c1c(ccc(c1)N[C@@H]1CCN(C1=O)c1cccc(c1)Cl)C(=O)NO	1
H-137	c1c(cccc1c1cn(nn1)CCc1ccccc1)C(=O)NO	1
H-138	c1(c([nH]c(c1)c1cccs1)C(=O)NCc1ncc(cc1)C(=O)NO)c1ccc(cc1)F	1
H-139	c1(ccc2c(c1)C[C@@H](CC2)NS(=O)(=O)c1c(cc(cc1)Cl)Cl)C(=O)NO	1
H-140	c1(c(cc(cc1)C(=O)NO)NC(=O)c1ccccc1)Br	1
H-141	Cc1nc2c(n1CC)ccc(c2)/C=C/C(=O)NO	1
H-142	c1(cc2cc(c1)/C=C\CO[C@H](C(=O)Nc1c(OC2)cccc1)CCCCCC(=O)NO)OC	1
H-143	O=S(=O)(c1cc(/C=C/C(=O)NO)ccc1)c1nc2c(cc1)cccc2F	1
H-144	c1ccc2c(c1)nc(n2CCN(C(C)C)C(C)C)c1cccc(c1)/C=C/C(=O)NO	1

H-145	c1cccc(c1)NS(=O)(=O)c1cc(ccc1)/C=C/C(=O)NO	1
H-146	c1(CNC(=O)c2cc3C(CC(=O)Nc3cc2)(C)C)cc(ccc1)/C=C/C(=O)NO	1
H-147	n1(c(c(nc1c1cccc(c1)/C=C/C(=O)NO)C)C)CCN1CCOCC1	1
H-148	n1(c2ccccc2nc1c1cccc(c1)/C=C/C(=O)NO)[C@@H]1CCCN(C1)C	1
H-149	N(Cc1ccc(cc1)C(=O)NO)Cc1nc(c2ccccc2)no1	1
H-150	c12c(ncn1C)cc(cc2)/C=C/C(=O)NO	1
H-151	C(c1nc2c(n1Cc1cccnc1)ccc(c2)/C=C/C(=O)NO)Cc1ccccc1	1
H-152	c1cc(cc2c1n(c(n2)C1CCCCC1)CCCO)/C=C/C(=O)NO	1
H-153	c1(c(cc(cc1)C(=O)NO)NC(=O)c1ccccc1)C	1
H-154	c1cccc2c1NC(=O)[C@@H](N2Cc1ccc(cc1)C(=O)NO)Cc1ccccc1	1
H-155	c1cc2c(cc1CCCCc1ccc(cc1)CC(=O)NO)OCO2	1
H-156	c1c(ccc(c1)N[C@H]1CCN(C1=O)c1ccccc1)C(=O)NO	1
H-157	c1(ccc2c(c1)C[C@@H](CC2)NS(=O)(=O)c1c(cc(cc1)F)F)C(=O)NO	1
H-158	c1(c(cc(cc1)C(=O)NO)NC(=O)c1ccccc1Cl)OC	1
H-159	c1(c(cc(cc1)C(=O)NO)NC(=O)c1cccc(c1)OCc1ccccc1)Cl	1
H-160	c1c(c(cc(c1)/C=C/C(=O)NO)F)CN1CCC[C@@H](C1)c1c([nH]c2c1cccc2)C(C)(C)C	1
H-161	C(=O)(N[C@@H](Cc1ccc(cc1)OCC(=O)NO)C(=O)Nc1ccccc1)OC(C)(C)C	1
H-162	c1c(ccc(c1)c1cc(c2ccoc2)[nH]c1C(=O)Nc1ccc(cc1)C(=O)NO)O	1
H-163	CN(C)c1ccc(C(=O)N/N=C/c2ccc(C(=O)NO)cc2)cc1	1
H-164	C(c1onc(c2ccc(cc2)F)n1)NCc1ccc(C(=O)NO)cc1	1
H-165	c1cc2cc(c1)C[C@H](NC(=O)[C@@H](NC(=O)[C@H](C2)NC(=O)C)CCCCCC(=O)NO)C(=O)OC	1
H-166	C(c1nc2c(n1CCc1ccccn1)ccc(c2)/C=C/C(=O)NO)C(C)C	1
H-167	c1c(ccc(c1)/C=C/C(=O)NO)/C=N/OCCN1CCOCC1	1
H-168	c1(c(cc(cc1)C(=O)NO)NC(=O)c1ccc(cc1)OC)Cl	1
H-169	c12c(NCN1CCC1=CCCC=N1)cc(cc2)/C=C/C(=O)NO	1
H-170	c1cc(cc2c1n(c(n2)CC(C)C)CCCO)/C=C/C(=O)NO	1
H-171	c1(c(cc(cc1)C(=O)NO)NC(=O)c1ccc(cc1)Cl)OC	1
H-172	C(=O)(CCCCC[C@@H](c1c[nH]c2c1cccc2)c1c[nH]c2c1cccc2)NO	1
H-173	c1cccc2c1NC(=O)[C@H](N2Cc1ccc(cc1)C(=O)NO)Cc1ccc(cc1)OC(C)(C)C	1
H-174	C(c1nc2c(n1CCCO)ccc(c2)/C=C/C(=O)NO)Cc1ccccc1	1
H-175	c1cc(cc2c1n(c(n2)CCc1ccccc1)CCN1CCCCC1)/C=C/C(=O)NO	1
H-176	c1cc(cc2c1n(c(n2)CCc1ccccc1)CCN(CC)CC)/C=C/C(=O)NO	1
H-177	c1(ccc2c(c1)C[C@@H](CC2)Nc1nccc(n1)c1ccc(cc1)F)C(=O)NO	1
H-178	c1c(ccc(c1)N[C@H]1CCN(C1=O)CCc1ccccc1)C(=O)NO	1
H-179	c1(c2nc3c(n2C[C@@H](CO)O)ccc(c3)/C=C/C(=O)NO)ccc(cc1)OC	1
H-180	c1cccc(c1)C(=O)NC(=O)NCCCCCCCC(=O)NO	1
H-181	c1cccc2c1OCCCCCCCCO[C@H](C(=O)N2)CCCCCC(=O)NO	1
H-182	C(c1nc2c(n1CCc1ccccn1)ccc(c2)/C=C/C(=O)NO)Cc1ccccc1	1
H-183	c1(ccc2c(c1)C[C@@H](CC2)Nc1nc(cc(n1)OCC)C)C(=O)NO	1
H-184	C([C@H]1Nc2c(N1C)ccc(c2)/C=C/C(=O)NO)Cc1ccccc1	1
H-185	c1(c(cc(cc1)C(=O)NO)NC(=O)c1ccc(cc1)Cl)Cl	1

H-186	ONC(=O)CCCCCn1c(=O)c2cccc3cccc(c1=O)c23	1
H-187	c1(c2c(ccc1)cccc2)c1ccc(C(=O)NO)cc1	1
H-188	C(c1nc2c(n1CCc1cccnc1)ccc(c2)/C=C/C(=O)NO)OCc1ccccc1	1
H-189	c1(ccc2c(c1)C[C@@H](CC2)Nc1nccc(n1)c1c(cccc1)Cl)C(=O)NO	1
H-190	c1(ccc2c(c1)C[C@@H](CC2)Nc1nccc(n1)C(F)(F)F)C(=O)NO	1
H-191	c1ccc2c(c1)nc(n2CC1CCNCC1)c1cccc(c1)/C=C/C(=O)NO	1
H-192	c12ccc(nc1cccc2)N(CCCCCCC(=O)NO)c1ccccn1	1
H-193	c1cc(cc2c1n(c(n2)CCc1ccccc1)CCCOC)/C=C/C(=O)NO	1
H-194	c1(c(cc(cc1)C(=O)NO)NC(=O)c1ccccc1)F	1
H-195	c1(ccc2c(c1)C[C@@H](CC2)Nc1nccc(n1)c1ccc(nc1)N1CCOCC1)C(=O)NO	1
H-196	C1CC[C@H]2[C@H](C1)[C@H](C[C@@H]2Cc1ccccc1)c1ccc(cc1)C(=O)NO	1
H-197	c1ccc2c(c1)n(cc2Cc1ccccc1)Cc1ccc(cc1)C(=O)NO	1
H-198	C(c1nc2c(n1CCc1cccnc1)ccc(c2)/C=C/C(=O)NO)Cc1ccccc1	1
H-199	c1(c2nc3c(n2C[C@@H](CO)O)ccc(c3)/C=C/C(=O)NO)cc(c(cc1)OCc1ccccc1)OC	1
H-200	c1c(ccc(c1)c1cc(c2ccccc2)[nH]c1C(=O)Nc1ccc(cc1)C(=O)NO)O	1
H-201	c1(c(cc(cc1)C(=O)NO)NC(=O)c1ccccc1)C(F)(F)F	1
H-202	[n+]1(onc(c1S(=O)(=O)c1ccccc1)OCCCCCC(=O)NO)[O-]	1
H-203	c1(c2nc3c(n2C[C@H](CO)O)ccc(c3)/C=C/C(=O)NO)ccccn1	1
H-204	c1c(cc2c(c1)n(c(c2CC(=O)NCCCCCC(=O)NO)C)C(=O)c1ccc(cc1)Cl)OC	1
H-205	C([C@H]1Nc2c(N1CCN1CCOCC1)ccc(c2)/C=C/C(=O)NO)Cc1ccccc1	1
H-206	N(Cc1ccc(cc1)C(=O)NO)Cc1nc(c2ccc(cc2)Cl)no1	1
H-207	c1c(cccc1c1cn(nn1)Cc1ccccc1)C(=O)NO	1
H-208	c1(ccc2c(c1)C[C@@H](CC2)NS(=O)(=O)c1cc(ccc1)F)C(=O)NO	1
H-209	c1cc(cc2c1n(c(n2)CCc1ccccc1)CC(C)(C)CN(C)C)/C=C/C(=O)NO	1
H-210	c1cc(cc2c1n(c(n2)CCc1ccccc1)Cc1cc(c(c(c1)OC)OC)OC)/C=C/C(=O)NO	1
H-211	c1c(c(cc(c1)/C=C/C(=O)NO)F)CN1CCC[C@H](C1)c1c([nH]c2c1cccc2)C(C)(C)C	1
H-212	c1cc(cc2c1n(c(n2)CCc1ccccc1)Cc1ccccn1)/C=C/C(=O)NO	1
H-213	c1c(cc2c(c1)C[C@H](N(C2)C(=O)[C@@H](N)Cc1ccccc1)C(=O)Nc1ccc(cc1)OC)OC C(=O)NO	1
H-214	c1(ccc2c(c1)C[C@@H](CC2)NS(=O)(=O)c1cnccc1)C(=O)NO	1
H-215	c1(ccc2c(c1)C[C@H](CC2)NS(=O)(=O)c1cc(ccc1)C(F)(F)F)C(=O)NO	1
H-216	C(c1onc(c2ccc(cc2)[N+](=O)[O-])n1)NCc1ccc(C(=O)NO)cc1	1
H-217	c1(ccc2c(c1)C[C@H](CC2)NS(=O)(=O)c1cc(c(cc1)OC)OC)C(=O)NO	1
H-218	c1ccc2c(c1)n(c(c2)C)Cc1ccc(cc1)C(=O)NO	1
H-219	C1CC[C@@H]2[C@H](C1)[C@H]([C@@H](C2)C)c1ccc(cc1)C(=O)NO	1
H-220	n1(c(nc(c1c1cccc(c1)/C=C/C(=O)NO)C)c1ccccc1)[C@@H]1CCCN(C1)CC	1
H-221	c1ccc2c(c1)nc(n2CCN1CCOCC1)c1cccc(c1)/C=C/C(=O)NO	1
H-222	C(Cc1ccc(cc1)CC(=O)NO)CCc1cccc(c1)C(F)(F)F	1
H-223	c1(c2nc3c(n2CCO)ccc(c3)/C=C/C(=O)NO)ccc(cc1)OC	1
H-224	C(CC(=O)NO)CCCCCNC(=O)NC(=O)c1ccccc1	1
H-225	c12c(cc(cc1)CCCCc1ccc(cc1)CC(=O)NO)cc[nH]2	1
H-226	C[C@H](/C=C/C(=O)NO)/C=C(\C)/C(=O)c1ccc(cc1)N(C)C	1

H-227	c12c(ncn1Cc1ccccc1)cc(cc2)/C=C/C(=O)NO	1
H-228	C1CC[C@@H]2[C@H](C1)[C@H](CC2)c1ccc(cc1)C(=O)NO	1
H-229	c1ccc2c(c1)n(cc2)Cc1ccc(cc1)C(=O)NO	1
H-230	c1cccc2c1NC(=O)[C@H](N2Cc1ccc(cc1)C(=O)NO)Cc1cc(c(cc1)F)F	1
H-231	C1CC[C@H]2[C@H](C1)[C@H](C[C@@H]2CCN(C)C)c1ccc(cc1)C(=O)NO	1
H-232	c1ccc2c(c1)n(cc2CCN(C)C)Cc1ccc(cc1)C(=O)NO	1
H-233	C(=O)(NO)C1=CCCCC1	1
H-234	c1(c(cc(cc1)C(=O)NO)NC(=O)c1ccc(cc1)OCC)OC	1
H-235	O=C1CNC(=O)[C@H](N1Cc1ccc(cc1)C(=O)NO)Cc1sccc1	1
H-236	c1cc(cc2c1n(c(n2)CCc1ccccc1)CCCO)C(=O)NO	1
H-237	c1(c(cc(cc1)C(=O)NO)NC(=O)c1cccc(c1)Oc1ccccc1)Cl	1
H-238	C(c1nc2c(n1C[C@H](CO)O)ccc(c2)/C=C/C(=O)NO)Cc1ccccc1	1
H-239	N[C@@H](Cc1ccc(cc1)OCC(=O)NO)C(=O)Nc1ccccc1	1
H-240	c1(ccc2c(c1)C[C@@H](CC2)NS(=O)(=O)c1cc(c(cc1)Cl)Cl)C(=O)NO	1
H-241	c1(ccc2c(c1)C[C@@H](CN2)Nc1nccc(n1)c1ccccnc1)C(=O)NO	1
H-242	c1(ccc2c(c1)C[C@@H](CC2)Nc1nccc(n1)c1cc2ccccc2nc1)C(=O)NO	1
H-243	c1(ccc2c(c1)C[C@@H](CC2)Nc1nccc(n1)c1ccc(nc1)C)C(=O)NO	1
H-244	C1CN[C@@H](C1)C(=O)N1Cc2cc(ccc2C[C@H]1C(=O)Nc1ccc(cc1)OC)OCC(=O)NO	1
H-245	n1(c(nc(c1c1cccc(c1)/C=C/C(=O)NO)C)C)[C@@H]1CCCN(C1)CC	1
H-246	C(=O)(N1Cc2cc(ccc2C[C@H]1C(=O)Nc1ccc(cc1)OC)OCC(=O)NO)CCc1ccccc1	1
H-247	c1(ccc2c(c1)C[C@H](CC2)Nc1nccc(n1)c1ccccnc1Cl)C(=O)NO	1
H-248	c1(c(cc(cc1)C(=O)NO)NC(=O)Cc1ccccc1)OC	1
H-249	c1cc(ccc1NC(=O)CCCCCCC(=O)NO)c1cnnn1c1ccccc1	1
H-250	c1(ccc2c(c1)C[C@H](CC2)Nc1nccc(n1)c1cc(cnc1)OC)C(=O)NO	1
H-251	c1cccc2c1NC(=O)CN2Cc1ccc(cc1)C(=O)NO	1
H-252	c1(ccc2c(c1)C[C@@H](CC2)Nc1nccc(n1)c1cc(cnc1)C)C(=O)NO	1
H-253	c1(c(cc(c(c1)F)CCCCc1ccc(cc1)CC(=O)NO)F)F	1
H-254	c1cccc2c1NC(=O)[C@H](N2Cc1ccc(cc1)C(=O)NO)Cc1ccccc1	1
H-255	c1cc(cc2c1n(c(n2)c1cscc1)CCCO)/C=C/C(=O)NO	1
H-256	O=S(=O)(c1ccc(n2nc(cc2c2ccc(cc2)C)C(=O)NCCCCCC(=O)NO)cc1)N	1
H-257	c1(c(cc(cc1)C(=O)NO)NC(=O)c1ccc(cc1Cl)Cl)OC	1
H-258	[nH]1c(c(cc1c1sccc1)c1ccc(cc1)O)C(=O)NCc1ccc(cc1)C(=O)NO	1
H-259	c1c(cc2c(c1)C[C@H](N(C2)C(=O)OCc1ccccc1)C(=O)NCCc1ccccc1)OCC(=O)NO	1
H-260	c1ccc2c(c1)c(c([nH]2)C)/C=C/c1c(cccc1)c1ccc(cc1)/C=C/C(=O)NO	1
H-261	c1c(cc(cc1)C(=O)NO)NC(=O)c1ccccc1	1
H-262	c1ccc2c(c1)ccc(n2)C(=O)NO	1
H-263	c1c(ccc(c1)N[C@]1(CCN(C1=O)c1ccccc1)C)C(=O)NO	1
H-264	c1c(ccc(c1)N[C@@]1(CCN(C1=O)c1ccc(cc1)Cl)C)C(=O)NO	1
H-265	C(=O)(CCCCC[C@H](c1c[nH]c2c1cc(cc2)[N+](=O)[O-])c1c[nH]c2c1cc(cc2)[N+](=O)[O-])NO	1
H-266	C(c1nc2c(n1CCc1ccccc1)ccc(c2)/C=C/C(=O)NO)C(C)C	1
H-267	c1c(ccc(c1)/C=C/C(=O)NO)/C=N/OCc1ccc(cc1)C(=O)OC	1

H-268	c1cccc(c1CCCCc1ccc(cc1)CC(=O)NO)C(F)(F)F	1
H-269	C(=O)(CCCCSc1nc(cc(=O)[nH]1)c1ccc(cc1)c1ccccc1)NO	1
H-270	C(=O)(/C=C/c1ccc(cn1)NC(=O)[C@H](Cc1ccccc1)c1ccccc1)NO	1
H-271	c1c(ccc2SCCC(=O)Nc12)C(=O)NO	1
H-272	c1cccc2c1NC(=O)[C@H](N2Cc1ccc(cc1)C(=O)NO)CCc1ccccc1	1
H-273	c1cccc2c1OCCCCCO[C@@H](C(=O)N2)CCCCCC(=O)NO	1
H-274	c1(NC(=O)CCCCCCCN(C=O)O)c2c(ccc1)cccc2	1
H-275	C(=C\C(=O)NO)/c1cc(ccc1)S(=O)(=O)N[C@H](C(=O)Nc1c2ccccc2ccc1)c1ccccc1	1
H-276	c1c(cc2c(c1)C[C@H](N(C(=O)[C@@H](N)CC(C)C)C2)C(=O)Nc1ccc(cc1)OC)OCC(=O)NO	1
H-277	c1(ccc2c(c1)C[C@H](CC2)Nc1ccc(cc1)Br)C(=O)NO	1
H-278	c1ccc2c(c1)n(c1c2CN(CC1)C)Cc1ccc(cc1)C(=O)NO	1
H-279	c1(ccccc1)NC(=O)c1ccc(cc1)C(=O)NO	1
H-280	C(=O)(c1ccc(cc1)CNC(=O)c1cccn1C)NO	1
H-281	C(=O)([C@H](C(=O)Nc1cc2c(nc1)cccc2)CCCCCN(C=O)O)Nc1cc2c(nc1)cccc2	1
H-282	c1cccc2c1NC(=O)[C@H](N2Cc1ccc(cc1)C(=O)NO)Cc1cccs1	1
H-283	C(=O)(N1Cc2cc(ccc2C[C@H]1C(=O)NCCc1ccccc1)OCC(=O)NO)CCc1ccccc1	1
H-284	c12ccccc1cccc2/C=C/C(=O)NO	1
H-285	C(CCCCCC(=O)NO)NC(=O)c1noc(c1)c1ccc(cc1)N=[N+]=[N-]	1
H-286	c1(ccc2c(c1)C[C@H](CC2)Nc1nccc(n1)c1cccnc1)C(=O)NO	1
H-287	c1cc(cc2c1n(c(n2)CCc1ccccc1)CCCN1CCCC1=O)/C=C/C(=O)NO	1
H-288	c1(ccc2c(c1)C[C@@H](CC2)Nc1ncccn1)C(=O)NO	1
H-289	c1cccc2c1NC(=O)[C@H](N2Cc1ccc(cc1)C(=O)NO)Cc1ccc(cc1)O	1
H-290	[C@H](c1c[nH]c2c1cccc2)(c1c[nH]c2c1cccc2)c1ccc(cc1)/C=C/C(=O)NO	1
H-291	c1cc2cc(c1)COC/C=C/COCc1c(ccc(Nc3nccc2n3)c1)OCCCCCCC(=O)NO	1
H-292	c1(ccc2c(c1)C[C@@H](CN2C)NS(=O)(=O)c1ccc(cc1)Cl)C(=O)NO	1
H-293	c1(ccccc1)NC(=O)[C@H]1N(C(=O)CCc2ccccc2)Cc2cc(ccc2C1)OCC(=O)NO	1
H-294	C(=O)(/C=C/c1ccccc1)NO	1
H-295	C1SC2(SC1)C[C@H](N(C2)C(=O)[C@@H]1CCCN1C(=O)OC(C)(C)C)C(=O)NCCCCCC(=O)NO	1
H-296	c1c(ccc(c1)N[C@@H]1CCN(C1=O)Cc1ccccc1)C(=O)NO	1
H-297	C(CCCCNC(=O)/C=C\1/c2c(cccc2)c2c1cccc2)C(=O)NO	1
H-298	C(=O)(Nc1cc2c(cc1)cccc2)CCCCCCCN(C=O)O	1
H-299	c12c(nc(n1CCCO)c1ccc(c(c1)OC)OCc1ccccc1)cc(cc2)/C=C/C(=O)NO	1
H-300	c1(ccc2c(c1)C[C@@H](CC2)Nc1nccc(n1)c1ccc(cc1)C)C(=O)NO	1
H-301	c1(ccc2c(c1)C[C@@H](CC2)Nc1nccc(n1)c1cc(ccc1)N(C)C)C(=O)NO	1
H-302	C(=O)([C@H](C(=O)Nc1cc2c(nccc2)cc1)CCCCCN(C=O)O)Nc1cc2c(nccc2)cc1	1
H-303	c1c(cc(cc1)C(=O)NO)NC1CCCCC1	1
H-304	c1(ccc2c(c1)C[C@H](CO2)Nc1nccc(n1)c1cnccc1)C(=O)NO	1
H-305	C(CCCCC(=O)NO)ONC(=O)c1cc(c(cc1)C)C	1
H-306	C1SC2(SC1)C[C@H](N(C2)C(=O)[C@@H](N)Cc1ccccc1)C(=O)NCCCCCC(=O)NO	1
H-307	C(c1nc2c(n1Cc1ccccc1)ccc(c2)/C=C/C(=O)NO)C(C)C	1

H-308	c1(ccc2c(c1)C[C@@H](CC2)NS(=O)(=O)c1ccc(cc1)Cl)C(=O)NO	1
H-309	N(Cc1ccc(cc1)C(=O)NO)Cc1nc(c2ccc(cc2)OC)no1	1
H-310	c1c(ccc(c1)N[C@H]1CCN(C1)c1ccc(cc1)Cl)C(=O)NO	1
H-311	c1(c2nc3c(n2CCO)ccc(c3)/C=C/C(=O)NO)ccncc1	1
H-312	c1(ccc2c(c1)C[C@@H](CC2)Nc1nccc(n1)c1ccc(nc1)Cl)C(=O)NO	1
H-313	c1(ccc2c(c1)C[C@@H](CC2)NS(=O)(=O)CCCC)C(=O)NO	1
H-314	c1ccc2c(c1)n(cc2C)Cc1ccc(cc1)C(=O)NO	1
H-315	C1CC[C@H]2[C@H](C1)[C@H](C[C@@H]2C)c1ccc(cc1)C(=O)NO	1
H-316	C1SC2(SC1)C[C@H](N(C2)C(=O)[C@@H](N)CC(C)C)C(=O)NCCCCCC(=O)NO	1
H-317	N1c2c(cccc2)[C@]2([C@@]1(N(CC2)Cc1ccc(cc1)/C=C/C(=O)NO)C)O	1
H-318	c1(c(cc2c(c1)C[C@H](CC2)NS(=O)(=O)c1cccc(c1)Cl)F)C(=O)NO	1
H-319	c1(ccc2c(c1)C[C@@H](CC2)Nc1ccc(cn1)[N+](=O)[O-])C(=O)NO	1
H-320	c1(onc(c1)C(=O)NCCCCCCC(=O)NO)c1cccc(c1)N	1
H-321	c1c(ccc(c1)NC)C(=O)NO	1
H-322	c1c(cccc1NC(=O)CCCCCCC(=O)NO)c1cnnn1c1ccccc1	1
H-323	C(=O)(c1ccc(cc1)CN(C(=O)Nc1ccccc1)CCCC)NO	1
H-324	C(=O)(/C=C/c1ccc(cc1)C(F)(F)F)NO	1
H-325	c1c(ccc2c1NC(=O)[C@@H](S2)C)C(=O)NO	1
H-326	c1(ccc2c(c1)C[C@H](CN2)NS(=O)(=O)c1cc(ccc1)Cl)C(=O)NO	1
H-327	c1(ccc2c(c1)C[C@@H](CC2)NC(=O)/C=C/c1cccnc1)C(=O)NO	1
H-328	c1c(cc2c(c1)C[C@H](N(C2)C(=O)OC(C)(C)C)C(=O)Nc1ccc(cc1)OC)OCC(=O)NO	1
H-329	c1(ccc2c(c1)C[C@@H](CC2)Nc1nccc(n1)c1ccc(nc1)OC)C(=O)NO	1
H-330	n1c(nc(N(c2ccc(cc2)OCCCCCC(=O)NO)C)c2c1CCC2)C	0
H-331	c1cc(cc2c1n(c(n2)CCc1ccccc1)CCc1ccccc1)/C=C/C(=O)NO	0
H-332	c1c(cc2c(c1)C[C@H](N(CCc1ccccc1)C2)C(=O)Nc1ccc(cc1)OC)OCC(=O)NO	0
H-333	c1c(cc2c(c1)C[C@H](N(C(=O)[C@@H](N)C(C)C)C2)C(=O)Nc1ccc(cc1)OC)OCC(=O)NO	0
H-334	C(=O)(CCCCc1nn(cc1)Cc1ccc(cc1)Nc1ccccc1)NO	0
H-335	c1ccccc1CNC(=O)c1ccc(cc1)C(=O)NO	0
H-336	c1c(cc2c(c1)C[C@H](N(C(=O)[C@@H](N)[C@@H](C)CC)C2)C(=O)Nc1ccc(cc1)OC)OCC(=O)NO	0
H-337	C(CCCCC(=O)NO)ONC(=O)c1cc(ccc1)C	0
H-338	c1c(ccc(c1)CNC(=O)NCCC(=O)NO)N(C)C	0
H-339	c1ccc2c(c1)c(ncn2)N(c1ccc(cc1)OCCCCCC(=O)NO)C	0
H-340	c1c(cc2c(c1)C[C@H](NC2)C(=O)Nc1cccc2c1cccc2)OCC(=O)NO	0
H-341	C1SC2(SC1)C[C@H](N(C2)C(=O)[C@@H](N)C(C)C)C(=O)NCCCCCC(=O)NO	0
H-342	C1SC2(SC1)C[C@H](N(C2)C(=O)[C@@H](N)[C@H](CC)C)C(=O)NCCCCCC(=O)NO	0
H-343	c1(c(cc(cc1)C(=O)NO)NC(=O)c1ccc(cc1)Oc1ccccc1)Cl	0
H-344	c1cc(cc2c1n(c(n2)CCc1ccccc1)CCCN1CCOCC1)/C=C/C(=O)NO	0
H-345	C(=O)(NO)C1=CCCC1	0
H-346	c1(ccc2c(c1)C[C@@H](CC2)Nc1nccc(n1)c1ccc(cc1F)C)C(=O)NO	0
H-347	c1cccc2c1OCCCCCCO[C@@H](C(=O)N2)CCCCCC(=O)NO	0

H-348	c1(ccc2c(c1)C[C@H](CN2)NS(=O)(=O)c1cc(ccc1)F)C(=O)NO	0
H-349	c1c(ccc(c1)C(=O)NO)C(=O)NCCc1ccccc1	0
H-350	c1cccc2c1NC(=O)[C@H](N2Cc1ccc(cc1)C(=O)NO)CCCCNC(=O)OC(C)(C)C	0
H-351	c1c(cc2c(c1)C[C@H](N(C2)C(=O)OC(C)(C)C)C(=O)Nc1cc(ccc1)Cl)OCC(=O)NO	0
H-352	c1ccc2c(c1)c(nc(n2)C)N(c1ccc(cc1)OCC(=O)NO)C	0
H-353	c1(c(cc(cc1)C(=O)NO)NC(=O)c1ccc(cc1Cl)Cl)Cl	0
H-354	c1c(cc(cc1)NC(=O)CCCCCCC(=O)NO)c1nnn(c1)C1CCCCC1	0
H-355	c1cccc2c1NC(=O)[C@@H](N2Cc1ccc(cc1)C(=O)NO)Cc1cccs1	0
H-356	c1c(cccc1)NC(=O)CCCCC[C@@H](C(=O)NO)Cc1ccccc1	0
H-357	C1CCCN1Cc1ccc(cc1)C(=O)NO	0
H-358	C1CCCC1c1ccc(cc1)C(=O)NO	0
H-359	O=C1CNC(=O)[C@H](N1Cc1ccc(cc1)C(=O)NO)Cc1c[nH]c2c1cccc2	0
H-360	c1(ccc2c(c1)C[C@H](CN2)NS(=O)(=O)c1cc(c(cc1)OC)OC)C(=O)NO	0
H-361	c1(ccc2c(c1)C[C@H](CC2)Nc1nccc(n1)c1ccc(cc1OC)OC)C(=O)NO	0
H-362	N(Cc1ccc(cc1)C(=O)NO)Cc1nc(c2ccc(cc2)C)no1	0
H-363	c1(ccc2c(c1)C[C@@H](CC2)NC(=O)OCc1cccnc1)C(=O)NO	0
H-364	C(CCCCC(=O)NO)ONC(=O)c1cc(cc(c1)C)C	0
H-365	c1c(cc2c(c1)C[C@H](N(C(=O)[C@@H](N)C)C2)C(=O)Nc1ccc(cc1)OC)OCC(=O)NO	0
H-366	c1(c(cc2c(c1)C[C@H](CC2)NS(=O)(=O)c1ccc(cc1)Cl)F)C(=O)NO	0
H-367	c1c(cc2c(c1)C[C@H](N(C2)C(=O)OC(C)(C)C)C(=O)Nc1ccccc1)OCC(=O)NO	0
H-368	c1c(ccc(c1)/C=C/C(=O)NO)/C=N/OCc1c(c(c(c(c1F)F)F)F)F	0
H-369	C1SC2(SC1)C[C@H](N(C2)C(=O)CN)C(=O)NCCCCCC(=O)NO	0
H-370	c1(ccc(cc1)CCCCc1ccc(cc1)CC(=O)NO)C(F)(F)F	0
H-371	c1ccc2c(c1)c(ncn2)N(c1ccc(cc1)OCCCCC(=O)NO)C	0
H-372	c1c(ccc(c1)C(=O)NO)C(=O)NCCc1ccncc1	0
H-373	N(Cc1ccc(cc1)C(=O)NO)Cc1nc(c2ccc(cc2)C(F)(F)F)no1	0
H-374	C(=O)(/C=C/c1cc(ccc1)S(=O)(=O)n1c2c(cccn2)cc1)NO	0
H-375	c1ccc2c(c1)c(ncn2)N(c1ccc(cc1)OCC(=O)NO)C	0
H-376	c1(ccc2c(c1)C[C@@H](CC2)Nc1nccc(n1)c1ccc(cc1)Oc1ccccc1)C(=O)NO	0
H-377	C1SC2(SC1)C[C@H](N(C2)C(=O)C1CCN(CC1)C(=O)OC(C)(C)C)C(=O)NCCCCC C(=O)NO	0
H-378	C(=O)(CCCCCNc1nc(nc2n(cnc12)Cc1ccccc1)Cl)NO	0
H-379	C(c1nc2c(n1Cc1ccccc1)ccc(c2)/C=C/C(=O)NO)Cc1ccccc1	0
H-380	c1(ccc2c(c1)C[C@H](CN2)NS(=O)(=O)c1ccc(cc1)Cl)C(=O)NO	0
H-381	c1ccc2c(c1)c(nc(n2)C)N(c1ccc(cc1)OCCCC(=O)NO)C	0
H-382	c1(ccc2c(c1)C[C@@H](CC2)Nc1nc(cc(Oc2ccccc2)n1)C)C(=O)NO	0
H-383	C(=O)([C@H](Cc1cc(c(cc1)O)Br)N=O)NCCC(=O)NO	0
H-384	c1(c(cc2c(c1)C[C@@H](CC2)Nc1nccc(n1)c1cccnc1)F)C(=O)NO	0
H-385	c1ccc2c(c1)c(nc(n2)C)N(c1ccc(cc1)OCCCCCC(=O)NO)C	0
H-386	c1(ccc2c(c1)C[C@@H](CC2)Nc1nccc(n1)c1ccc(cc1Cl)Cl)C(=O)NO	0
H-387	c1cccc(c1)[C@H](NC(=O)OC(C)(C)C)C(=O)Nc1ccc(cc1)C(=O)NO	0
H-388	c1ccc2c(c1)c(nc(n2)C)N(c1cc(c(cc1)OC)OCCCCCC(=O)NO)C	0

H-389	c1c(cc2c(c1)C[C@H](N(C2)C(=O)OC(C)(C)C)C(=O)Nc1cc(c(cc1)F)Cl)OCC(=O)NO	0
H-390	c1c(ccc(c1)/C=C/C=C/C(=O)NO)c1ccc(cc1)OC	0
H-391	c1(ccc2c(c1)C[C@H](CN2)NS(=O)(=O)c1cc(ccc1)OC(F)(F)F)C(=O)NO	0
H-392	c1(ccc(cc1F)Cl)/C=C/C(=O)NCCCCCC(=O)NO	0
H-393	c1c(cc2c(c1)C[C@H](N(C2)C(=O)OC(C)(C)C)C(=O)Nc1ccc(cc1)C)OCC(=O)NO	0
H-394	c1(ccc2c(c1)C[C@@H](CC2)Nc1nccc(n1)c1cc(ccc1)Cl)C(=O)NO	0
H-395	c1(ccc2c(c1)C[C@@H](CC2)Nc1nccc(n1)c1ccc(cc1)C(F)(F)F)C(=O)NO	0
H-396	c1ccc2c(c1)c(nc(n2)C)N(c1ccc(cc1)OCCCCC(=O)NO)C	0
H-397	c1(c2nc3c(n2C)ccc(c3)/C=C/C(=O)NO)cc(c(cc1)OCc1ccccc1)OC	0
H-398	c1c(cc2c(c1)C[C@H](N(CCCc1ccccc1)C2)C(=O)Nc1ccc(cc1)OC)OCC(=O)NO	0
H-399	c1c(ccc(c1)NC(=O)NCCCCCCC(=O)NO)N(C)C	0
H-400	[C@@]12(CCN(CC1)Cc1ccccc1)Oc1ccc(cc1C(=O)C2)/C=C/C(=O)NO	0
H-401	C(=O)(c1c(cc(c(c1)C(C)C)O)O)N1CCc2onc(c2C1)C(=O)NCCCCCCC(=O)NO	0
H-402	c1c(cc2c(c1)C[C@H](N(C2)C(=O)OC(C)(C)C)C(=O)Nc1cc(ccc1)C)OCC(=O)NO	0
H-403	c1(ccc2c(c1)C[C@@H](CC2)Nc1ncc2c(n1)ccc(c2)F)C(=O)NO	0
H-404	C1CN([C@@H](C1)COC)Cc1ccc(cc1)C(=O)NO	0
H-405	[C@H]1(CCC[C@H]1c1ccc(cc1)C(=O)NO)COC	0
H-406	C(CCCCC(=O)NO)Cc1nc(no1)c1cnccc1	0
H-407	C1SC2(SC1)C[C@H](N(C2)C(=O)OC(C)(C)C)C(=O)NCCCCCC(=O)NO	0
H-408	c1cc(cc2c1n(c(n2)CCc1ccccc1)CCC(=O)O)/C=C/C(=O)NO	0
H-409	c1ccc(cc1)C(=O)NO	0
H-410	c1c(cc2c(c1)C[C@H](N(Cc1ccccc1)C2)C(=O)Nc1ccc(cc1)OC)OCC(=O)NO	0
H-411	c1(ccc(cc1)C(=O)NO)CN(C(C)C)C(C)C	0
H-412	C(C)(C)C(C(C)C)c1ccc(cc1)C(=O)NO	0
H-413	C(CCCCC(=O)NO)Cc1nc(no1)c1sccc1	0
H-414	C1SC2(SC1)C[C@H](N(C2)C(=O)CCN)C(=O)NCCCCCC(=O)NO	0
H-415	CNC(=O)c1ccc(cc1)C(=O)NO	0
H-416	c1cc(ccc1NC(=O)CCCCCCC(=O)NO)c1cn(nn1)c1ccccc1	0
H-417	c1c(cc2c(c1)C[C@H](N(C2)C(=O)OC(C)(C)C)C(=O)Nc1ccc(cc1)c1ccccc1)OC C(=O)NO	0
H-418	n1c(nc(N(c2ccc(cc2)OCCCCC(=O)NO)C)c2c1CCC2)C	0
H-419	CN(C)c1ccc(C(=O)N(C)/N=C/c2cc(C(=O)NO)ccc2)cc1	0
H-420	c1cc(ccc1/C=C/C(=O)NO)OC[C@@H](NC(=O)c1ccc(cc1)Cl)Cc1c2ccccc2[nH]c1	0
H-421	C(=O)(CCCCCCNc1nc(nc2n(cnc12)CC(C)C)Cl)NO	0
H-422	c1(ccc2c(c1)nccc2)/C=C/C(=O)NCCCCCC(=O)NO	0
H-423	C(CCCCC(=O)NO)Cc1nc(no1)c1ccccc1	0
H-424	c1cc(cc2c1CN(CC2)C(=O)c1cccn1C)C(=O)NO	0
H-425	C(CCCCNC(=O)/C=C(/C=C/c1ccccc1)\C)C(=O)NO	0
H-426	c1(ccc2c(c1)C[C@H](CC2)Nc1nccc(n1)c1ccccc1)C(=O)NO	0
H-427	c1c(cc2c(c1)C[C@H](N(C2)C(=O)CN)C(=O)Nc1ccc(cc1)OC)OCC(=O)NO	0
H-428	c1(ccc2c(c1)C[C@@H](CC2)Nc1nccc(n1)c1ccc(cc1C)Cl)C(=O)NO	0
H-429	c1c(cc(cc1)C(=O)NO)N(Cc1ccccc1)Cc1ccccc1	0

H-430	CN(C)c1ccc(C(=O)N/N=C/c2cc(C(=O)NO)ccc2)cc1	0
H-431	c1(ccc2c(c1)C[C@@H](CC2)Nc1nccc(n1)c1ccc(cc1)Cl)C(=O)NO	0
H-432	C(CCCCC(=O)NO)CC[NH3+]	0
H-433	c1c(cc2c(c1)C[C@H](NC2)C(=O)Nc1ccc(cc1)c1ccccc1)OCC(=O)NO	0
H-434	c1(ccc2c(c1)C[C@H](CC2)Nc1nccc(n1)c1ccc(F)c(c1)Cl)C(=O)NO	0
H-435	O=C1CNC(=O)[C@H](N1Cc1ccc(cc1)C(=O)NO)Cc1ccccc1	0
H-436	C(=O)(NO)CCc1ccccc1	0
H-437	c1cccc(c1)N(c1ccccc1)Cc1ccc(cc1)C(=O)NO	0
H-438	c1cccc(c1)[C@@H](c1ccccc1)c1ccc(cc1)C(=O)NO	0
H-439	C(CCCCC(=O)NO)Cc1nc(no1)c1cccc(c1)[N+](=O)[O-]	0
H-440	c1(ccc2c(c1)C[C@@H](CN2)NC(=O)c1ccc(cc1)Cl)C(=O)NO	0
H-441	c1ccc2c(c1)c(ncn2)N(c1ccc(cc1)OCCCC(=O)NO)C	0
H-442	C(=O)(CCCCc1nn(cc1)c1ccccc1)NO	0
H-443	c1c(cc2c(c1)C[C@H](N(C2)C(=O)OC(C)(C)C)C(=O)Nc1ccc(cc1)F)OCC(=O)NO	0
H-444	C(CCCCC(=O)NO)Cc1nc(no1)c1ccc(cc1)[N+](=O)[O-]	0
H-445	C1SC2(SC1)C[C@H](NC2)C(=O)NCCCCCC(=O)NO	0
H-446	c1(ccc2c(c1)C[C@@H](CN2)NC(=O)c1cc(c(cc1)Cl)Cl)C(=O)NO	0
H-447	c1c(cc2c(c1)C[C@H](N(C2)C(=O)OC(C)(C)C)C(=O)NCCc1ccccc1)OCC(=O)NO	0
H-448	c1(ccc2c(c1)C[C@H](CN2)NC(=O)c1cc(ccc1)C(F)(F)F)C(=O)NO	0
H-449	c1(ccc2c(c1)C[C@H](CC2)Nc1ccc(cc1)F)C(=O)NO	0
H-450	ONC(=O)c1coc([C@@H](c2ccccc2)c2ccccc2)n1	0
H-451	N(C(=O)CCCCCCC(=O)NO)c1nc(cs1)c1ccc(cc1)N=[N+]=[N-]	0
H-452	c1c(cc(cc1)NC(=O)CCCCCCC(=O)NO)n1nnc(c1)C1CCCCC1	0
H-453	c1c(cccc1NC(=O)CCCCCCC(=O)NO)c1cn(nn1)c1ccccc1	0
H-454	C1SC2(SC1)C[C@H](N(C2)C(=O)C1CCNCC1)C(=O)NCCCCCC(=O)NO	0
H-455	C(=O)(Nc1ccccc1)CCCCCCCN(C=O)O	0
H-456	c1(ccc2c(c1)C[C@@H](CN2)NC(=O)c1cc(ccc1)OC)C(=O)NO	0
H-457	c1(onc(c1)C(=O)NCCCCC(=O)NO)c1ccc(cc1)N	0
H-458	c1(ccc2c(c1)C[C@@H](CN2)NC(=O)c1ccc(cc1)c1ccccc1)C(=O)NO	0
H-459	c1(ccc2c(c1)C[C@@H](CC2)Nc1ccccn1)C(=O)NO	0
H-460	c1(cc(ccc1CC#N)c1c(cc(cc1)/C=C/C(=O)NO)Cl)[C@]12C[C@@H]3C[C@H](C1)C[C@@H](C3)C2	0
H-461	n1c(nc(N(c2ccc(cc2)OCC(=O)NO)C)c2c1CCC2)C	0
H-462	C(=O)(CCCCc1nn(cc1)Cc1cc(ccc1)c1ccccc1)NO	0
H-463	c1c(cc2c(c1)C[C@H](N(C2)C(=O)OC(C)(C)C)C(=O)NCCCCC)OCC(=O)NO	0
H-464	c1(ccc2c(c1)C[C@H](CC2)N(c1nccc(n1)c1cccnc1)C)C(=O)NO	0
H-465	C(=O)(CCCCCCNc1nc(nc2n(cnc12)C(C)C)N)NO	0
H-466	c1c(cc2c(c1)C[C@H](NC2)C(=O)Nc1cc(ccc1)Cl)OCC(=O)NO	0
H-467	c1c(cc2c(c1)C[C@H](NC2)C(=O)Nc1ccc(cc1)F)OCC(=O)NO	0
H-468	C1N(Cc2n(C1)cc(c2)C(=O)NO)C(=O)c1cccn1C	0
H-469	c1(onc(c1)COCCCCC(=O)NO)c1ccccc1	0
H-470	c1c(cc2c(c1)C[C@H](NC2)C(=O)Nc1cc(c(cc1)F)Cl)OCC(=O)NO	0

H-471	c1(ccc2c(c1)C[C@H](CN2)NC(=O)c1cc(ccc1)Cl)C(=O)NO	0
H-472	c1c(cc2c(c1)C[C@H](NC2)C(=O)Nc1c(cc(cc1)C)C)OCC(=O)NO	0
H-473	c1ccc2c(c1)c(nc(n2)C)N(c1cc(c(cc1)OC)OCCCC(=O)NO)C	0
H-474	c1c(cc2c(c1)C[C@H](N(C2)C(=O)OC(C)(C)C)C(=O)NCc1ccccc1)OCC(=O)NO	0
H-475	C1[C@@H]2C[C@@H]3C[C@H]1C[C@](C2)(C3)NC(=O)NCCCCCC(=O)NO	0
H-476	c1(onc(c1)C(=O)NCCCCC(=O)NO)c1cccc(c1)N	0
H-477	c1(onc(c1)C(=O)NCCCCCCC(=O)NO)c1ccc(cc1)N	0
H-478	c1c(cc2c(c1)C[C@H](NC2)C(=O)NCCCCC)OCC(=O)NO	0
H-479	c1(onc(c1)C(=O)NCCCCC(=O)NO)c1ccccc1	0
H-480	N(O)C(=O)[C@H](Cc1ccc(cc1)OCc1ccccc1)NS(=O)(=O)C	0
H-481	c1c(cc2c(c1)C[C@H](NC2)C(=O)Nc1cc(ccc1)C)OCC(=O)NO	0
H-482	c1(onc(c1)C(=O)NCCCCC(=O)NO)c1ccc(cc1)NC(=O)OC(C)(C)C	0
H-483	C(CCCCC(=O)NO)Cc1nc(no1)c1ccccc1Cl	0
H-484	C(=O)(NO)C1CCCCC1	0
H-485	c1(ccc2c(c1)C[C@H](CC2)Nc1ccc(c(c1)Cl)C#N)C(=O)NO	0
H-486	c1(ccc2c(c1)C[C@H](CC2)Nc1ccc(cc1)[N+](=O)[O-])C(=O)NO	0
H-487	c1c(cc2c(c1)C[C@H](N(C2)C(=O)OC(C)(C)C)C(=O)Nc1c(cc(cc1)C)C)OCC(=O)NO	0
H-488	c1(ccc2c(c1)C[C@@H](CC2)Nc1nccc(n1)c1cc2ccccc2cc1)C(=O)NO	0
H-489	c1c(cc2c(c1)C[C@H](NC2)C(=O)Nc1ccc(cc1)C)OCC(=O)NO	0
H-490	C(=O)(NO)CCCc1ccccc1	0
H-491	c1c(cc2c(c1)C[C@H](N(C2)C(=O)OC(C)(C)C)C(=O)Nc1c(cccc1)C)OCC(=O)NO	0
H-492	C(=O)(Nc1ccccc1)CCCCCCN(C=O)O	0
H-493	c1c(cc2c(c1)C[C@H](NC2)C(=O)NCCc1ccccc1)OCC(=O)NO	0
H-494	c1c(cc(cc1)c1csc(n1)NC(=O)CCCCCCC(=O)NO)[N+](=O)[O-]	0
H-495	NCCCC(=O)N1[C@@H](CC2(SCCS2)C1)C(=O)NCCCCCC(=O)NO	0
H-496	c1c(cc2c(c1)C[C@H](NC2)C(=O)Nc1c(cccc1)C)OCC(=O)NO	0
H-497	c1c(cc(cc1)NC(=O)CCCCCCC(=O)NO)n1nnc(c1)c1ccccc1	0
H-498	c1c(cc2c(c1)C[C@H](N(C2)C(=O)OC(C)(C)C)C(=O)Nc1cccc2c1cccc2)OCC(=O)NO	0
H-499	C1(CCC(c2c1ccc(c2)NC(=O)c1ccc(cc1)C(=O)NO)(C)C)(C)C	0
H-500	c1c(cc2c(c1)C[C@H](N(C2)C(=O)OC(C)(C)C)C(=O)NC(C)(C)C)OCC(=O)NO	0
H-501	c1(onc(c1)C(=O)NCCCCCCC(=O)NO)c1ccc(cc1)NC(=O)C	0
H-502	C(=O)(CCCCc1nn(cc1)Cc1ccc(cc1)n1ccc2ccccc12)NO	0
H-503	c1c(ccc(c1)O[C@H]1CCN(C1=O)c1ccccc1)C(=O)NO	0
H-504	c1c(cc2c(c1)C[C@H](NC2)C(=O)NCc1ccccc1)OCC(=O)NO	0
H-505	c1ccc2c(c1)c(nc(n2)C)N(c1cc(c(cc1)OC)OCCCCC(=O)NO)C	0
H-506	C(=O)(CCCCc1nn(cc1)Cc1ccc(cc1)c1ccccc1)NO	0
H-507	C(CCCCC(=O)NO)C[NH3+]	0
H-508	C(CCCCC(=O)NO)Cc1nc(no1)c1ccc(cc1)C	0
H-509	c1cc(ccc1C(=O)NO)C(=O)N[C@@H](c1c2c([nH]c1)cccc2)C(=O)Nc1ccc(cc1)C	0
H-510	c1c(cc2c(c1)C[C@H](NC2)C(=O)Nc1ccc(cc1)OC)OCC(=O)NO	0
H-511	C1CN([C@H](C1)COC)Cc1ccc(cc1)C(=O)NO	0

H-512	[C@@H]1(CCC[C@@H]1c1ccc(cc1)C(=O)NO)COC	0
H-513	c1c(cc2c(c1)C[C@H](NC2)C(=O)NCCCCCC)OCC(=O)NO	0
H-514	N(O)C(=O)[C@H](Cc1ccc(cc1)OCc1ccccc1)NC(=O)C	0
H-515	c1(onc(c1)C(=O)NCCCCC(=O)NO)c1cccc(c1)NC(=O)OC(C)(C)C	0
H-516	C1SC2(SC1)C[C@H](N(C2)C(=O)[C@@H](N)C)C(=O)NCCCCCC(=O)NO	0
H-517	n1c(nc(N(c2ccc(cc2)OCCCC(=O)NO)C)c2c1CCC2)C	0
H-518	c1c(ccc(c1)N[C@H]1CC(=O)N(C1)c1ccccc1)C(=O)NO	0
H-519	c1cc(cc(c1)Oc1ccccc1)C(=O)NO	0
H-520	C(=O)(Nc1ccccc1)CCCCCN(C=O)O	0
H-521	c1(c(ccc(c1)c1ccc(cc1)/C=C/C(=O)NO)O)[C@]12C[C@@H]3C[C@H](C1)C[C@@H](C3)C2	0
H-522	C(=O)(c1cc2c(cc1)cccc2)NCCCCCN(C=O)O	0
H-523	ONC(=O)c1coc(c2cccs2)n1	0
H-524	c1c(ccc(c1)N([C@@H]1CCN(C1=O)c1ccccc1)C)C(=O)NO	0
H-525	c1c(cc2c(c1)C[C@H](NC2)C(=O)Nc1ccccc1)OCC(=O)NO	0
H-526	C(c1onc(c2sccc2)n1)NCc1ccc(C(=O)NO)cc1	0
H-527	C(CCCCC(=O)NO)Cc1nc(no1)c1ccc(cc1)F	0
H-528	c1c(ccc(c1)C[C@@H](C(=O)NO)NC(=O)c1ccccc1)OCc1ccccc1	0
H-529	C(/C(=C/c1ccc(cc1)/C=C/C(=O)NO)/c1ccc(cc1)F)NC1CC1	0
H-530	c1(ccc(cc1)C(=O)NO)CN(CC)CC	0
H-531	C(C)C(CC)c1ccc(cc1)C(=O)NO	0
H-532	N(O)C(=O)[C@H](Cc1ccc(cc1)OCCc1ccccc1)NS(=O)(=O)C	0
H-533	C(=O)(NCCCCCN(C=O)O)CCc1ccccc1	0
H-534	ONC(=O)c1coc(c2cc(ccc2)c2ccccc2)n1	0
H-535	C1SC2(SC1)C[C@H](N(C2)C(=O)[C@@H]1CCCN1)C(=O)NCCCCCC(=O)NO	0
H-536	C(=O)(NO)Cc1ccccc1	0
H-537	c1c(cc(cc1)NC(=O)CCCCCCC(=O)NO)c1nnn(c1)c1ccc(cc1)F	0
H-538	ONC(=O)c1csc(c2ccccc2)n1	0
H-539	c1c(cc2c(c1)C[C@H](NC2)C(=O)NC(C)(C)C)OCC(=O)NO	0
H-540	ONC(=O)c1csc([C@@H](c2ccccc2)c2ccccc2)n1	0
H-541	[NH3+]CCC[NH2+]CCCCCC(=O)NO	0
H-542	c1(C(=O)NO)c2c(ccc1)cccc2	0
H-543	ONC(=O)c1coc(c2ccc(cc2)Br)n1	0
H-544	N(O)C(=O)[C@H](Cc1ccc(cc1)OCCc1ccccc1)NC(=O)C	0
H-545	C(CCCCC(=O)NO)[NH3+]	0
H-546	C(=O)(c1cc(c2ccccc2)ccc1)NO	0
H-547	ONC(=O)c1noc(c2ccc(cc2)Br)n1	0
H-548	ONC(=O)c1coc(c2c(cccc2)Br)n1	0
H-549	c1c(ccc(c1)C(=O)NO)C(=O)NCCN1CCN(CC1)C	0
H-550	C(=O)(c1ccccc1)NCCCCCN(C=O)O	0
H-551	c1c(cc(c(c1)N[C@H]1CCN(C1=O)c1ccc(cc1)Cl)Cl)C(=O)NO	0
H-552	CCCC(=O)NO	0

H-553	ONC(=O)c1coc(c2ccc3c(c2)cccc3)n1	0
H-554	ONC(=O)c1coc(c2ccc(cc2)c2ccccc2)n1	0
H-555	N(O)C(=O)[C@H](Cc1ccc(cc1)OCCc1ccccc1)NC(=O)c1ccccc1	0
H-556	ONC(=O)c1coc(c2ccc3c(c2)ccc(c3)OC)n1	0
H-557	N(O)C(=O)[C@H](Cc1ccc(cc1)OCc1ccccc1)NC(=O)c1ccc(cc1)C	0
H-558	ONC(=O)c1coc(c2ccc(cc2)Cl)n1	0
H-559	C(=O)(NO)/C=C/C=C/c1ccc(c2ccc(c(c2)[C@]23C[C@@H]4C[C@H](C2)C[C@@H](C4)C3)OC)cc1	0
H-560	C(=N\NC(=S)N1CCN(CC1)C(=O)NO)/c1c(cccc1)O	0
H-561	ONC(=O)c1coc(c2ccc(cc2)C)n1	0
H-562	c1cc(cc2c1n(c(n2)CC(C)C)CCCO)CCC(=O)NO	0
H-563	ONC(=O)c1csc(Cc2ccccc2)n1	0
H-564	ONC(=O)c1csc(c2ccc(cc2)Br)n1	0
H-565	ONC(=O)c1noc(c2ccccc2)n1	0
H-566	C(=O)(NO)C(CCC)CCC	0
H-567	ONC(=O)c1coc(c2ccccc2)n1	0
H-568	S(=O)(=O)(N[C@@H](Cc1ccc(cc1)OCc1ccccc1)C(=O)NO)c1ccc(cc1)C	0
H-569	C(=N\NC(=S)N1CCN(CC1)C(=O)NO)/c1ccc(cc1)Cl	0
H-570	ONC(=O)c1coc(c2ccc(cc2)F)n1	0
H-571	ONC(=O)c1coc(c2ccc(cc2)OC)n1	0
H-572	N(O)C(=O)[C@H](Cc1ccc(cc1)OCCc1ccccc1)NC(=O)c1ccc(cc1)C	0
H-573	ONC(=O)c1csc(c2nccnc2)n1	0
H-574	c1ccc(cc1)[C@H](C(=O)NO)c1ccccc1	0
H-575	N(O)C(=O)[C@H](Cc1ccc(cc1)OCCc1ccccc1)NS(=O)(=O)c1ccc(cc1)C	0
H-576	C1C=C(C(=O)N1CCCc1cc2c(cc1)cccc2)CCC(=O)NO	0
H-577	[NH3+]CCCCC(=O)NO	0
H-578	c1ccc2c(c1)c(nc(n2)C)N(c1cc(c(cc1)OC)OCC(=O)NO)C	0
H-579	c1ccc2c(c1)c(nc(n2)C)N(c1cc(ccc1)OCCCCCC(=O)NO)C	0
H-580	c1ccc2c(c1)c(nc(n2)C)N(c1cc(ccc1)OCCCCC(=O)NO)C	0
H-581	c1ccc2c(c1)c(nc(n2)C)Nc1cc(c(cc1)OC)OCCCC(=O)NO	0
H-582	c1ccc2c(c1)c(nc(n2)C)N(c1cc(ccc1)OCCCC(=O)NO)C	0
H-583	c1ccc2c(c1)c(nc(n2)C)N(c1cc(ccc1)OCC(=O)NO)C	0
H-584	C(CCCCC(=O)NO)Cc1nc(no1)c1ccc(cc1)OC	0
H-585	C(CCCCC(=O)NO)Cc1nc(no1)c1ccc(cc1)C(F)(F)F	0
H-586	C(CCCCC(=O)NO)Cc1nc(no1)c1ccc(cc1)Cl	0
H-587	c1cccc(c1)C(=O)NC(=O)NCCCC(=O)NO	0
H-588	C(=O)(N(O)CCCCCCCC(=O)Nc1ccccc1)C	0
H-589	C(=O)(N(O)CCCCCC(=O)Nc1ccccc1)C	0
H-590	C(=O)(N(O)CCCCCCC(=O)Nc1ccccc1)OC	0
H-591	c1c(cc(cc1)NC(=O)CCCCCCC(=O)NO)c1nnn(c1)c1ccc(cc1)I	0
H-592	c1c(cc2c(c1)Cc1n(C2)c(=O)n(c1O)c1ccc(cc1)c1ccccc1)OCC(=O)NO	0
H-593	c1c(cc2c(c1)Cc1n(C2)c(=O)n(c1O)c1ccccc1)OCC(=O)NO	0

Cl* = Class of the compounds (*1 = Active; 0 = Inactive*)

4.2.2. Dataset Division

Prior to the model developments, the 593 compounds of the dataset is divided into two different sets namely the test set and the training set. The 593 compounds of this hydroxamate-based dataset are separated into the training and the test set by the random splitting of the data, using "Generate Training and Test Data" module present in the Discovery studio 3.0 software. The constructed training set contained 445 compounds whereas a test set containing 148 compounds to maintain a ration of 3:1 for the training set and the test set.

4.2.3. Bayesian classification study

It is seen that, the concepts of fragment-based Bayesian classification study not only provided a great success across numerous disciplines including drug design and discovery [Xia et al. 2004, Klon et al. 2006, Prathipati et al. 2008, Liu et al. 2014, Amin et al. 2018a] but also produced good results in the preliminary study on the tetrahydroisoquinoline derivatives. Bayesian modeling has an advantage not only to obtain the data frequency statistics but also this technique is effective for larger datasets.

Bayes' theorem is a theory that, given enough data, can predict the probability of a certain event [Amin et al. 2018a, Berger 2013, Box & Tiao 2011].

Here, in this classification based study on the basis of the biological activity, these compounds were classified into two different classes using a threshold value. In this study, using the mean biological activity of the dataset was used as threshold value where the compounds possessed higher HDAC8 inhibition than the threshold were classified as active compounds and compounds possessed activity lower than or equals to threshold were assigned as inactive compounds. For the development of a Bayesian classification model on this dataset, the active compounds were assigned a value of 1 where the inactive ones were given a value of 0 in a binary manner.

In this current study, the Bayesian classification models constructed in Discovery Studio 3.0 software in which the molecular properties of the compounds like the physicochemical and structural information including lipophilicity (*AlogP*), molecular weight (*MW*), molecular fractional polar surface area (*FPSA*), total number of aromatic

rings (*nAR)*, total number of rings (*nR*), number of hydrogen bond donor (*nHBD*) and hydrogen bond acceptor (*nHBA*) features and number of rotatable bonds (*nRB*) are used for model development. Additionally, with extended connector of molecular fingerprint of diameter 6 (*ECFP_6*) and Functional classed extended connectivity Fingerprint of diameter 6 (*FCFP_6*) of the Discovery Studio 3.0 software which belongs to the class of 2D topological fingerprints (circular) were also taken into account for development of the Bayesian model using the training set in order to characterize the structural features of these hydroxamate-based HDAC8 inhibitors. In this modeling, the combinations of molecular properties, *ECFP_6* and *FCFP_6* [Sastry et al. 2010, O'Boyle & Sayle 2016] are used to develop 3 different Bayesian models which are also validated externally, using the help of the constructed test set.

4.2.2. Recursive partitioning study

Recursive partitioning (RP) is a multivariate analysis used frequently to classify members of the population by constructing one or more decision trees and uses the molecular descriptors step by step to discriminate the compounds in active and inactive and is able to provide different physic-chemical, structural and sub-structural features have a significant influence on the biological activity of the molecules [Chen et al. 2011, Halder et al. 2013, Adhikari et al. 2016].

In this study, Similar to the Bayesian classification model development, the Recursive Partitioning models for these diverse set of hydroxamate derivatives are also constructed using the combination of the physicochemical and structural properties such as *AlogP, MW, FPSA, nAR, nHBA, nR*, *nHBD, nRB* and the connectivity fingerprints like *ECFP_6* and *FCFP_6* similar to the Bayesian classification study.

4.2.3. Statistical analysis and evaluation of Models

The performance of the constructed model was internally and externally evaluated by computing the receiver operating characteristic (*ROC*) curve of the training and the test sets HDAC8 inhibitors [Amin et al. 2017c].

Moreover, the accuracy (*Acc*), sensitivity or the True positive rate (*Se*), specificity (*Sp*) and precision *(Pr)* were also considered to justify the constructed Bayesian as well as the

Recursive partitioning models using the ***Equation 4.8*** - ***Equation 4.11*** [Amin et al. 2017c, Amin et al 2018a].

$$Se = \frac{TP}{TP+FN} \qquad \textbf{\textit{Equation 4.8}}$$

$$Sp = \frac{TN}{TN+FP} \qquad \textbf{\textit{Equation 4.9}}$$

$$Acc = \frac{TP+TN}{TP+TN+FP+FN} \qquad \textbf{\textit{Equation 4.10}}$$

$$Pr = \frac{TP}{TP+FP} \qquad \textbf{\textit{Equation 4.11}}$$

Whereas TP is true positives value; TN is true negatives value; FP is false positives value and FN is the false negative value.

Chapter 5: *Result Discussion*

Chapter 5: *Result Discussion*

5.1. Results of the preliminary study using a small dataset

5.1.1. Regression-based 2D-QSAR study

By the implementation of the stepwise-multiple linear regression (S-MLR) method on the training set molecules, the model with the best statistical outcomes is constructed using 8 2D-PaDEL descriptors and is given in ***Equation 5.1***. Additionally, the contributions of these selected molecular descriptors of these tetrahydroisoquinoline in their HDAC8 inhibitory activity derivatives are provided n ***Table 5.1***.

pIC_{50} (HDAC8) = -8.530 (±1.124) +0.385 (±0.057) *BCUTp-1h* +1.631 (±0.249) *IC4* +0.150 (±0.019) *minHBint3* -8.029 (±2.007) *VCH-6* +0.079 (±0.018) *ATSC8*p +0.000 (±0.000) *VR1_Dt* +0.014 (±0.003) *AATS8v* -0.000 (±0.000) *VR1_Dzi*. ***Equation 5.1***

Table 5.1. Summary of the description and contribution of the molecular descriptors present in the S-MLR model.

Descriptor	***Full description***	***Correlation***
BCUTp-1h	nlow highest polarizibility weighted BCUTS	Positive
IC4	Information content index (neighborhood symmetry of 4 order)	Positive
minHBint3	Minimum E-state descriptors of strength for potential Hydrogen Bonds of path length 3	Positive
VCH-6	Valance chain, order 6	Negative
ATSC8p	Centered Broto-Moreau autocorrelation of lag 8 Weighted by polarizibility	Positive
VR1_Dt	Randic-like eigenvector-based index from detour matrix	Positive
AATS8v	Average Broto-Moreau auto correlation-lag 8/weighted by van der waals volumes	Positive
VR1_Dzi	Randic-like eigenvector-based index from Barysz matrix / weighted by first ionization potential	Negative

The MLR model (***Equation 5.1***) which was constructed on the 61 compounds in the training set (N_{train} = 61) and externally validation of the model was done using the test set molecules (N_{test} = 20) which provided significant statistical outcomes such as: R^2 = 0.851, *SEE* = 0.278, R^2_{adj} = 0.828, *F* (8, 52) = 37.190, *PRESS* = 4.018, *average* $r_m{}^2{}_{LOO}$ = 0.722, *average* $r_m{}^2{}_{(test)}$ = 0.507, Q^2 = 0.799, R^2_{pred} = 0.508, *RMSEP* = 0.455, $cR_p{}^2$ = 0.792, Q^2_{f1} = 0.508, Q^2_{f2} = 0.507.

Chapter 5: *Result Discussion*

From these statistical outcomes of the S-MLR model, it is clearly seen that the model equation (***Equation 5.1***) predicts 79.88% variance and explains 82.83% variance in the inhibitory activity of these compounds against HDAC8. It is also seen that the external validation of the model provided an externally-validated R^2 value of R^2_{pred} = 0.508 along with an externally and externally validated average r_m^2 values such as average $r_m^2{}_{(test)}$ = 0.507 and average $r_m^2{}_{LOO}$ of 0.722. Besides that, the S-MLR model passed the Golbraikh and Tropsha validation criteria [Golbraikh & Tropsha, 2002] and provided significant p-values whereas the proximal Q^2_{f1} and Q^2_{f2} values of this model indicated the systematic splitting of biological activity for the training and the test set. Additionally, experimental (observed) and the predicted activity for the compounds of this model is given in ***Figure 5.1*** **(A)** along with the normalized mean distance values of these compounds calculated during the Applicability domain (AD) analysis provided in ***Figure 5.1*** **(B)** [Banerjee et al. 2019b]. Aside from the original model (***Equation 5.1***), another 100 MLR models were constructed using the same 8 descriptors by scrambling the test and the training set compounds which is given in ***Table 5.2***.

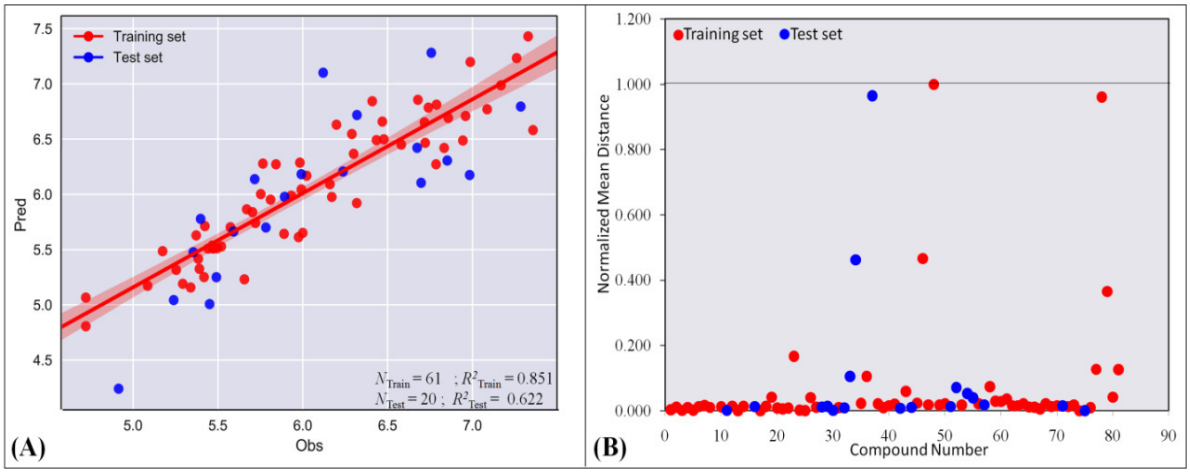

Figure 5.1. **(A)** The observed and predicted values obtained from S-MLR model along with the correlation between the variables used in the developed 2D-QSAR model. **(B)** Applicability domain (AD) of this data set compounds.

Table 5.2. Summary of constructed 100 MLR models along with the ***Equation 5.1***.

Model No	R^2	R^2_{adj}	Q^2	*SEE*	*PRESS*	*P value*	R^2_{pred}
01	0.836	0.810	0.765	0.292	4.449	Passed	0.572
02	0.793	0.762	0.646	0.314	5.117	Failed	0.746
03	0.797	0.769	0.694	0.318	5.258	Failed	0.753
04	0.813	0.784	0.702	0.324	5.443	Failed	0.659
05	0.849	0.826	0.779	0.284	4.189	Passed	0.424
06	0.821	0.794	0.726	0.299	4.640	Failed	0.650
07	0.850	0.827	0.768	0.284	4.183	Failed	0.385
08	0.854	0.832	0.776	0.288	4.315	Passed	0.297
09	0.817	0.789	0.742	0.314	5.114	Passed	0.629
10	0.850	0.827	0.750	0.280	4.081	Passed	0.451
11	0.834	0.808	0.735	0.291	4.394	Failed	0.597
12	0.824	0.796	0.725	0.313	5.101	Passed	0.641
13	0.834	0.808	0.764	0.295	4.534	Passed	0.563
14	0.771	0.736	0.649	0.325	5.491	Passed	0.825
15	0.860	0.839	0.795	0.274	3.907	Passed	0.398
16	0.870	0.850	0.804	0.260	3.506	Passed	0.264
17	0.825	0.798	0.732	0.309	4.979	Failed	0.532
18	0.793	0.761	0.680	0.342	6.081	Failed	0.771
19	0.814	0.785	0.699	0.308	4.942	Passed	0.520
20	0.865	0.844	0.800	0.278	4.020	Failed	-0.141
21	0.851	0.828	0.767	0.288	4.311	Failed	0.351
22	0.765	0.728	0.652	0.335	5.851	Failed	0.754
23	0.806	0.776	0.708	0.324	5.452	Failed	0.728
24	0.787	0.754	0.690	0.322	5.389	Passed	0.752
25	0.818	0.790	0.710	0.307	4.916	Failed	0.679
26	0.810	0.781	0.709	0.317	5.242	Failed	0.706
27	0.851	0.829	0.786	0.289	4.354	Passed	0.378
28	0.831	0.805	0.754	0.299	4.643	Passed	0.606
29	0.820	0.792	0.707	0.291	4.397	Failed	0.718
30	0.853	0.831	0.781	0.287	4.279	Passed	0.431
31	0.784	0.750	0.625	0.308	4.942	Passed	0.786
32	0.829	0.803	0.736	0.288	4.309	Failed	0.623
33	0.853	0.831	0.785	0.275	3.945	Failed	0.528
34	0.759	0.721	0.633	0.327	5.561	Failed	0.812
35	0.841	0.817	0.763	0.294	4.499	Passed	0.482
36	0.798	0.767	0.697	0.323	5.429	Failed	0.528
37	0.789	0.756	0.612	0.318	5.263	Failed	0.723
38	0.817	0.788	0.737	0.310	4.993	passed	0.612
39	0.829	0.803	0.752	0.290	4.378	Passed	0.613
40	0.835	0.810	0.753	0.296	4.547	Failed	0.509
41	0.770	0.735	0.629	0.339	5.964	Failed	0.816
42	0.802	0.771	0.704	0.334	5.800	Failed	0.708
43	0.821	0.793	0.710	0.293	4.451	Failed	0.650

44	0.820	0.792	0.737	0.304	4.820	Passed	0.595
45	0.821	0.793	0.709	0.287	4.272	Failed	0.678
46	0.796	0.764	0.707	0.323	5.432	Passed	0.728
47	0.816	0.788	0.737	0.312	5.070	Passed	0.638
48	0.768	0.732	0.657	0.333	5.755	Failed	0.831
49	0.851	0.828	0.770	0.285	4.213	Failed	0.424
50	0.805	0.775	0.713	0.317	5.240	Passed	0.710
51	0.758	0.721	0.630	0.342	6.077	Failed	0.870
52	0.785	0.752	0.677	0.335	5.832	Failed	0.789
53	0.794	0.763	0.699	0.324	5.442	Failed	0.640
54	0.823	0.796	0.749	0.301	4.705	Failed	0.649
55	0.809	0.780	0.740	0.304	4.797	Passed	0.682
56	0.845	0.821	0.746	0.286	4.257	Failed	0.589
57	0.833	0.808	0.749	0.298	4.613	Passed	0.505
58	0.832	0.806	0.745	0.306	4.860	Passed	0.473
59	0.807	0.777	0.686	0.313	5.109	Failed	0.727
60	0.808	0.778	0.729	0.296	4.553	Passed	0.669
61	0.826	0.799	0.721	0.296	4.564	Failed	`0.656
62	0.772	0.736	0.632	0.328	5.584	Failed	0.741
63	0.814	0.786	0.713	0.308	4.938	Failed	0.659
64	0.787	0.754	0.688	0.322	5.394	Failed	0.772
65	0.807	0.778	0.701	0.322	5.389	Passed	0.579
66	0.827	0.800	0.760	0.282	4.146	Passed	0.649
67	0.814	0.786	0.703	0.300	4.680	Failed	0.707
68	0.825	0.798	0.748	0.312	5.056	Passed	0.537
69	0.800	0.769	0.662	0.320	5.330	Failed	0.731
70	0.834	0.809	0.736	0.292	4.449	Failed	0.648
71	0.818	0.790	0.716	0.303	4.955	Passed	0.572
72	0.809	0.780	0.707	0.320	5.333	Failed	0.719
73	0.798	0.767	0.703	0.323	5.414	Passed	0.662
74	0.804	0.774	0.680	0.322	5.395	Passed	0.723
75	0.802	0.772	0.694	0.320	5.326	Failed	0.724
76	0.771	0.736	0.644	0.346	6.212	Failed	0.865
77	0.824	0.797	0.741	0.307	4.905	Failed	0.528
78	0.821	0.794	0.737	0.307	4.914	Passed	0.647
79	0.827	0.801	0.729	0.291	4.399	Failed	0.520
80	0.799	0.768	0.686	0.314	5.122	Failed	0.760
81	0.798	0.767	0.664	0.313	5.100	Passed	0.750
82	0.817	0.789	0.718	0.317	5.228	Failed	0.677
83	0.792	0.759	0.653	0.329	5.623	Failed	0.775
84	0.811	0.782	0.705	0.311	5.045	Failed	0.736
85	0.838	0.814	0.763	0.292	4.435	Failed	0.580
86	0.859	0.838	0.795	0.283	4.170	Passed	0.340
87	0.785	0.752	0.649	0.331	5.681	Failed	0.809
88	0.832	0.806	0.760	0.285	4.221	Passed	0.515
89	0.820	0.792	0.724	0.303	4.784	Failed	0.653

90	0.818	0.790	0.715	0.302	4.747	Failed	0.663
91	0.790	0.758	0.678	0.318	5.248	Failed	0.761
92	0.817	0.789	0.718	0.315	5.173	Failed	0.561
93	0.804	0.774	0.628	0.304	4.814	Passed	0.743
94	0.855	0.833	0.782	0.279	4.056	Failed	0.030
95	0.839	0.814	0.765	0.279	4.054	Passed	0.619
96	0.800	0.770	0.707	0.310	5.006	Failed	0.727
97	0.814	0.786	0.691	0.295	4.528	Failed	0.700
98	0.788	0.755	0.669	0.333	5.753	Failed	0.806
99	0.822	0.795	0.747	0.296	4.569	Passed	0.638
100	0.795	0.764	0.690	0.318	5.255	Passed	0.767
Equation 5	**0.851**	**0.828**	**0.799**	**0.278**	**4.018**	**Passed**	**0.508**

5.1.1.1. Contributions of molecular descriptors

The contributions of the 8 selected molecular descriptors toward the HDAC8 inhibitory activity of these tetrahydroisoquinoline based hydroxamate derivatives were clearly suggested by the ***Equation 5.1***, depicted in ***Table 5.1*** whereas the ***Figure 5.2*** is additionally provided to display the correlation matrix of these descriptors with the biological activity [Banerjee et al. 2019b].

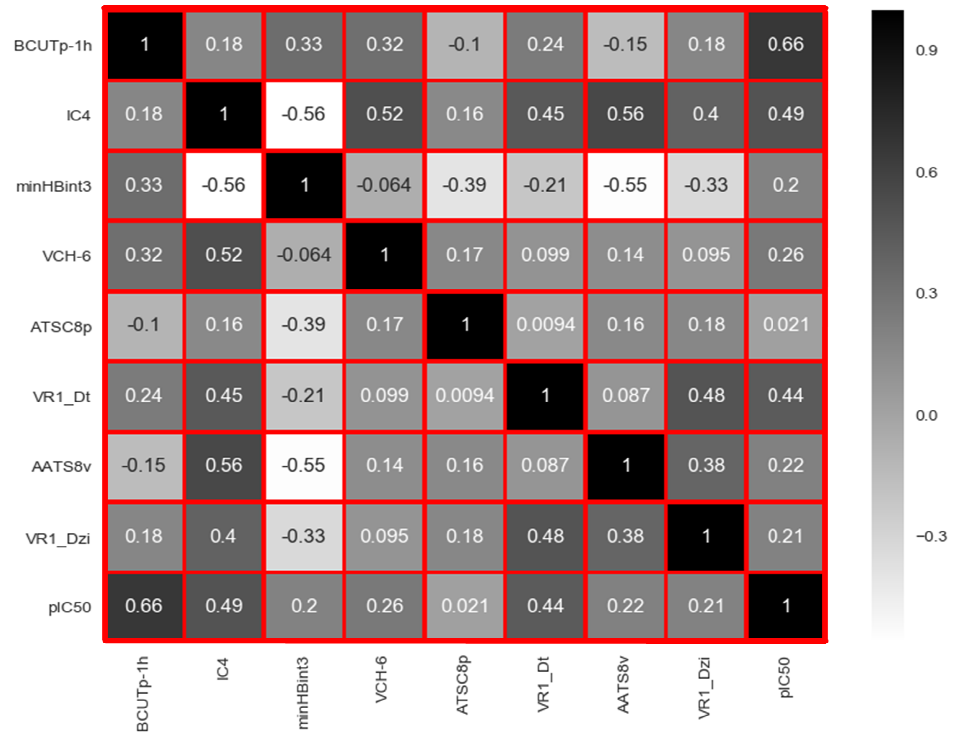

Figure 5.2. Heatmap of the correlation matrix of the selected molecular descriptors with the pIC_{50} values of the compounds

From the ***Equation 5.1***, the descriptor *BCUTp-1h* (nlow highest polarizibility weighted BCUTS) depicted a positive correlation with the HDAC8 inhibitory potency of these compounds. This might suggest the significance of the large, bulky hydrophobic group substitution in the R_2 and R_3 positions of area-B of the scaffold ***Figure 4.1*****(A)**. Several compounds of this tetrahydroisoquinoline dataset (Compounds **T-62, T-63, T-65 to T-69** and **T-71 to T-73**) exhibited higher HDAC8 inhibition while possessing higher values of *BCUTP-1h*. The only exception of this scenario is the compound **T-70** which though having higher *BCUTp-1h* values and bulky cyclohexyl moiety exhibited poor HDAC8 inhibition. This observation may signify the important effects of the unsaturated pi bonds present in the other compounds (Compounds **T-62, T-63, T-65** to **T-69** and **T-71** to **T-73**) except the compound **T-70** containing unsaturated pi bond-less cyclohexyl group for their higher HDAC8 inhibition [Banerjee et al. 2019b].

IC4 is the Information content index of neighborhood symmetry of order 4 exhibited its positive correlation with the inhibitory potency of these tetrahydroisoquinoline hydroxamate derivated HDAC8 inhibitors. This descriptor (*IC4*) may indicate the positive contributions of the 4-methoxy phenyl amino carboxyl moiety present in the R_4 positions in area-C [***Figure 4.1*****(A)**] of these derivatives, where the compounds **(**compounds **T-24, T-33** to **T-59** and **T-74** to **T-81**) containing such type of functions [CONH(4-OMePh) function] also possessed higher HDAC8 inhibition as well as higher *IC4* values.

The *VR1_Dt* (Randic-like eigenvector-based index from detour matrix) descriptor from the S-MLR model, was positively correlated itself with the HDAC8 inhibitory activity of these tetrahydroisoquinoline compounds and also indicated the positive influences of the 4-methoxy phenyl amino carboxyl [CONH(4-OMePh)] moiety for better HDAC8 inhibition. The compounds (Compounds **T-34, T-46** and **T-77** to **T-79**) which contained higher *VR1_Dt* values exhibited higher HDAC8 inhibition compared to the compounds (Compounds **T-10, T-12, T-14, T-16, T-18, T-20** and **T-22**) don not possess a 4-methoxy phenyl amino carboxyl have lower values of *VR1_Dt* and were also poorly active against HDAC8.

The negative correlation of the descriptor *VCH-6* (Valance chain of order 6) clearly indicated about that presence of any larger alkyl chain in the structure of these

compounds can deduce the activity whereas it is observed that compounds such as **T-28** to **T-31** and **T-61** containing a large alkyl chain exhibited poor HDAC8 inhibition.

The ***Equation 5.1*** showed the descriptor *minHBint3* (Minimum E-state descriptors of strength for potential Hydrogen Bonds of path length 3) as a positive influencer of the HDAC8 inhibitory activity of these tetrahydroisoquinoline hydroxamate derivatives which can be correlated with the hydrogen bond forming capability in the area-B ***Figure 4.1*****(A)** of the tetrahydroisoquinoline scaffold and with the alkyl chain length of the substitutions of the area-B. Also, several compounds like compounds **T-60** to **T-73** showed higher values of *minHBint3* and some of them have good HDAC8 inhibitory activity.

The positive correlation between the descriptor *ATSC8p* (Centered Broto-Moreau autocorrelation of lag 8 weighted by polarizability) and the biological activity (HDAC8 inhibitory activity) was shown in the ***Equation 5.1***., which can be correlated with the Boc substitutions of these compounds. Compounds such as compounds **T-40, T-42, T-44, T-48, T-50, T-74** and **T-76** containing Boc group substitution at the area-B and a bulky group expressed higher HDAC8 inhibition.

VR1_Dzi (Randic-like eigenvector-based index from Barysz matrix/weighted by first ionization potential) was suggested as the negative influencer for the activity of these HDAC8 inhibitors where the descriptor *AATS8v* (Average Broto-Moreau auto correlation-lag 8/weighted by Van der Waal volumes) showed positive contributions toward the activity and may be correlated with the van der Waal volume of the area-B. Different groups namely $CO(CH_2)_3Ph$ (Cpd **T-58**), COPh (Cpd **T-56**), COBnz (Cpd **T-54**), and $COCH_2OPh$ (Cpd **T-33**) may possess higher van der Waal volume in the area-B and exhibited higher HDAC8 inhibition. This observation might indicate the beneficial effects of carboxy alkyl aryl or carboxyaryl moiety substitution at the area-B of the compounds ***Figure 4.1*****(A)** for higher HDAC8 inhibition [Banerjee et al. 2019b].

5.1.2. Bayesian Classification-based 2D QSAR study

The Receiver Operating Characteristics (*ROC*) based Bayesian classification study was conducted for the fragmental analysis of these HDAC8 inhibitors [Banerjee et al. 2019b]. The *ROC*-based statistical validation of the constructed Bayesian model delivered

significant results and provided a Leave-One-Out cross validation *ROC* value of ROC_{CV} = 0.885, five-fold cross-validation *ROC* of 0.871 for the training set where the *ROC* plots obtained from the model is given in ***Figure 5.3*** and the other *ROC* based statistical outcomes of the model is shown in ***Table 5.3***.

Additionally, the Bayesian classification model delivered a total of 40 molecular sub-structures containing 20 good and 20 bad sub-structural features responsible for modulating the HDAC8 inhibitory activity of these tetrahydroisoquinoline compounds which are provided in ***Figure 5.4*** and ***Figure 5.5*** respectively**.**

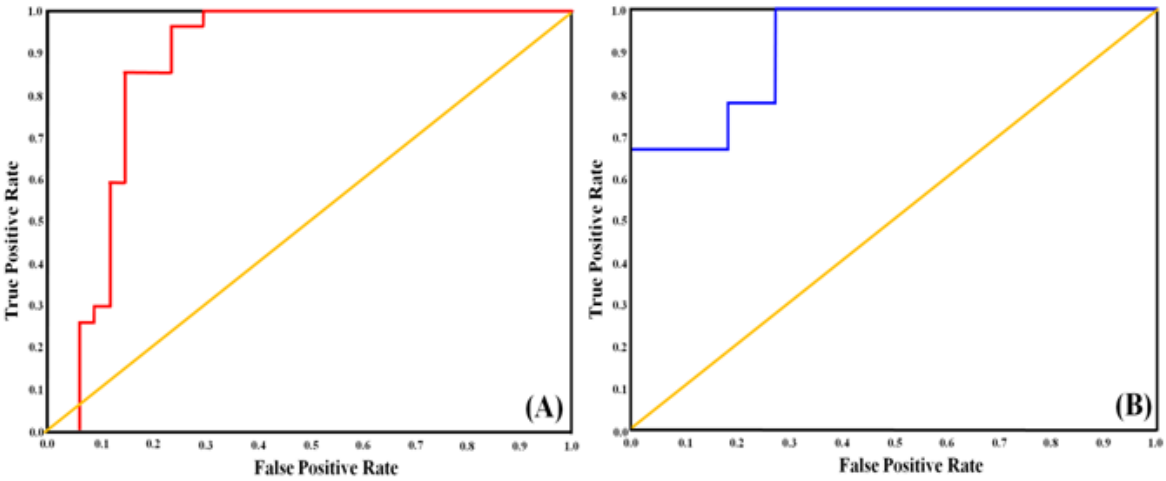

Figure 5.3. ROC plots obtained from the Bayesian model (A) Training set (5-fold CV), (B) Test set.

Table 5.3. Summary of the validation parameters given by the Bayesian classification model.

Set	*ROC*	ROC_{CV}	*TP*	*FN*	*FP*	*TN*	*Sensitivity*	*Specificity*	*Concordance*
Training	0.871	0.885	27	0	10	24	1.000	0.706	0.836
Test set	0.919	--	8	1	3	8	0.889	0.727	0.800

By the help of the Bayesian classification study identification of the influences of the molecular substructural features responsible for regulating the HDAC8 inhibitory activity of these tetrahydroisoquinoline derivatives became possible. The aminoester (G1) and the animobutoxy carbonyl (NHBoc) moieties (G2) including the sub-structures features G4-G5 displayed their positive influence of the NHBoc group for the higher HDAC8 inhibition of these compounds. A large number of these derivatives bearing the NHBoc

group in their structure (Cpds **T-38, T-40, T-42, T-44, T-46, T-48, T-50, T-52, T-74** to **T-75** and **T-77**) seemed to have excellent HDAC8 inhibitory activity in the nanomolar range. During the comparison of these HDAC8 inhibitors to their corresponding NHBoc group analogs, these molecules seemed to have better HDAC8 inhibitory activity than their NHBoc group unsubstituted analogs (compound **T-1** *vs* compound **T-2,** compound **T-3** *vs* compound **T-4,** compound **T-5** *vs* compound **T-6,** compound **T-7** *v***s** compound **T-8,** compound **T-9** *vs* compound **T-10,** compound **T-13** *vs* compound **T-14,** compound **T-15** *vs* compound **T-16,** compound **T-17** *vs* compound **T-18,** compound **T-21** *vs* compound **T-22,** compound **T-25** *vs* compound **T-26,** compound **T-27** *vs* compound **T-28,** compound **T-29** *vs* compound **T-30** and compound **T-31** *vs* compound **T-32**) which clearly explained the beneficial influence of the NHBoc group present in the structure of these compounds for providing better HDAC8 inhibitory activity [Banerjee et al. 2019b]. The substructures G7-G11 was able to identify the important contribution of aryl group substituted tetrahydropyridine ring along with the dimethylene group substitution at the heterocyclic nitrogen atom. Compounds containing these types of substructural feature such as compounds **T-63, T-65** to **T-67** and **T-71** to **T-73** were also seemed to have highly effective against HDAC8 enzymatic activity. The Substructural features G13 and G16 showed the significance of the benzyl group substitution at the chiral carbon atom of these tetrahydroisoquinoline derivatives for the higher HDAC8 inhibitory potency. Several molecules (Compounds **T-40, T-42 and T-43)** possessing such type of benzyl group were seemed to have higher HDAC8 inhibitory activity.

The substructural features G15 and G17 depicted the significance of the dicarboxamido group substitution in the tetrahydropyridine scaffold of these HDAC8 inhibitors. Compounds with this type of structure seemed to bear higher HDAC8 inhibitory potency (Compounds **T-35** to **T-37, T-41, T-43, T-49, T-51, T-53** and **T-58**). The importance of substituted amine groups was well attributed in the substructural feature G12 at the tetrahydroisoquinoline chiral carbon atom. Besides, substructural feature G14 and G18 displayed the significance of the tertiary nitrogen atom attached to a chiral carbon atom of the tetrahydroisoquinoline ring and the dimethylene carbonyl group. The compounds containing these features (Compounds **T-40, T-41** and **T-43**) showed promising HDAC8 inhibitory activity [Banerjee et al. 2019b].

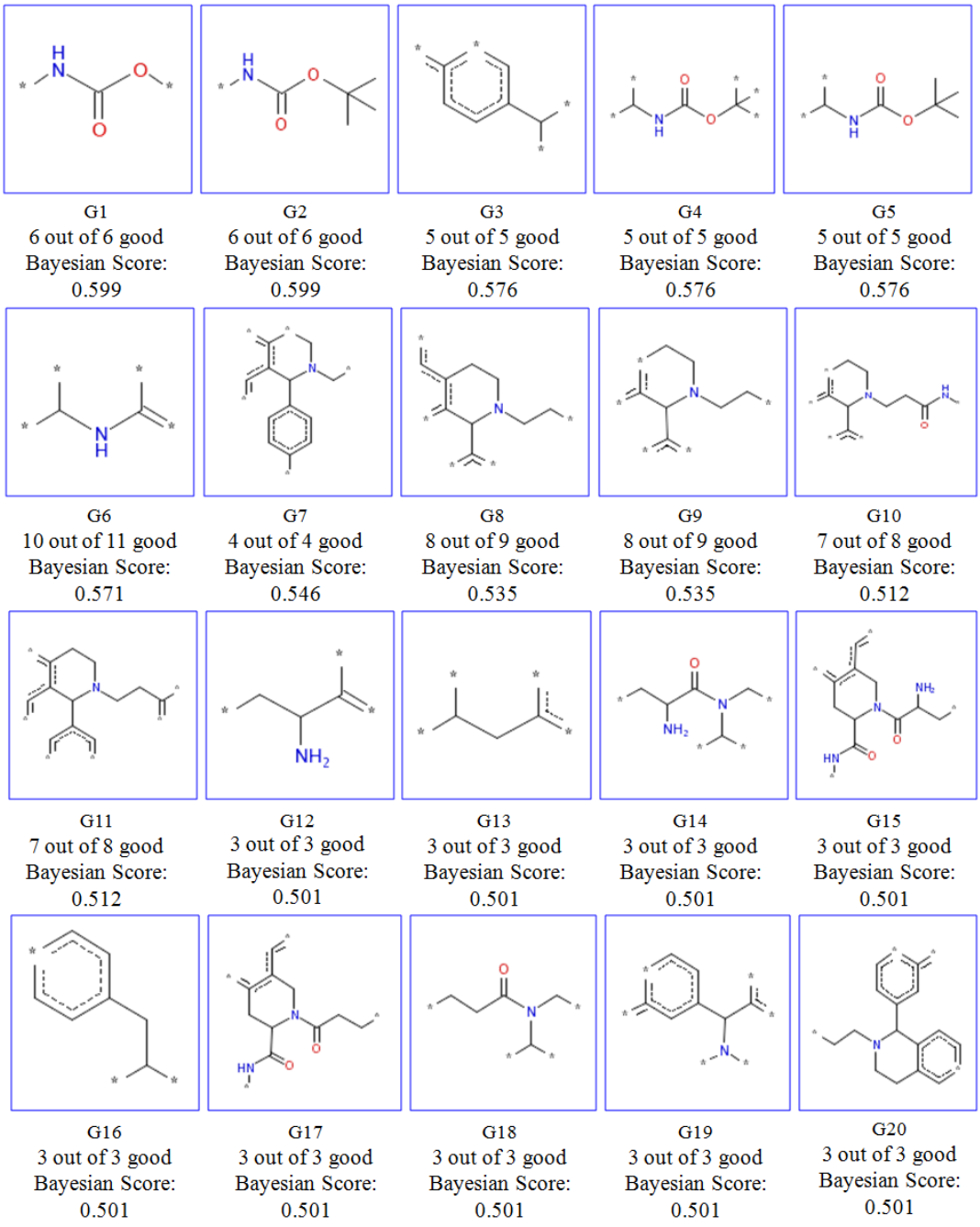

Figure 5.4. Good molecular fingerprints generated by Bayesian classification model.

While the analysis of the bad molecular substructures with negative influence on the activity of these compounds, surprisingly, the tetrahydroisoquinoline scaffold alone (B13), the ether function containing tetrahydroisoquinoline scaffold (B1 and B2) or the

tetrahydroisoquinoline scaffold containing carboxyl (B3-B4) or ester (B9) or carboxamide (B14) group substitutions were suggested as a detrimental factor for HDAC8 inhibitory potency of these compounds.

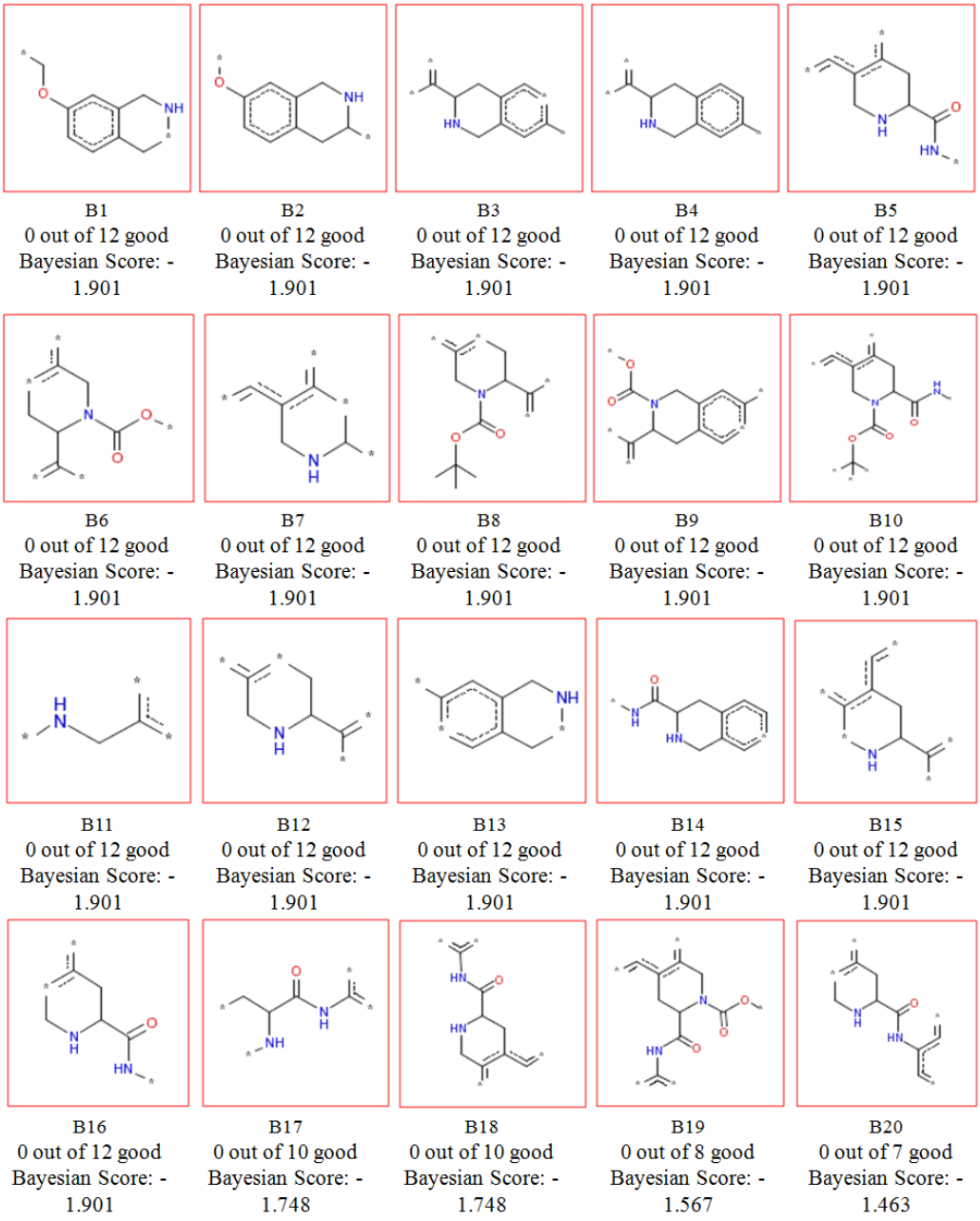

Figure 5.5. Bad molecular fingerprints generated by Bayesian classification model.

As because all of the compounds of this hydroxamate-based dataset posses a common tetrahydroisoquinoline scaffold as its core, it can be assumed that the HDAC8 inhibitory

potency of these compounds may be dependent on the R_1 and R_2 group substituents and on the hydroxamate moiety. From these observations, it can be said that in order to better higher HDAC8 inhibition, replacement of the tetrahydroisoquinoline scaffold with different groups can be useful. Also, the structural fragments B6, B8-B10 and B19 suggested the ester group substitution at the tetrahydropyridine nitrogen atom can act as a detrimental factor for the HDAC8 inhibitory potency of these HDAC8 inhibitors. From the observation of the experimental inhibitory activity of these compounds against HDAC8, it was observed that the compounds with these of structural features produce lesser active HDAC8 inhibitors (Compounds **T-3, T-11, T-15, T-19, T-23, T-25, T-27, T-29** and **T-31**). Additionally, the carboxamido substitution near the nitrogen atom tetrahydroisoquinoline scaffold was also identified as unfavorable for HDAC8 inhibitory activity which is displayed in substructural features B5, B10, B16, B18, and B20. The dataset compounds containing these features (Compounds **T-1** to **T-32**) are seemed to deliver lower HDAC8 inhibition. Finally, the substructure B11 suggested about the negative influence of the aminobenzyl substitution on HDAC8 inhibition of the compounds. The aminoaryl group containing molecules were therefore lower active inhibitors (Compounds **T-3** and **T-4**) whereas the substructure B17 displayed the detrimental effect of the aryl carboxamido group substitution near the tetrahydropyridine nitrogen atom (Compounds **T-1** to **T-2, T-8, T-10, T-11** to **T-16, T-18, T-19 5** to **T-20, T-22 to T-23** and **T-25** to **T-26**) [Banerjee et al. 2019b].

5.1.3. 3D CoMFA study

From the statistical aspects, The CoMFA model built using these tetrahydroisoquinoline derivated compounds yielded significant statistically outcomes. The CoMFA model yielded an internally cross-validated Q^2 value of Q^2 = 0.554 using 5 optimum components whereas the non-cross validation R^2 value delivered by the model was 0.927 along with *SEE* of 0.188. Additionally, the 10-fold internally cross-validated R^2 value was R^2_{CV} = 0.564 with 4 optimal components while providing a bootstrap R^2 of $R^2_{\text{Bootstrap}}$ = 0.961 and a scrambled Q^2 = 0.504 **(*Table 5.4*)** which was lesser than its value of cross-validation Q^2. This signifies that the constructed CoMFA model was not obtained by chance. From all these statistical outcomes this model seemed to be explaining the

significance of electrostatic and steric contributions of 41.30% and 58.70% respectively. The electrostatic and steric contours maps of the compounds **T-61**, **T-62** and **T-64** are shown in ***Figure 5.6*** [Banerjee et al. 2019b].

Table 5.4. Summary of the CoMFA model of the tetrahydroisoquinoline analogs.

Model	R^2	R^2_{CV}	$R^2_{Bootstrap}$ (10 runs)	Q^2	Q^2(Scrambled)	SEE
CoMFA	0.927	0.564	0.961	0.554	0.504	0.188

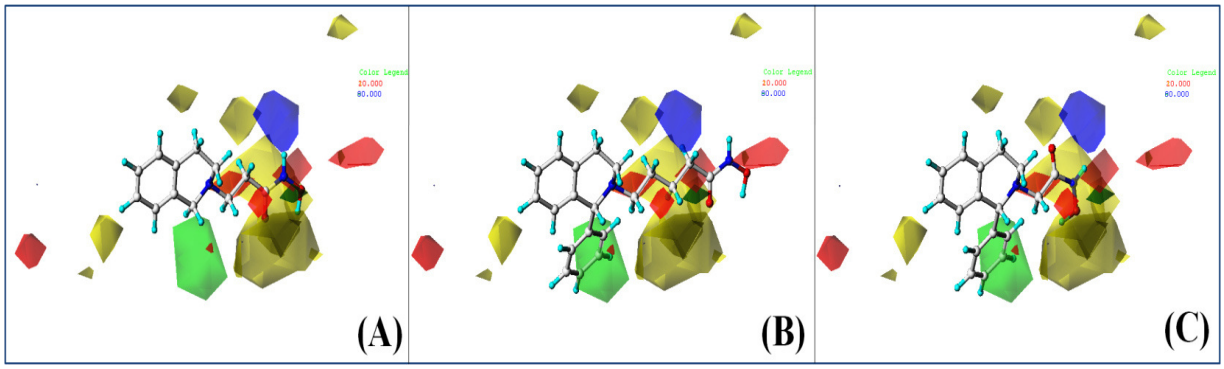

Figure 5.6. Contour maps of the Compound **T-61** (A), Compound **T-62** (B) and Compound **T-64** (C) obtained from CoMFA study.

From the CoMFA contour maps of the most active molecule generated by the CoMFA study (Compound **T-62**) it was seen that the phenyl moiety of the compound substituted at the 1-position of the tetrahydroisoquinoline ring has entered into a steric favorable area (**green**) [***Figure 5.6***] indicated toward the positive influences of the bulky steric group substitution at the 1-position of the tetrahydroisoquinoline ring for the higher HDAC8 inhibitory potency. Additionally, near the area-A ***Figure 4.1*****(A)** of the tetrahydroisoquinoline moiety, a steric unfavorable region (**yellow**) has been shown which suggested detrimental effects of the bulky steric group substitution at that position for the activity. It is seen that the compounds (Compounds **T-1** to **T-32)** possessing oxymethyl hydroxamate function at that position may be a crucial factor for reducing their HDAC8 inhibitory activity [Banerjee et al. 2019b].

Also, a steric unfavorable region (**yellow**) was shown by the contour in the area-A of the scaffold of ***Figure 4.1*****(A)** Compounds suggesting the unfavorability of bulky steric substitution at that position for the activity. Compounds **T-1** to **T-32** which possesses an oxymethyl hydroxamate group at that position is maybe an important factor for reduction

of the HDAC8 inhibition of those compounds. Also, the backbone structure of these compounds was encompassed by a bigger steric unfavorable region suggesting bulky steric substitution at this position is unfavorable for the activity.

In case of the effects of the electrostatic fields toward the activity of these compounds, it is seen that an electrostatic unfavorable region (**red**) is present proximal to the hydroxamate function. This may be suggesting that greater electronegativity shown by the group at that position may produce better coordination with the catalytic Zn^{2+} ion of HDAC8. The importance of that nitrogen atom for the activity of these compounds was indicated by an electrostatic unfavorable region proximal to the tetrahydroisoquinoline heterocyclic nitrogen atom. A heterocyclic favorable electropositive (**blue**) field was observed at a distance from the molecule. From these observations, the CoMFA study may be clearly indicated toward the significance of the different substitutions at R_2, R_3 and R_4 positions of the tetrahydroisoquinoline moiety for regulating the HDAC8 inhibitory potency of these molecules [Banerjee et al. 2019b].

5.1.4. H-QSAR study

During the development process of H-QSAR model on these tetrahydroisoquinoline derivatives, different combinations of carbon atom (**C**), bond (**B**), atom (**A**), chirality (**Ch**), hydrogen atom (**H**) and donor-acceptor feature (**DA**) are used for the model construction in which a few of these models were unable to cross-validation criteria because of their lower R^2_{cv} values (acceptable limit < 0.5) (***Table 5.5***). On the basis of the highest values of the internally validated R^2 value of the models, **Model-A** (R^2_{cv} = 0.576) was identified as the best model among all the constructed H-QSAR models **(*Table 5.5*)**.

Table 5.5. Summary of the constructed H-QSAR model of the tetrahydroisoquinoline analogs.

Model	*Fragment distinction*	R^2_{CV}	R^2	*SE*	*Length*	*Component*
A	**A/B/C**	**0.576**	**0.664**	**0.395**	**353**	**2**
B	A/B/H	0.461	0.697	0.383	353	4
C	A/B/Ch	0.525	0.731	0.360	59	4
D	A/B/DA	0.503	0.612	0.425	307	2
E	A/B/C/H	0.541	0.659	0.402	53	3
F	A/B/C/Ch	0.564	0.675	0.389	353	2
G	A/B/C/DA	0.518	0.701	0.376	353	3

H	A/B/H/Ch	0.476	0.699	0.381	97	4
I	A/B/H/DA	0.476	0.632	0.418	71	3
J	A/B/Ch/DA	0.503	0.607	0.428	151	2
K	A/B/C/H/Ch	0.517	0.661	0.401	53	3
L	A/B/C/Ch/DA	0.518	0.627	0.417	257	2
M	A/B/C/H/DA	0.476	0.710	0.374	307	4
N	A/B/H/DA/Ch	0.471	0.673	0.397	353	4
O	A/B/C/H/Ch/DA	0.481	0.720	0.368	307	4

N.B.: Bold faces indicate the best model.

The development of the Model-A was done using different fragment distinctions of C, B and A along with the atom counts exhibited an R^2 of 0.664 and a *SE* of 0.395. To judge the superiority of the model, further development was das using different atom counts which yielded the best model with an atom count of 4-7 according to its R^2_{cv} value, highest with respect of the other models (***Table 5.6***). The external validation of this model provided a predicted R^2 value R^2_{pred} = 0.795 which suggested that the model successfully passed bothe internal and external validation criteria [Banerjee et al. 2019b]. Additionally, the H-QSAR generated contour maps of the compounds **T-61**, **T-62** and **T-64** are provided in ***Figure 5.7***.

Table 5.6. Summary of the atom counts of model-A of H-QSAR study

Model	*Atom Coun*	R^2_{CV}	R^2	*SE*	*Length*	*Component*
A-1	1-4	0.484	0.660	0.405	59	4
A-2	2-5	0.535	0.654	0.405	59	3
A-3	3-6	0.564	0.672	0.391	257	2
A-4	**4-7**	**0.576**	**0.664**	**0.395**	**353**	**2**
A-5	5-8	0.573	0.684	0.387	53	3
A-6	6-9	0.553	0.699	0.377	61	3
A-7	7-10	0.554	0.693	0.381	61	3

N.B.: Bold faces indicate the best model.

The model generated fragments, displayed their significance in the modulation of the HDAC8 inhibitory potency of these compounds in different colour coding such as greenish-blue and green coloured fragments denoted their positive effects whereas the orange-red and red coloured fragments pointed at the fragments with a detrimental impact on the activity. Interestingly for most active compound (Compound **T-62**), the presence of only green and yellow fragments reflected their positive influence in HDAC8 inhibitory activity of the compounds such as the green coloured carbon fragments, noticed in the fused phenyl ring of the scaffold. From the tetrahydroisoquinoline ring, two

hydrogen atoms of the marked in yellow colour including a hydrogen atom in green colour reflected their positive influence for HDAC8inhibitory potency of the compounds **T-62** and **T-64** (***Figure 5.7***).

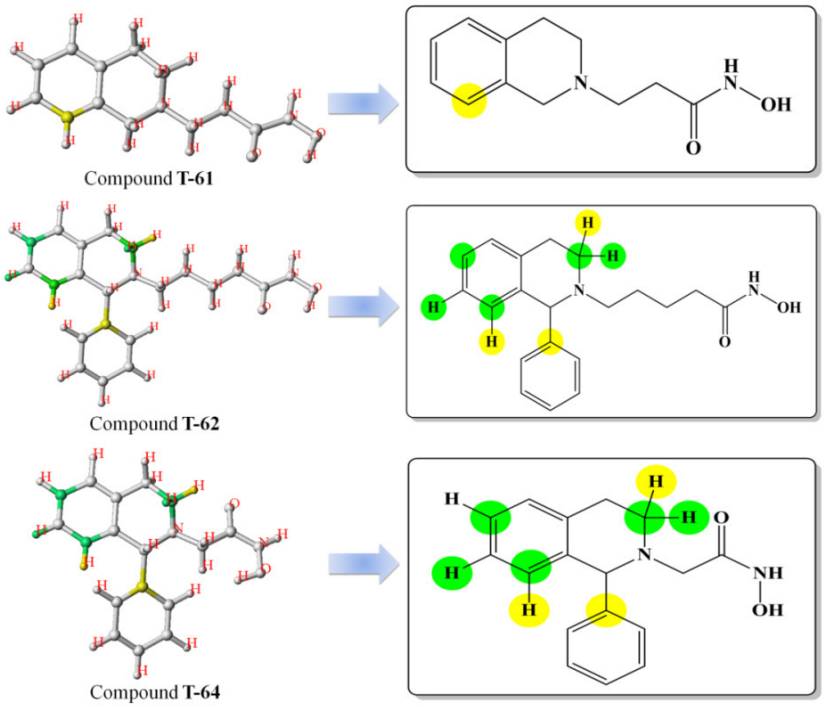

Figure 5.7. Contour maps of compounds **T-62, T-61**and **T-64** generated by HQSAR model.

The fragments compound showing white colour fragments indicate their moderate or ineffectiveness toward the HDAC8 inhibition. Also, no red or orange-red fragments were noticed in case of all the three compounds (Compounds **T-61**, **T-62**, **T-64**). Nevertheless, some similar fragments with similar contributions were also seen both the most active (Compound **T-62**) and the least active compound (Compound **T-64**). However, the other least active compound (Compound **T-61**) displayed dissimilarity and exhibited just a yellow coloured carbon atom in the fused phenyl ring of its tetrahydroisoquinoline scaffold presenting a moderately positive influence toward its activity. No red or red-orange coloured fragments were compound **T-61** also (***Figure 5.7***). Therefore, the HQSAR study signified the importance of tetrahydroisoquinoline ring along with 1-phenyl group substitution near the alkyl hydroxamate function of these compounds for higher HDAC8 inhibition [Banerjee et al. 2019b].

Chapter 5: *Result Discussion*

5.2. Study of the diverse large dataset of Hydroxamate derivatives

5.2.1. Bayesian classification study

The employment of the fragment-based Bayesian classification technique was quite helpful in order to identify important molecular fragments influencing HDAC8 inhibitory activity of these diverse set of hydroxamate derivatives obtained from the Binding database. Three different Bayesian models were constructed using the molecular properties of these compounds, combining the molecular properties with the Extended connectivity fingerprints of diameter 6 (*ECFP_6*) and also combining the molecular properties of these compounds along with the *FCFP_6* descriptors of these molecules. The study disclosed a total of different substructural fragments of these molecules responsible for modulating the HDAC8 inhibitory activity. The molecular fingerprints are shown in ***Figure 5.8-Figure 5.11*** respectively. Among the total 593 compounds of this dataset (***Table 4.2***), 455 compounds were taken to construct the training set where the remaining 148 compounds were taken as the test set to conduct this classification based molecular modeling studies. The results of a *ROC* based statistical analysis on the constructed Bayesian model was also appeared to statistically significant for these models. The other statistical parameters of both the sets (training set and test set) are displayed in ***Table 5.7***.

Table 5.7. Statistical parameters of the constructed Bayesian classification models.

Model	***Descriptors***	***Set***	***ROC***	***ROC_{CV}***	***TP***	***FN***	***FP***	***TN***	***Se***	***Sp***
I	*MP*	Training	0.717	0.688	170	79	60	136	0.683	0.694
		Test	0.673	--	39	41	10	58	0.487	0.853
II	*MP, ECFP_6*	Training	0.853	0.838	190	59	11	185	0.763	0.944
		Test	0.855	--	53	27	9	59	0.662	0.868
III	*MP, FCFP_6*	Training	0.846	0.829	188	61	14	182	0.755	0.929
		Test	0.847	--	53	27	10	58	0.622	0.853

Se: Sensitivity; ***Sp:*** Specificity; ***Con:*** Concordance; ***ROC_{CV}*:** Five-fold cross-validated ROC score.

4.2.1.1. Statistical outcomes of the Bayesian models

From the above statistics, it is clearly seen that Model-I with only the molecular properties of the molecules such as *AlogP, MW, FPSA, nAR, nHBA, nR*, *nHBD, nRB* depicted that they do have contributions for modifying the HDAC8 inhibitory potency of these molecules and provided a five-fold cross-validation *ROC* score of 0.688 for the training set, depicting their poor discriminant power for the Model-I. Moreover, it provided the *Se* and *Sp* values for the training set compounds as 0.683 and 0.694, respectively (for Model-I). The overall prediction accuracy of the training set was 67.3% as per model-1.

On the other hand, other two models (Model-II and Model-III) containing the molecular properties along with the molecular fingerprints (*ECFP_6* and *FCFP_6*) were able to provide better discrimination for the compounds of this diverse set of hydroxamate group containing HDAC8 inhibitors than the Model-I. The Model-II, constructed using the *ECFP_6* and the molecular properties of these compounds, was able to provide a ROC value of 0.853 and 0.855 for the constructed training and the test set compounds respectively. The Model-II also provided *ROC* score (ROC_{CV}) of 0.838 for five-fold cross-validation along with a sensitivity of 0.763 and specificity of 0.944 for the training set with an 84.3% accuracy.

The ***Figure 5.8*** and ***Figure 5.9*** shows the Model-II generated good and bad molecular fingerprints generated respectively.

While discussing the third model constructed using the molecular properties and the *FCFP_6* descriptors (Model-III), the model produced statistical outcomes almost similar to the outcomes of the Model-II. This model provided a *ROC* score of 0.846, ROC_{CV} of 0.829, sensitivity 0.755 and specificity of 0.929 for the training set with an overall prediction accuracy of 84.7%. Additionally, ***Figure 5.10*** and ***Figure 5.11 shows*** the Model-III generated good and bad molecular fingerprints respectively.

From the study of these statistical outcomes, it was observed that the Model-II and Model-III provided a good amount of discrimination capability for these hydroxamate derivatives better than the Model-I. These models were also able to identify the

significant molecular fingerprints of these molecules responsible for modulation of the HDAC8 inhibitory potency of these molecules.

5.2.1.2. Analysis of the ECFP_6 fingerprint descriptors generated molecular fingerprints (Model-II)

The molecular fragments with positive effects on HDAC8 inhibitory potency of these HDAC8 inhibitors, generated by the *ECFP_6 descriptors* are provided in ***Figure 5.8***. From these fingerprints it is observed that the sub-structure G1-G4 reflected the beneficial effects of the meta-acryl group substituted phenyl ring for the inhibitory activity of these compounds against HDAC8, suggesting the meta-substituted phenyl ring may act as a linker group of these HDAC8 inhibitors for better HDAC8 inhibition.

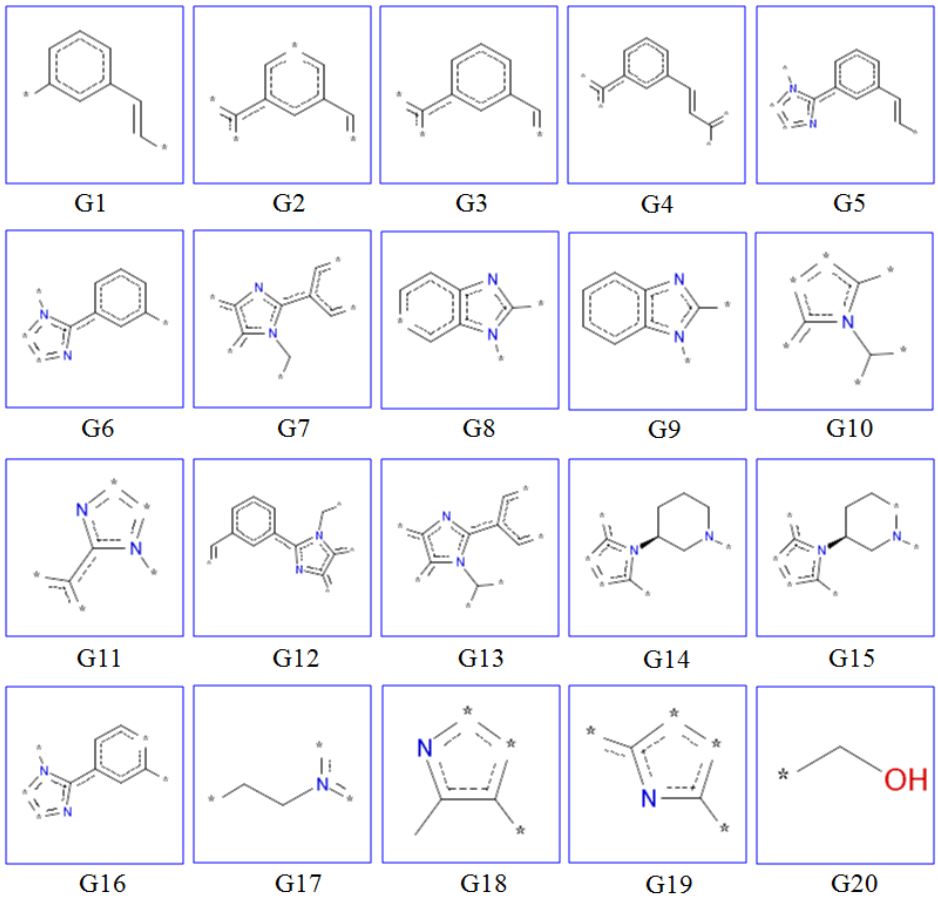

Figure 5.8. The good molecular fingerprints generated by *ECFP_6 fingerprint descriptor* of Model-II

The molecular fragments G5-G7, G10-G13, and G16 suggested about the *N*-substituted 2-phenyl imidazole moiety as a positive influencer of the activity of these compounds. Substructural feature G5 also shows the importance of olefinic bond substituted at 3-position of the phenyl ring. Moreover, G5-G7, G12, G16, G18-G19 substructures have structural similarity with substructure and represent *N*-substituted-2-phenyl imidazole which reflects the importance of *m*-substitution at the phenyl ring for the better HDAC8 inhibition.

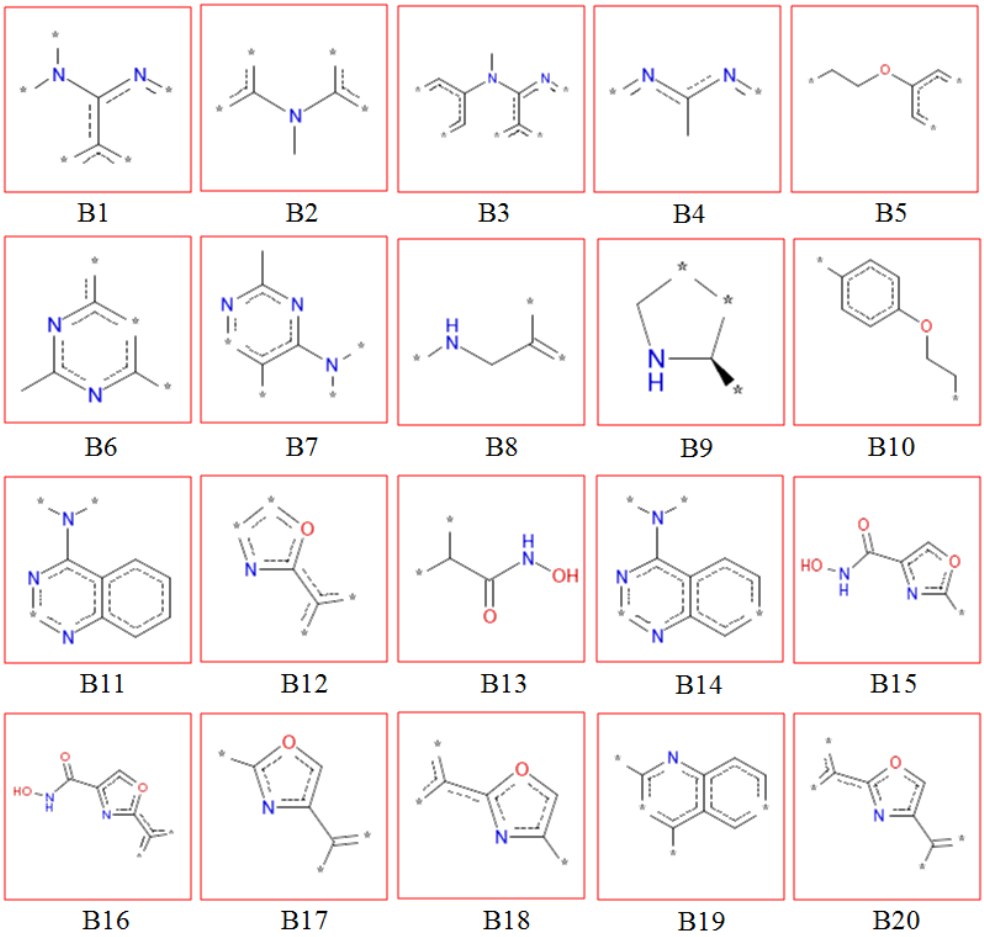

Figure 5.9. The bad molecular fingerprints generated by *ECFP_6 fingerprint descriptor* of Model-II

The molecular fingerprints G8 and G9 represented the N-substituted benzimidazole moiety as an important and good moiety for the activity of these compounds. This might suggest the role of the benzimidazole moiety as a cap group for the better interaction

inside the HDAC8 active site. The sub-structure G14 and G15 may display the positive effects of the *N*-piperidine substituted imidazole, benzimidazole or pyrrole moiety on the inhibitory activity of these molecules against HDAC8 activity. Also, the fragment G17 indicated the n-alkyl group substitution at the imidazole heterocyclic nitrogen atom as a positive influencer for the activity whereas G20 identified the hydroxymethyl moiety as a good substructure for HDAC8 inhibition.

Bad molecular sub-structures produced by *ECFP_6* fingerprint descriptors having negative effects on the HDAC8 inhibitory potency are provided in ***Figure 5.9***. The sub-structure B1, B4, B6-B7, B11, B14, and B19 may signify the negative influence of the quinazoline, naphthyridine and pyrimidine moiety for the HDAC8 inhibitory activity of these compounds. It may suggest that these moieties are a poor surface recognition factor for the compounds and as a cap group either does not provide good interaction with the active site amino acid residues of the HDAC8 or hinders the entry of the molecule inside the narrow pocket of HDAC8 because of its large structure.

Sub-structure B2 and B3 signified that the *N, N*-biaryl group in the cap group can decrease the HDAC8 inhibitory activity of the compounds. Moieties like aryloxy alkyl groups (B5, B10) and 2-substituted pyrrolidine groups (B9) are also suggested as a detrimental moiety for the activity of these compounds. The molecular fragments B12 and B17-B18 indicated the detrimental effects of the oxazole moiety in the structure for their HDAC8 inhibition. The sub-structures B13, B15, B16, B17, and B20 demonstrated the presence of oxazole is detrimental as the liker motif of the compound for their HDAC8 inhibition. This also proposes to eliminate the oxazole-3-hydroxamate group as the liker-ZBG motif for better HDAC8 inhibition of these compounds.

5.2.1.3. Analysis of the FCFP_6 fingerprint descriptors generated molecular fingerprints (Model-III)

The sub-molecular fragments with beneficial effects and the detrimental effects on the inhibitory potency of these compounds against HDAC8 activity, fabricated by the *FCFP_6 fingerprint descriptors* are furnished in ***Figure 5.10*** and ***Figure 5.11*** respectively.

Chapter 5: *Result Discussion*

By studying the molecular fingerprints delivered by the *FCFP_6 fingerprint descriptors* of the Model-III, it is observed that many of the good molecular fingerprints such as the G21-G33 and G36-G37 are almost identical with the fingerprints produced by the *ECFP_6 fingerprint descriptors* of Model-II. All these descriptors seemed to be suggesting the constructive effects of the acrylamide group, *N*-substituted benzimidazole moiety, *N*-piperidine substituted imidazole, benzimidazole and pyrrole moiety on the HDAC8 inhibition of these compounds. Additionally, the *FCFP_6 fingerprint descriptors* provided some other fingerprints such as the molecular fingerprint G34 displayed branched alkyl chain substituted pyrrole moiety and the fingerprint G35 and G39 suggested the n-alkyl group substituted imidazoline moiety as good contributors for the activity of these compounds.

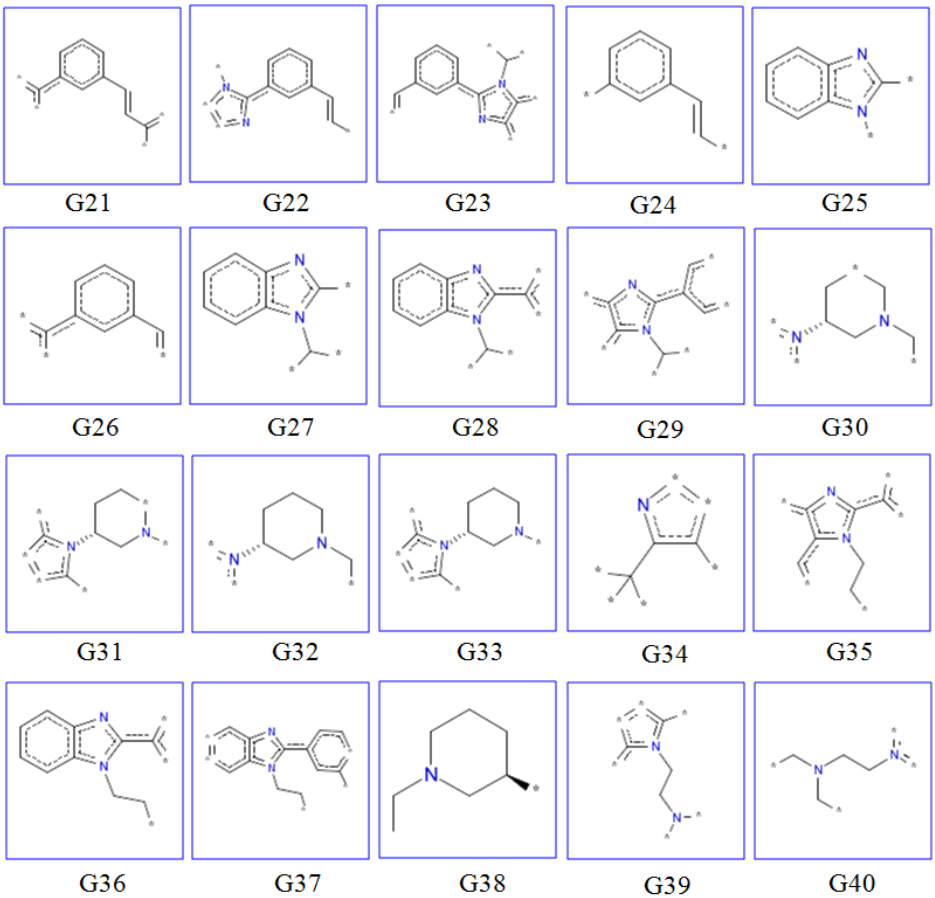

Figure 5.10. The good molecular fingerprints generated by *FCFP_6 fingerprint descriptor* of Model-III

Chapter 5: *Result Discussion*

In case of the bad molecular substructures with detrimental effects on the HDAC8 inhibitory potency of these compounds, the *FCFP_6 fingerprint descriptors* produced some molecular sub-structures such as B21-B24, B26 and B29-36 are similar to the bad molecular sub-structures provided by *ECFP_6 fingerprint descriptors* from Model-II. Besides, there are also some new *FCFP_6 fingerprint descriptors generated* molecular fingerprints by Model-II.

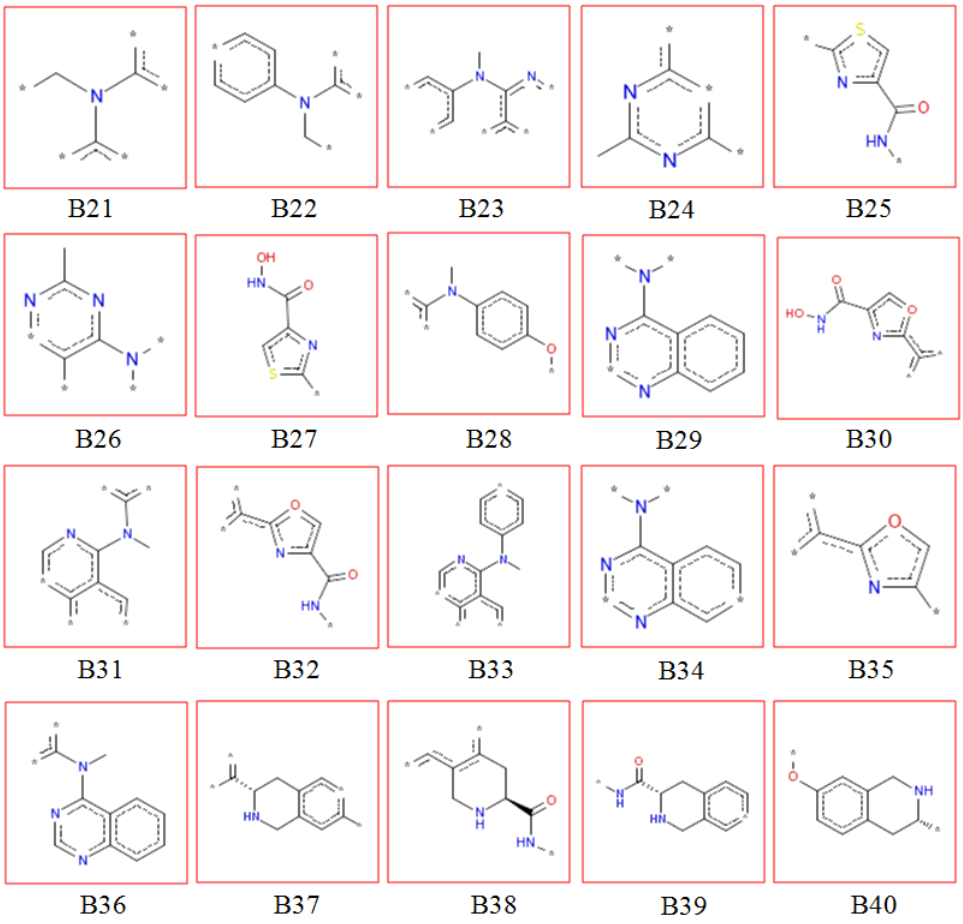

Figure 5.11. The bad molecular fingerprints generated by *FCFP_6 fingerprint descriptor* of Model-III

The molecular sub-structure B25 and B27 indicated the detrimental effects of the thiazole moiety in the linker motif of the compounds as well as the thiazole hydroxamate group as the linker-ZBG moiety for these hydroxamate derivatives. The molecular fragment B38 also suggested the presence of the 2-carnoxamino group substituted piperidine moiety in the structure of the compounds can be detrimental toward HDAC8 inhibitory potency of

these HDAC8 inhibitors. Moreover, the sub-structures B37 and B39-B80 depicted that the presence of 2-carboxamino group substituted tetrahydroisoquinoline moiety or the 6-oxyalkyl group substituted tetrahydroisoquinoline moiety either in the cap group or in the linker motif of the compounds can be negatively correlated with HDAC8 inhibitory potency of these HDAC8 inhibitors.

.5.2.2. Recursive partitioning study

For the construction of more understandable and precise classification based models, Recursive Partitioning (RP) study is conducted on the large dataset of diverse hydroxamate group containing HDAC8 inhibitors by forming the decision trees for the classification of these ligands into the group of compounds like the active compounds and inactive compounds [Chen et al. 2011, Halder et al. 2013, Adhikari et al. 2016].

The decision trees for the recursive partitioning models are constructed by the molecular properties (*MP*) and fingerprints like *ECFP_6* and *FCFP_6*. Different combinations of molecular properties and the molecular fingerprints were used to find the best combination. Five-fold cross-validation method was employed to understand the best predictive performance of the constructed models. The statistical performances of the RP models are shown in ***Table 5.8***. From the ROC_{CV} values generated by the five-fold cross-validation and the externally validated *ROC* score (ROC_{Test}), it is observed that the RP model with the different *molecular* properties of these molecules along with the *ECFP_6 fingerprint descriptors* showed the best results among the three constructed RP models. While comparing the RP model based on molecular properties and the models based on the molecular properties and the fingerprints descriptors it is observed that the addition of the molecular fingerprint descriptors are able to significantly improve the classification where the model provided several significant molecular fingerprints also.

Table 5.8. Comparison of the *ROC*, ROC_{CV} and the ROC_{TEST} values of the PR models.

Model	*Descriptors*	*ROC*	ROC_{CV}	ROC_{Test}
Model-IV	Molecular Properties	0.816	0.723	0.710
Model-V	Molecular Properties + *ECFP_6*	0.908	0.773	0.848
Model-VI	Molecular Properties + *FCFP_6*	0.896	0.750	0.813

From this observation, it can be said that the molecular properties alone are unable to characterize the important sub-structures features which are important and provides a significant contribution to the inhibitory potency of these molecules against HDAC8. Hence, the molecular fingerprints and with the molecular properties together were employed as the molecular descriptors for the RP analysis. Through observations, it is seen that considering these fingerprints during the model development can enhance the model performance and shows better statistical outcomes while comparing with the model developed using only the molecular properties of the compounds. Besides, ***Table 5.9*** contains the statistical outcomes of Model-IV, Model-V, and Model-VI.

Table 5.9. Statistical outcomes of the constructed Recursive Partitioning models

Model	*Descriptors*	*Tree*	*Leaves*	*ROC*	ROC_{CV}	*TN*	*FP*	*FN*	*TP*	ROC_{Test}
IV	*MP*	1	19	0.816	0.723	151	45	63	186	0.710
		2	14	0.801	0.715	144	52	55	194	0.691
		3	13	0.799	0.702	148	48	61	188	0.699
		4	12	0.789	0.702	140	56	52	197	0.702
		5	9	0.774	0.703	138	58	55	194	0.663
		6	7	0.751	0.706	148	48	72	177	0.646
		7	5	0.724	0.661	160	36	104	145	0.698
		8	4	0.705	0.602	149	47	100	149	0.690
		9	2	0.601	0.602	182	14	181	68	0.555
V	*MP* + *ECFP_6*	1	24	0.908	0.773	169	27	55	194	0.848
		2	22	0.905	0.770	169	27	55	194	0.851
		3	13	0.851	0.770	158	38	48	201	0.814
		4	10	0.845	0.767	160	36	56	193	0.808
		5	8	0.836	0.740	151	45	49	200	0.811
		6	6	0.814	0.740	154	42	59	190	0.806
		7	5	0.810	0.749	157	39	69	180	0.797
		8	4	0.793	0.749	159	37	78	171	0.771
		9	3	0.776	0.752	125	71	46	203	0.765
		10	2	0.667	0.654	186	10	153	96	0.608
VI	*MP* + *FCFP_6*	1	23	0.896	0.750	152	44	35	214	0.813
		2	20	0.891	0.741	152	44	35	214	0.813
		3	11	0.852	0.745	155	41	47	202	0.799
		4	10	0.850	0.745	150	46	42	207	0.798
		5	8	0.832	0.756	155	41	52	197	0.794
		6	6	0.807	0.759	159	37	65	184	0.778
		7	5	0.800	0.741	150	46	58	191	0.760
		8	4	0.797	0.741	157	39	73	176	0.758
		9	3	0.781	0.742	123	73	42	207	0.751

		10	2	0.680	0.742	183	13	143	106	0.618

N.B.> *MP*: Molecular properties; *Tree:* Tree number; *Leaves:* Number of leaves.

5.2.2.1. Analysis of the molecular fragments produced by the RP models.

The Recursive partitioning model (Model-V) constructed using the molecular properties and the *ECFP_6* fingerprint descriptors produced 10 molecular fragments which it used to split the decision tree to discriminate the HDAC8 inhibitors. These *ECFP_6* fingerprints are given in ***Figure 5.12***.

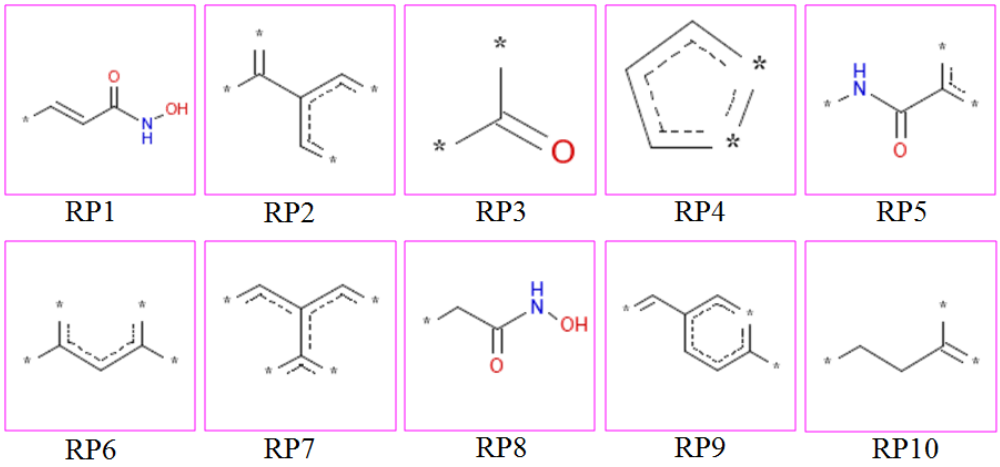

Figure 5.12. *ECFP_6* fingerprints obtained from RP Model-V

Regarding the *ECFP_6* molecular fingerprints produced by the Model-V, all the molecular fingerprints provide either good or bad influence on the HDAC8 inhibitory activity of this large set of hydroxamate-based HDAC8 inhibitors. The fingerprint RP1 signified the importance of the cinnamoyl hydroxamate moiety whereas the fingerprint RP6 suggested the importance of the methyl hydroxamate moiety for the activity of these compounds. The sub-structure RP2 suggested the carboxyphenyl moiety as a regulating factor for the activity. The importance of the carbonyl group for the activity of these hydroxamate group-containing compounds is displayed by the model using the fingerprint RP3 and the RP5 where the fingerprint RP5 not only signifies the importance of the carbonyl moiety as well as the carboxamido group for these compounds. Substructure RP7 and RP9 identified the importance of substitution at the *meta*- and the *para*- positions of the phenyl ring of these compounds for their HDAC8 inhibitory potency. The molecular fragment RP4 signifies the importance of the 5-membered

heterocyclic moieties like pyrrole, pyrrolidine, etc whereas the RP10 signified the ethylcarboxyl moiety for the HDAC8 inhibitory activity of these hydroxamate derivatives.

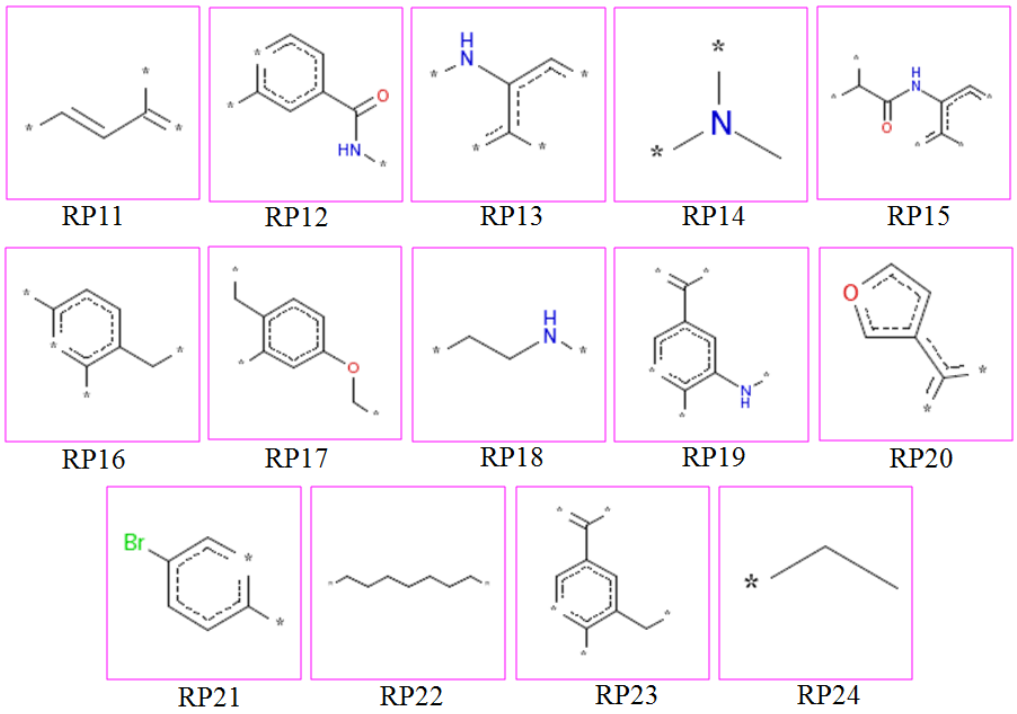

Figure 5.13. *FCFP_6* fingerprints obtained from RP Model-VI

In case of the *FCFP_6* molecular fingerprints produced by the *FCFP_6* fingerprint descriptor used in the Model-VI also identified a group of 14 molecular fragments important to the HDAC8 inhibitory activity if these hydroxamate derivatives which are used to split the compounds into active and inactive. The molecular fingerprints produced by the *FCFP_6* molecules are provided in ***Figure 5.13***.

The molecular fingerprint RP11signified the importance of cinnamoyl moiety for the activity of the compounds whereas the fingerprint RP12 and RP23 suggested the importance of the *meta*-aryl carboxamind aryl moiety as an important molecular sub-structure for the activity. Sub-structural feature RP13, RP15, and RP19 indicated the importance of the *ortho*-, *para*- and *meta*-amino phenyl group for the activity of these compounds. The molecular fragment RP16- RP17 suggested the *ortho*- and *para*-di substituted benzyl moiety as an important structural feature whereas the fingerprint RP21

suggested *para*-bromo phenyl group as an influencer for the activity of the compounds. Fragments RP18, RP22, and RP24 suggested the ethyl amino, *n*-heptyl and methylene groups respectively as important fragments to identify the active and the inactive compounds from this diverse large dataset of hydroxamate group containing HDAC8 inhibitors. The fingerprint RP14 and RP20 helped to identify the significance of the tertiary nitrogen atom and the 3-substituted furan ring for the activity of these compounds.

Chapter 6: *Designing of newer HDAC8 inhibitors*

Chapter 6: *Designing of newer HDAC8 inhibitors*

Using the observations of this study on these HDAC8 inhibitors, a group of newer molecules HDAC8 inhibitors (Compounds **N-1** to **N-6**) is designed (***Table 6.1***) and the ***Equation 5.1*** is used to predict the HDAC8 inhibitory activity of these compounds.

Table 6.1. Newer designed HDAC8 inhibitors with higher predicted HDAC8 inhibitory activity.

Scaffold-A	Scaffold-B
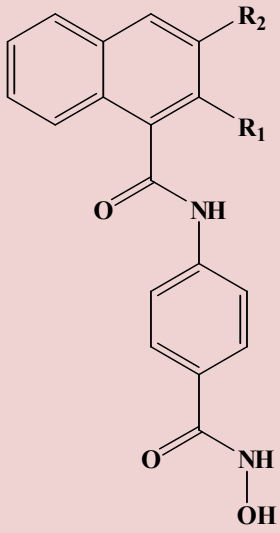	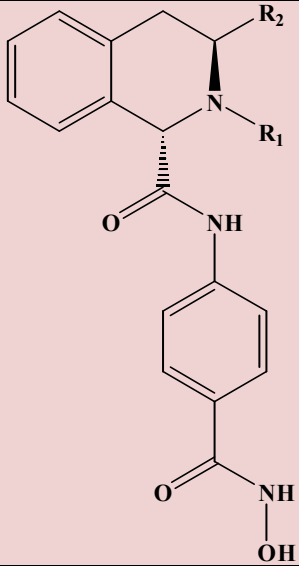

Cpd	*Scaffold*	*R_1*	*R_2*	*IC50 (nM)[a]*	*pIC50[a]*
N-1	A	Bnz	CONH4-BrPh	6.90	8.161
N-4[c]	B	Bnz	*(S)*-CONH4-BrPh	255.00	6.593
N-2	A	(1H-isoindol-1-yl)methyl	CONH4-OMePh	5.73	8.242
N-5[c]	B	(1H-isoindol-1-yl)methyl	*(S)*-CONH4-OMePh	87.35	7.059
N-3	A	CO-O-Bnz	CONH4-OMePh	5.36	8.271
N-6[c]	B	CO-O-Bnz	*(S)*-CONH4-OMePh	122.70	6.911

a: HDAC8 inhibitory activity predicted by ***Equation 5.1***;
b: Reported HDAC8 inhibitory activities are provided for the purpose of comparison.
*c:*Compounds possess *(S)*-conformation at the 1-position of their scaffold-B.

From the predicted activity of these compounds, it is observed that these newly designed molecules (***Table 6.1***) provided higher predicted activity (Compounds **N-1** to **N-3**) for the naphthyl derivatives over their tetrahydroisoquinoline analogs (Compounds **N-4** to **N-6**). As per the suggestions of the 2D-QSAR study, these newly designed molecules depicted the carboxy amidophenyl (CONH4-OMePh) moiety and bulky steric groups as important factors for higher HDAC8 inhibition. The Bayesian classification studies showed the

tetrahydroisoquinoline scaffold as a negative influencer for HDAC8 inhibition. The newer designed HDAC8 inhibitors (***Table 6.1***) also preferred the naphthyl moiety as a better cap group than the tetrahydroisoquinoline moiety for higher activity against HDAC8 [Banerjee et al. 2019b].

Chapter 7: *Observation and Conclusion*

Chapter 7: *Observation and Conclusion*

7.1. Observation and Conclusions of the preliminary study of small dataset

In the preliminary study, the multi-QSAR analysis of the tetrahydroisoquinoline hydroxamate derivated HDAC8 inhibitors was successfully able to identify several significant molecular features of these compounds responsible for regulating the biological activity of the compounds. The summary of these outcomes are graphically represented in ***Figure 7.1*** which also resembles with the SAR study of these HDAC8 inhibitors [Zhang et al. 2010, Zhang et al. 2011a, Zhang et al. 2011b, Taha et al. 2017].

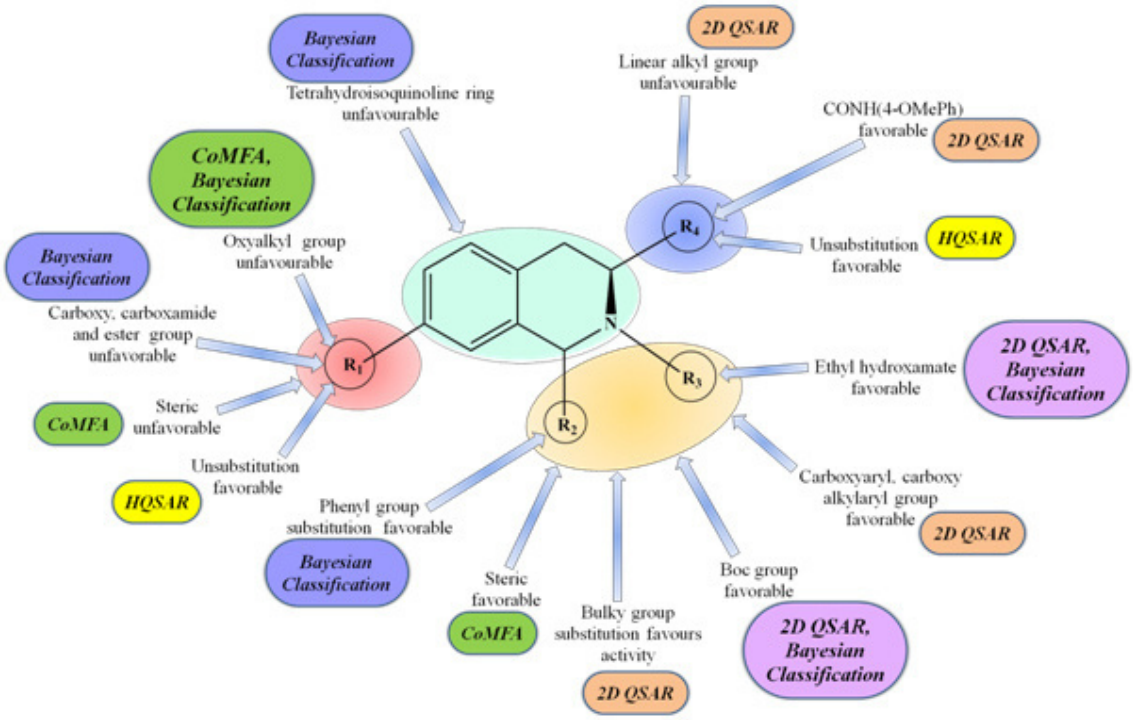

Figure 7.1. Schematic represented a summary of the outcomes of the multi-QSAR study on the tetrahydroisoquinoline hydroxamate-based HDAC8 inhibitors.

From the results of the 3D- and 2D-QSAR studies conducted on these HDAC8 inhibitors suggested the detrimental effects of the R_1 substitution of the scaffold in area-A on their HDAC8 inhibition. Substitution of the oxymethyl function at the R_1 position of several compounds (Compounds **T-1** to **T-59** and **T-74** to **T-81**) was suggested to provide negative influence on the HDAC8 inhibition of these inhibitors and was displayed as bad molecular structures by the Bayesian classification study. The unsubstituted hydrogen atom present at the R_1 position of the most active compounds of the series (Compound **T-**

62) was displayed as a good fragment for HDAC8 inhibition by the H-QSAR study. The steric unfavorable field near the R_1 position showed in the 3D-QSAR CoMFA generated contour maps also suggested the unfavorability of steric substitution at that position.

During the observation of the substitutions present at the R_2 and R_3 positions of the scaffold (area-B), the substitution of the bulky steric group in those positions was suggested to be beneficial for the activity by the 2D-QSAR study. Substitution of different groups such as Boc, carboxy aryl alkyl, carboxy aryl groups along groups with larger van der Waal volume was also suggested to provide beneficial effects on the activity. The Bayesian classification study also found the Boc group as a good molecular fragment for higher HDAC8 inhibition. The CoMFA generated contours showed a steric favorable field near the area-B substitutions (R_2 and R_3 positions) and suggested bulky steric group substitution at that area have a chance to increase the activity of these HDAC8 inhibitors. The 2D molecular descriptor *VCH-6* and *mintHBint3* signified the importance of the alkyl chain length of these compounds in the area-B for their activity while suggested detrimental effects of larger alkyl chain length at that area for the activity of the compounds (Compounds **T-28** to **T-32** and **T-61**). The Bayesian study suggested ethyl hydroxamate group as good fingerprint for HDAC8 indicating that 2 carbon distance between the ZBG (hydroxamate moiety) and the surface recognition group (tetrahydroisoquinoline scaffold) of these tetrahydroisoquinoline derivated compounds (Compounds **T-63** and **T-65** to **T-73**) as the optimal distance for better HDAC8 inhibition. Also, the most active compound of this series contained an n-butyl linker in its structure which suggests that the 2-4 carbon distances between the ZBG and the cap of these compounds may provide optimal distance for better HDAC8 inhibition.

For the substitutions of the R_4 position of area-C, it is seen that the Bayesian classification study suggested the tetrahydroisoquinoline moiety along with its R_1 and R_4 substitution as a detrimental feature for the HDAC8 inhibition of these compounds where the 2D-QSAR study identified the R_4 4-methoxy phenylamino carboxyl moiety as positive contributor toward the activity of these compounds. The H-QSAR study identified the unsubstituted nitrogen atoms present at the R4 position of the most active compound (Compound **T-62**) as the positive contributors for the activity while suggesting the importance of the tetrahydroisoquinoline moiety for HDAC8 inhibition. This

incidence might be occurring due to the dual-role played by the tetrahydroisoquinoline scaffold itself for these compounds. For the compounds **T-1 to T-59** and **T-74 to T-81**, because while having the hydroxamate group at the R_1 and 4-methoxyphenyl amino carboxy group at R_4 positions, the tetrahydroisoquinoline ring acts as the linker motif where the hydroxamate group acts as the ZBG and R_4 substitution as the cap group (Zhang et al. 2010). On the other hand, for the compounds **T-60** to **T-73** the tetrahydroisoquinoline group serves as the cap moiety with its R_2 substitution where the R_3 n-alkyl hydroxamate group serves as the linker and the ZBG groups respectively (Taha et al. 2017). Hence, this study may have suggested that the tetrahydroisoquinoline group might be more beneficial for HDAC8 inhibition as the cap group instead of acting as a linker motif.

Additionally, the newly designed compound (Compounds **N-82** to **N-87**) suggested that the replacement of the tetrahydroisoquinoline moiety with other fused ring containing moieties like the napthyl group can be more effective than their corresponding tetrahydroisoquinoline analogs. This work is accepted for publication in the Journal of Biomolecular Structure and Dynamics [Banerjee et al. 2019b].

7.2. Observation of the Classification study conducted on the diverse large dataset of hydroxamate derivatives

7.2.1. Observation of the Bayesian classification study

Bayesian classification study on the dataset containing diverse group of hydroxamate containing HDAC8 inhibitors was conducted using different combinations of molecular properties of the molecules, the *ECFP_6* and the *FCFP_6 fingerprint descriptors,* it is observed that the molecular properties such as *AlogP, MW, FPSA, nAR, nHBA, nR*, *nHBD, nRB* of these compounds are unable to discriminate these compounds into active and inactive thus provided poor statistical outcomes. On the other hand, the addition of the fingerprint descriptors such as the *ECFP_6* and the *FCFP_6* molecular descriptors are able to discriminate these molecules in the active and inactive quite well and provided better statistical outcomes in comparison with the model constructed using only the molecular properties of these compounds. Although the statistical outcomes provided by the models containing the *ECFP_6* and the *FCFP_6* descriptors provided almost similar

outcomes, the model containing the *ECFP_6* descriptors provided a better result than the model containing the *FCFP_6* descriptors.

In case of the molecular fingerprints provided by the *ECFP_6* and *FCFP_6* descriptors, many of the molecular fingerprints were identical to each other. The Bayesian study on these hydroxamate derivatives suggested that bulky groups like phenyl imidazole or benzimidazole moiety can be suitable as the cap/surface recognition feature for these compounds whereas the presence of groups like quinazoline, naphthyridine, tetrahydroisoquinoline and pyrimidine moiety in the cap group of the moiety can be detrimental for HDAC8 inhibitory potency of these compounds. Also, this study indicated the beneficial effects of the piperidine, pyrrole and pyrrolidine moiety in the cap group for the activity of these compounds. In case of the linker motif, the presence of oxazole, thiazole, tetrahydroisoquinoline moiety and the *n*-alkyloxy phenyl moiety in the linker motif, of these compounds is also suggested to be detrimental toward the potency of these compounds. Additionally, the study indicated that the meta-alkyl group substituted phenyl ring in the linker region of these compounds can be beneficial for the activity of the compounds might be suggesting a lesser number of rotatable bonds in the linker moiety as an important factor for the HDAC8 inhibition of these compounds.

7.2.1. Observation of the Recursive partitioning study

By studying the outcomes of the recursive partitioning study conducted for this diverse set of hydroxamate group containing HDAC8 inhibitors, it is observed that the model constructed using the molecular properties of these compounds cannot split the compounds into the active and the inactive compounds properly. In addition to the fingerprint descriptors with the molecular properties are able to discriminate these compounds much more efficiently and provided better statistical outcomes. This was also observed in case of the Bayesian classification study of these compounds, suggesting the importance of the fingerprint descriptors like *ECFP_6* and *FCFP_6* in the identification of the molecular factors responsible for regulating the HDAC8 inhibitory potency of these molecules.

The constructed recursive partitioning models also produced a total of 24 molecular fragments containing 10 *ECFP_6* and 14 *FCFP_6* molecular fragments which the RP models used to split the decision tree and to discriminate these compounds into active and

inactive HDAC8 inhibitors. The study revealed some of the important molecular fragments such as, meta-carboxy amido benzyl phenyl, furan, 4-bromo phenyl, 3-alkyl amino group substituted phenyl ring for the HDAC8 inhibitory potency of the compounds which may indicate that presence of such groups in the cap group can affect the interaction of the surface recognition group of these compounds inside the HDAC8 active site. Besides these molecular fragments, the study also suggested several linear groups like n-alkyl group, n-alkyl amino group, phenyl amino carbonyl moiety, 4-alkyloxy benzyl moiety along with cinnamoyl group have significant importance in the HDAC8 inhibition of these molecules. This may suggest that the presence of such groups in the linker region can affect the binding of the ligand inside the long and tunnel-like pocket HDAC8 which might alter the HDAC8 inhibitory activity of the compounds.

Finally, from both the Bayesian classification study and the Recursive partitioning study of this diverse large set of hydroxamate containing HDAC8 inhibitors it is observed that the Bayesian and the Recursive Partitioning studies were very efficient techniques to study the regulatory factor influencing the activity of these compounds. These studies were helpful to identify a different important sub-structural molecular fragment which influences the HDAC8 inhibitory activity of these compounds but also able to discriminate the molecular fragments with the positive and negative influences of the activity of these hydroxamate derivatives.

Chapter 8: *Future Directions*

Chapter 8: *Future Directions*

From this study, it was observed that the enzymatic activity of the HDAC8 isoform is correlated with a large group of cancer and other pathophysiological disorders. Hence, the designing of HDAC8 selective inhibitors for effective HDAC8 inhibition is a major concern in order to combat cancer and pathophysiological conditions influenced by the activity of HDAC8 through various mechanisms. Also, it is seen that in this effort to design HDAC8 specific potent inhibitors, numerous molecules containing a variety of different pharmacophoric features provided a wide range of HDAC8 inhibition. Besides the synthetic approaches, employment of different computational and molecular modeling based techniques are also performed to identify and screen potent HDAC8 inhibitors from different databases. Our group is also one of them, trying to explore the HDAC8 enzyme and in order to design target-specific HDAC8 inhibitors with higher HDAC8 inhibitory activity [Amin et al. 2017a, 2017b, 2018a, 2018b, Halder et al. 2015].

From the different SAR studies, it was observed that there are a number of ZBG groups for the HDAC8 inhibitors are available for chelation with the Zn^{2+} ion of HDAC8. It was noticed that hydroxamic acid moiety is more suitable as the ZBG for the HDAC8 inhibitors than the other groups [Amin et al. 2017a, 2018b]. On the other hand as for the cap and the liker moiety it is observed that there are several groups and factors such as, the presence of tertiary nitrogen, aromatic heterocyclic groups, alky chain, alkyl chain length, unsaturation in the cap and linker moiety, aromatic ring substitutions, moieties like carboxamido, alkyloxy, aryloxy-alkyl groups, hydrogen bond donor and acceptor groups which may affect the function of the cap and the linker moieties as well as the activity and the selectivity of the HDAC8 inhibitors. Additionally, hydrophobicity of the surface recognition group and the unsaturation in the cap moiety may provide better interaction in the HDAC8 pocket while increasing the selectivity and potency of the compounds. As for the linker moieties of the HDAC8 inhibitors, it is seen that, though the hydroxamate function of the compounds is an excellent zinc binder for HDAC8 inhibition, a linker moiety must provide the optimal distance to interact the cap and the ZBG at their proper site of interaction inside the HDAC8 pocket and any further interactions of the linker moiety inside the HDAC8 active site may be more convenient for the compound to provide better HDAC8 inhibition.

Chapter 8: *Future Directions*

Nevertheless, the chemo-metrics and computational studies seemed to be an effective tool in order to identification, screening, and designing of target-selective HDAC8 inhibitors. These techniques along with the molecular docking and study of the available ligand-bound crystal structures of HDAC8 are quite useful to identify and extract the essential structural features of the HDAC8 inhibitors for better comprehension of the ligand-protein interaction inside the HDAC8 active. Hence, studies like quantitative structure-activity relationship (QSAR), quantitative structure-selectivity relationship along with database screening, molecular docking and synthetic approaches can be able to provide the desiring potent and target specific HDAC8 inhibitors in future in order to combat the pathophysiological disorders, cancer conditions, epigenetic disorders and diseases related to the abnormal activity of the HDAC8 enzyme.

References

References

- A. Golbraikh, & A. Tropsha, Beware of q2!. *J. Mol. Graph. Model.* 20 (2002) 269-276.
- A. Montero, J.M. Beierle, C.A. Olsen, M.R. Ghadiri, Design, synthesis, biological evaluation, and structural characterization of potent Histone Deacetylase inhibitors based on cyclic alpha/beta-tetrapeptide architectures, J. Am. Chem. Soc. 131 (2009) 3033-3041.
- A. Saha, G.N. Pandian, S. Sato, J. Taniguchi, K. Hashiya, T. Bando, H. Sugiyama, Synthesis and biological evaluation of a targeted DNA-binding transcriptional activator with HDAC8 inhibitory activity. Bioorg. Med. Chem. 21 (2013) 4201-4209.
- A. Vannini, C. Volpari, G. Filocamo, E.C. Casavola, M. Brunetti, D. Renzoni, P. Chakravarty, C. Paolini, R. De Francesco, P. Gallinari, C. Steinkühler, S. Di Marco, Crystal structure of a eukaryotic zinc-dependent histone deacetylase, human HDAC8, complexed with a hydroxamic acid inhibitor. Proc. Natl Acad. Sci. USA 101 (2004) 15064-15069.
- A. Vannini, C. Volpari, P. Gallinari, P. Jones, M. Mattu, A. Carfí, R. De Francesco, C. Steinkühler, S. Di Marco, Substrate binding to histone deacetylases as shown by the crystal structure of the HDAC8-substrate complex. EMBO Rep. 8 (2007) 879-884.
- A.A. Tabackman, R. Frankson, E.S. Marsan, K. Perry, K.E. Cole, Structure of 'linkerless' hydroxamic acid inhibitor-HDAC8 complex confirms the formation of an isoform-specific subpocket. J. Struct. Biol. 195 (2016) 373-378.
- A.E. Klon, J.F. Lowrie, D.J. Diller, Improved naive Bayesian modeling of numeriacl data for absorption, destribution, metabolism and excretion (ADME) property prediction. J. Chem. Inf. Model. 46 (2006)1945–1956.
- A.K. Halder, A. Saha, T. Jha, Exploring QSAR and pharmacophore mapping of structurally diverse selective matrix metalloproteinase-2 inhibitors, J. Pharm. Pharmacol. 65 (2013) 1541-1554.
- A.K. Halder, S. Mallick, D. Shikha, A. Saha, K.D. Sahab, T. Jha, Design of dual MMP-2/HDAC8 inhibitors by pharmacophore mapping, molecular docking, synthesis and biological activity. RSC. Adv. 5 (2015) 72373-72386.

References

- A.K. Oyelere, P.C. Chen, W. Guerrant, S.C. Mwakwari, R. Hood, Y. Zhang, Y. Fan, Non-peptide macrocyclic histone deacetylase inhibitors. J. Med. Chem. 52 (2009) 456-468.
- A.P. Kozikowski, S. Tapadar, D.N. Luchini, K.H. Kim, D.D. Billadeau, Use of the nitrile oxide cycloaddition (NOC) reaction for molecular probe generation: A new class of enzyme selective histone deacetylase inhibitors (HDACIs) showing picomolar activity at HDAC6. J. Med. Chem. 51 (2008) 4370-4373.
- A.P. Kozikowski, Y. Chen, A. Gaysin, B. Chen, M.A. D'Annibale, C.M. Suto, B.C. Langley, Functional differences in epigenetic modulators superiority of mercaptoacetamide-based histone deacetylase inhibitors relative to hydroxamates in cortical neuron neuroprotection Studies. J. Med. Chem. 50 (2007) 3054-3061.
- A.S. Vaidya, R. Neelarapu, A. Madriaga, H. Bai, E. Mendonca, H. Abdelkarim, R.B. van Breemen, S.Y. Blond, P.A. Petukhov, Novel histone deacetylase 8 ligands without a zinc chelating group: Exploring an 'upside-down' binding pose. Bioorg. Med. Chem. Lett. 22 (2012) 6621-6627.
- B. He, S. Velaparthi, G. Pieffet, C. Pennington, A. Mahesh, D.L. Holzle, M. Brunsteiner, R. van Breemen, Y. Sylvie, P. Blond, A. Petukhov, Binding Ensemble Profiling with Photoaffinity Labeling (BEProFL) approach: Mapping the binding poses of HDAC8 inhibitors. J. Med. Chem. 52 (2009) 7003-7013.
- B. Jose, Y. Oniki, T. Kato, N. Nishino, Y. Sumida, M. Yoshida, Novel histone deacetylase inhibitors: cyclic tetrapeptide with trifluoromethyl and pentafluoroethyl ketones. Bioorg. Med. Chem. Lett. 14 (2004) 5343-5346.
- B. Lutterbach, and S.W. Hiebert, Role of the transcription factor AML-1 in acute leukemia and hematopoietic differentiation. Gene 245 (2000) 223-235.
- B.J. Wilson, A.M. Tremblay, G. Deblois, G. Sylvain-Drolet, V. Giguère, An acetylation switch modulates the transcriptional activity of estrogen-related receptor alpha. Mol. Endocrinol. 24 (2010) 1349-1358.
- C. Zhao, J. Zang, Q. Ding, E.S. Inks, W. Xu, C.J. Chou, Y. Zhang, Discovery of meta-sulfamoyl N-hydroxybenzamides as HDAC8 selective inhibitors. Eur. J. Med. Chem. 150 (2018) 282-291.

References

- C.A. Lipinski, F. Lombardo, B.W. Dominy, P.J. Feeney, Experimental and computational approaches to estimate solubility and permeability in drug discovery and development settings. Adv. Drug Deliv. Rev. 46 (2001) 3-26.
- C.A. Olsen, and M.R. Ghadiri, Discovery of potent and selective histone deacetylase inhibitors via focused combinatorial libraries of cyclic alpha3 β-tetrapeptides. J. Med. Chem. 52 (2009) 7836-7846.
- C.B. Botta, W. Cabri, E. Cini, L. De Cesare, C. Fattorusso, G. Giannini, M. Persico, A. Petrella, F. Rondinelli, M. Rodriquez, A. Russo, M. Taddei, Oxime amides as a novel zinc binding group in histone deacetylase inhibitors: Synthesis, biological activity and computational evaluation. J. Med. Chem. 54 (2011) 2165-2182.
- C.Q. Chen, K. Yu, Q.X. Yan, C.Y. Xing, Y. Chen, Z. Yan, Y.F. Shi, K.W. Zhao, S.M. Gao, , Pure curcumin increases the expression of SOCS1 and SOCS3 in myeloproliferative neoplasms through suppressing class I histone deacetylases. Carcinogenesis 34 (2013) 1442-1449.
- C.W. Yap, PaDEL Descriptor: an open source software to calculate molecular descriptors and fingerprints. J. Comput. Chem. 32 (2011) 1466-1474.
- Chakrabarti, I. Oehme, O. Witt, G. Oliveira, W. Sippl, C. Romier, R.J. Pierce, M. Jung, HDAC8: A multifaceted target for therapeutic interventions Trends Pharmacol. Sci. 36 (2015) 481-492.
- Chakrabarti, J. Melesina, F.R. Kolbinger, I. Oehme, J. Senger, O. Witt, W. Sippl, M. Jung, Targeting histone deacetylase 8 as a therapeutic approach to cancer and neurodegenerative diseases. Future Med. Chem. 8 (2016) 1609-1634.
- C-W. Yu, P-T. Chang, L-W. Hsin, J-W. Chern, Quinazolin-4-one derivatives as selective histone deacetylase‑6 inhibitors for the treatment of alzheimer's disease. J. Med. Chem. 56 (2013) 6775-6791
- D. Lamaa, H-P. Lin, L. Zig, C. Bauvais, G. Bollot, J. Bignon, H. Levaique, O. Pamlard, J. Dubois, M. Ouaissi, M. Souce, A. Kasselouri, F. Saller, D. Borgel, C. Jayat-Vignoles, H. Al-Mouhammad, J. Feuillard, K. Benihoud, M. Alami, A. Hamze, Design and synthesis of tubulin and histone deacetylase inhibitor based on iso-combretastatin A‑4. J. Med. Chem. 61 (2018) 6574-6591.

References

- D.F. Veber, S.R. Johnson, H.Y. Cheng, B.R. Smith, K.W. Ward, K.D. Kopple, Molecular properties that influence the oral bioavailability of drug candidates. J. Med. Chem. 45 (2002) 2615-2623.
- D.M. Fass, R. Shah, B. Ghosh, K. Hennig, S. Norton, W-N. Zhao, S.A. Reis, P.S. Klein, R. Mazitschek, R.L. Maglathlin, T.A. Lewis,S.J. Haggarty, Short-chain HDAC inhibitors differentially affect vertebrate development and neuronal chromatin. ACS Med. Chem. Lett. 2 (2011) 39-42.
- D.P. Dowling, S.L. Gantt, S.G. Gattis, C.A. Fierke, D.W. Christianson, Structural studies of human histone deacetylase 8 and its site-specific variants complexed with substrate and inhibitors. *Biochemistry* 47 (2008) 13554-13563.
- D.V. Smil, S. Manku, Y.A. Chantigny, S. Leit, A. Wahhab, T.P. Yan, M. Fournel, C. Maroun, Z. Li, A.M. Lemieux, A. Nicolescu, J. Rahil, S. Lefebvre, A. Panetta, J.M. Besterman, R. Déziel, Novel HDAC6 isoform selective chiral small molecule histone deacetylase inhibitors. Bioorg. Med. Chem. Lett. 19 (2009) 688-692.
- F.F. Wagner, D.E. Olson, J.P. Gale, T. Kaya, M. Weïwer, N. Aidoud, M. Thomas, E.L. Davoine, B.C. Lemercier, Y-L Zhang, E.B. Holson, Potent and selective inhibition of histone deacetylase 6 (HDAC6) does not require a surface-binding motif. J. Med. Chem. 56 (2013) 1772-1776.
- F.Z. Tassine, M. Elhallaoui, DFT-based QSAR study of N-hydroxyfurylacrylamide and its derivatives, principal inhibitors of histone deacetylase. J. Mater. Environ. Sci. 7 (2016) 2252-2258.
- G. Estiu, N. West, R. Mazitschek, E. Greenberg, J.E. Bradner, O. Wiest, On the inhibition of histone deacetylase 8. Bioorg. Med. Chem. 18 (2010) 4103–4110.
- G. Giannini, M. Marzi, R. Pezzi, T. Brunetti, G. Battistuzzi, M.D. Marzo, W. Cabri, L. Vesci, C. Pisano, N-Hydroxy-(4-oxime)-cinnamide: a versatile scaffold for the synthesis of novel histone deacetylase (HDAC) inhibitors. Bioorg. Med. Chem. Lett. 19 (2009) 2346-2349.
- G. Ortore, F.D. Colo, A. Martinelli, Docking of hydroxamic acids into HDAC1 and HDAC8: A rationalization of activity trends and selectivities. J. Chem. Inf. Model. 49 (2009) 2774-2785.

References

- G. Tang, J.C. Wong, W. Zhang, Z. Wang, N. Zhang, Z. Peng, Z. Zhang, Y. Rong, S. Li, M. Zhang, L. Yu, T. Feng, X. Zhang, X. Wu, J.Z. Wu, L. Chen, Identification of a novel aminotetralin class of HDAC6 and HDAC8 selective inhibitors. J. Med. Chem. 57 (2014) 8026-8034.
- G.E. Box & C.C. Tiao, Bayesian Inference in Statistical Analysis. John Wiley & Sons, NY, USA (2011).
- G.P. Cao, M. Arooj, S. Thangapandian, C. Park, V. Arulalapperumal, Y. Kim, Y.J. Kwon, H.H. Kim, J.K. Suh, K.W. Lee, A lazy learning-based QSAR classification study for screening potential histone deacetylase 8 (HDAC8) inhibitors. SAR QSAR Environ Res. 26 (2015) 397-420.
- G.P. Cao, S. Thangapandian, M. Son, R. Kumar, Y.-J. Choi, Y. Kim, Y.J. Kwon, H-H. Kim, J-K Suh, K.W. Lee, QSAR modeling to design selective histone deacetylase 8 (HDAC8) inhibitors. Arch. Pharm. Res. 39 (2016) 1356-1369.
- H. Martínez-Pacheco, G. Ramírez-Galicia, M. Vergara-Arias, J. Gertsch, M.J. Fragoso-Vázquez, D. Méndez-Luna, A.L. Abujamra, C-P.L. Cristina, R-H.M. Cecilia, I.Mendoza-Lujambio, J. Correa-Basurto, Docking and QSAR studies of aryl-valproic acid derivatives to identify anti-proliferative agents targeting the HDAC8. Anticancer Agents Med. Chem. 17 (2017) 927-940.
- H. Matter, M. Schudok, W. Schwab, W. Thorwart, D. Barbier, G. Billen, B. Haase, B. Neises, K. Weithmann, T. Wollmann, Tetrahydroisoquinoline-3-carboxylate based matrix-metalloproteinase inhibitors: design, synthesis and structure-activity relationship. Bioorg. Med. Chem. 10 (2002) 3529-3544.
- H. Nian, W.H. Bisson, W-M. Dashwood, J.T. Pinto, R.H. Dashwood, Alpha-keto acid metabolites of organoselenium compounds inhibit histone deacetylase activity in human colon cancer cells. Carcinogenesis 30 (2009) 1416-1423.
- H. Wang, Z-Y Lim, Y. Zhou, M. Ng, T. Lu, K. Lee, K. Sangthongpitag, K.C. Goh, X. Wang, X. Wu, H.H. Khng, S.K. Goh, W.C. Ong, Z. Bonday, E.T. Sun, Acylurea connected straight chain hydroxamates as novel histone deacetylase inhibitors: Synthesis, SAR, and in vivo antitumor activity. Bioorg. Med. Chem. Lett. 20 (2010) 3314-3321.

References

- I. Van den Wyngaert, W. de Vries, A. Kremer, J. Neefs, P. Verhasselt, W.H. Luyten, S.U. Kass, Cloning and characterization of human histone deacetylase 8. FEBS Lett. 478 (2000) 77-83.
- I.V. Gregoretti, Y.M. Lee, H.V. Goodson, Molecular evolution of the histone deacetylase family: Functional implications of phylogenetic analysis. J. Mol. Biol. 338 (2004) 17-31.
- J. Arts, P. Angibaud, A. Mariën, W. Floren, B. Janssens, P. King, J. van Dun, L. Janssen, T. Geerts, R.W. Tuman, D.L. Johnson, L. Andries, M. Jung, M. Janicot, K. van Emelen, R306465 is a novel potent inhibitor of class I histone deacetylases with broad-spectrum antitumoral activity against solid and haematological malignancies. British J. Cancer 97 (2007) 1344-1353.
- J. Arts, P. King, A. Mariën, W. Floren, A. Beliën, L. Janssen, I. Pilatte, B. Roux, L. Decrane, R. Gilissen, I. Hickson, V. Vreys, E. Cox, K. Bol, W. Talloen, I. Goris, L. Andries, M.D. Jardin, M. Janicot, M. Page, K. van Emelen, and P. Angibaud, JNJ-26481585, a novel 'second-generation' oral histone deacetylase inhibitor, shows broad-spectrum preclinical antitumoral activity. Cancer Ther. Clin. Can. Res. 15 (2009) 6841-6851.
- J. Cai, H. Wei, K.H. Hong, X. Wu, M. Cao, X. Zong, L. Li, C. Sun, J. Chen, M. Ji, Discovery and preliminary evaluation of 2-aminobenzamide and hydroxamate derivatives containing 1, 2, 4-oxadiazole moiety as potent histone deacetylase inhibitors. Eur. J. Med. Chem. 96 (2015) 1-13.
- J. Gao, B. Siddoway, Q. Huang, H. Xia, Inactivation of CREB mediated gene transcription by HDAC8 bound protein phosphatase. Biochem. Biophys. Res. Commun. 379 (2009) 1-5.
- J. Gasteiger, & M. Marsili, Iterative partial equalization of orbital electronegativity-a rapid access to atomic charges. Tetrahedron, 36, (1980) 3219-3228.
- J. Liu, and I.D. Krantz, Cornelia de Lange syndrome, cohesin, and beyond. Clin. Genet. 76 (2009) 303-314.
- J. Spencer, J. Amin, M. Wang, G. Packham, S.S.S. Alwi, G.J. Tizzard, S.J. Coles, R.M. Paranal, J.E. Bradner, T.D. Heightman, Synthesis and biological evaluation of

JAHAs: ferrocene-based histone deacetylase inhibitors. ACS Med. Chem. Lett. 2 (2011) 358-362.

- J. Wu, C. Du, Z. Lv, C. Ding, J. Cheng, H. Xie, L. Zhou, S. Zheng, The up-regulation of histone deacetylase 8 promotes proliferation and inhibits apoptosis in hepatocellular carcinoma. Dig. Dis. Sci. 58 (2013) 3545-3553.
- J.C. Canzoneri, P.C. Chen, A.K. Oyelere, Design and synthesis of novel histone deacetylase inhibitor derived from nuclear localization signal peptide. Bioorg. Med. Chem. Lett. 19 (2009) 6588-6590.
- J.J. Buggy, M.L. Sideris, P. Mak, D.D. Lorimer, B. McIntosh, J.M. Clark, Cloning and characterization of a novel human histone deacetylase, HDAC8. Biochem. J. 350 (2000) 199-205.
- J.O. Berger, Statistical Decision Theory and Bayesian Analysis. Springer Science & Business Media, NY, USA (2013).
- J.R. Somoza, R.J. Skene, B.A. Katz, C. Mol, J.D. Ho, A.J. Jennings, C. Luong, A. Arvai, J.J. Buggy, E. Chi, J. Tang, B.C. Sang, E. Verner, R. Wynands, E.M. Leahy, D.R. Dougan, G. Snell, M. Navre, M.W. Knuth, R.V. Swanson, D.E. McRee, L.W. Tari, Structural snapshots of human HDAC8 provide insights into the class I histone deacetylases. Structure 12 (2004) 1325-1334.
- J-H. Lee, Y. Yao, A. Mahendran, L. Ngo, G. Venta-Perez, M.L. Choy, R. Breslow, P.A. Marks, Creation of a histone deacetylase 6 inhibitor and its biological effects. PNAS. 112 (2015) 12005-12010.
- K. Krennhrubec, B.L. Marshall, M. Hedglin, E. Verdin, S.M. Ulrich, Design and evaluation of 'Linkerless' hydroxamic acids as selective HDAC8 inhibitors. Bioorg. Med. Chem. Lett. 17 (2007) 2874-2878.
- K.L. Durst, B. Lutterbach, T. Kummalue, A.D. Friedman, S.W. Hiebert, The inv (16) fusion protein associates with corepressors via a smooth muscle myosin heavy-chain domain. Mol. Cell. Biol. 23 (2003) 607-619.
- L. Zhang, X. Wang, X. Li, L. Zhang, W. Xu, Discovery of a series of hydroxamic acid derivatives as potent histone deacetylase inhibitors. J. Enzyme. Inhib. Med. Chem. 29 (2014) 582-589.

References

- L. Chen, Y. Li, Q. Zhao, H. Peng, T. Hou, ADME evaluation in drug discovery. 10. Predictions of P-glycoprotein inhibitors using recursive partitioning and Naive Bayesian classification techniques, Mol. Pharmaceutics 8 (2011) 889–900.
- L. Marek, A. Hamacher, F.K. Hansen, K. Kuna, H. Gohlke, M.U. Kassack, T. Kurz, Histone deacetylase (HDAC) inhibitors with a novel connecting unit linker region reveal a selectivity profile for HDAC4 and HDAC5 with improved activity against chemo resistant cancer cells. J. Med. Chem. 56 (2013) 427-436.
- L. Whitehead, M.R. Dobler, B. Radetich, Y. Zhu, P.W. Atadja, T. Claiborne, J.E. Grob, A. McRiner, M.R. Pancost, A. Patnaik, W. Shao, M. Shultz, R. Tichkule, R.A. Tommasi, B. Vash, P. Wang, T. Stams, Human HDAC isoform selectivity achieved via exploitation of the acetate release channel with structurally unique small molecule inhibitors. Bioorg. Med. Chem. 19 (2011) 4626-4634.
- L.E. Choi, M. Cho, B. Lee, S.J. Oh, S.K. Park, K. Lee, H.M. Kim, G. Han, Structure and property based design, synthesis and biological evaluation of gamma-lactam based HDAC inhibitors. Bioorg. Med. Chem. Lett. 21 (2011) 1218-1221.
- L.M. Henkes, P. Haus, F. Jäger, J. Ludwig, F.J. Meyer-Almes, Synthesis and biochemical analysis of 2,2,3,3,4,4,5,5,6,6,7,7-dodecafluoro-N-hydroxy-octanediamides as inhibitors of human histone deacetylases. Bioorg. Med. Chem. 20 (2012) 985-995.
- L-L. Liu, J. Lu, Y. Lu, M-Y. Zheng, X-M. Luo, W-L. Zhu, H-L. Jiang, K-X. Chen, Novel Bayesian classification models for predicting compounds blocking hERG potassium channels. Acta Pharmacol. Sin. 35 (2014) 1093–1102.
- M. Bergsland, M. Werme, M. Malewicz, T. Perlmann, J. Muhr, The establishment of neuronal properties is controlled by Sox4 and Sox11. Genes Dev. 20 (2006) 3475-3486.
- M. Haberland, M.H. Mokalled, R.L. Montgomery, E.N. Olson, Epigenetic control of skull morphogenesis by histone deacetylase 8. Genes Dev. 23 (2009) 1625-1630.
- M. Manal, K. Manish, D. Sanal, A. Selvaraj, V. Devadasan, M.J.N. Chandrasekar, Novel HDAC8 inhibitors: A multi-computational approach. SAR QSAR Environ Res. 28 (2017) 707-733.

References

- M. Marek, S. Kannan, A-T. Hauser, M.M. Mourão, S. Caby, V. Cura, D.A. Stolfa, K. Schmidtkunz, J. Lancelot, L. Andrade, J-P Renaud, G. Oliveira, W. Sippl, M. Jung, J. Cavarelli, R.J. Pierce , C. Romier, Structural basis for the inhibition of histone deacetylase 8 (HDAC8), a key epigenetic player in the blood fluke Schistosoma mansoni. PLoS Pathog. 9 (2013) e1003645.
- M. Marek, T.B. Shaik, T. Heimburg, A. Chakrabarti, J. Lancelot, E. Ramos-Morales, C. Da Veiga, D. Kalinin, J. Melesina, D. Robaa, K. Schmidtkunz, T. Suzuki, R. Holl, E. Ennifar, R.J. Pierce, M. Jung, W. Sippl, C. Romier, Characterization of Histone Deacetylase 8 (HDAC8) Selective Inhibition Reveals Specific Active Site Structural and Functional Determinants. J. Med. Chem. 61 (2018) 10000-10016.
- M. Mottamal, S. Zheng, T.L. Huang, G. Wang, Histone deacetylase inhibitors in clinical studies as templates for new anticancer agents. Molecules 20 (2015) 3898-3941.
- M. Nakagawa, Y. Oda, T. Eguchi, S. Aishima, T. Yao, F. Hosoi, Y. Basaki, M. Ono, M. Kuwano, M. Tanaka, M. Tsuneyoshi, Expression profile of class I histone deacetylases in human cancer tissues. Oncol. Rep. 18 (2007) 769-774.
- M. Sastry, J.F. Lowrie, S.L. Dixon, W. Sherman, Large-scale systematic analysis of 2D fingerprint methods and parameters to improve virtual screening enrichments, J. Chem. Inf. Model. 50 (2010) 771-784.
- M. Wünsch, J. Senger, P. Schultheisz, S. Schwarzbich, K. Schmidtkunz, C. Michalek, M. Klaß, S. Goskowitz, P. Borchert, L. Praetorius, W. Sippl, M. Jung, N. Sewald, Structure–activity relationship of propargylamine-based HDAC inhibitors. ChemMedChem. 12 (2017) 2044-2053.
- M.A. Deardorff, M. Bando, R. Nakato, E. Watrin, T. Itoh, M. Minamino, K. Saitoh, M. Komata, Y. Katou, D. Clark, K.E. Cole, E. De Baere, C. Decroos, N. Di Donato, S. Ernst, L.J. Francey, Y. Gyftodimou, K. Hirashima, M. Hullings, Y. Ishikawa, C. Jaulin, M. Kaur, T. Kiyono, P.M. Lombardi, L. Magnaghi-Jaulin, G.R. Mortier, N. Nozaki, M.B. Petersen, H. Seimiya, V.M. Siu, Y. Suzuki, K. Takagaki, J.J. Wilde, P.J. Willems, C. Prigent, G. Gillessen-Kaesbach, D.W. Christianson, F.J. Kaiser, L.G. Jackson, T. Hirota, I.D. Krantz, K. Shirahige, HDAC8 mutations in Cornelia de Lange syndrome affect the cohesin acetylation cycle. Nature 489 (2012) 313-317.

References

- M.R. Potzner, K. Tsarovina, E. Binder, A. Penzo-Méndez, V. Lefebvre, H. Rohrer, M. Wegner, E. Sock, Sequential requirement of Sox4 and Sox11 during development of the sympathetic nervous system. Development 137 (2010) 775-784.
- M.W. Schilham, M.A. Oosterwegel, P. Moerer, J. Ya, P.A.J. de Boer, M. van de Wetering, S. Verbeek, W.H. Lamers, A.M. Kruisbeek, A. Cumano, H. Clevers, Defects in cardiac outflow tract formation and pro-B-lymphocyte expansion in mice lacking Sox-4. Nature 380 (1996) 711-714.
- N. Adhikari, A.K. Halder, S. Mallick, A. Saha, K.D. Saha, T. Jha, Robust design of some selective matrix metalloproteinase-2 inhibitors over matrix metalloproteinase-9 through in silico/fragment-based lead identification and de novo lead modification: Syntheses and biological assays, Bioorg. Med. Chem. 24 (2016) 4291-4309.
- N. Adhikari, S.A. Amin, P. Trivedi, T. Jha, B. Ghosh, HDAC3 is a potential validated target for cancer: An overview on the benzamide-based selective HDAC3 inhibitors through comparative SAR/QSAR/QAAR approaches. Eur. J. Med. Chem. 157 (2018) 1127-1142.
- N. Suzuki, T. Suzuki, Y. Ota, T. Nakano, M. Kurihara, H. Okuda, T. Yamori, H. Tsumoto, H. Nakagawa, N. Miyata, Design, synthesis, and biological activity of boronic acid-based histone deacetylase inhibitors. J. Med. Chem. 52 (2009) 2909-2922.
- N.J. Porter, N.H. Christianson, C. Decroos, D.W. Christianson, Structural and functional influence of the glycine-rich loop G302GGGY on the catalytic tyrosine of histone deacetylase 8. Biochem 55 (2016) 6718-6729.
- N.M. O'Boyle, R.A. Sayle, Comparing structural fingerprints using a literature‐based similarity benchmark, J. Cheminform. 8 (2016) 36.
- O.J. Ingham, R.M. Paranal, W.B. Smith, R.A. Escobar, H. Yueh, T. Snyder, J.A. Porco Jr., J.E. Bradner, A.B. Beeler, Development of a potent and selective HDAC8 inhibitor. ACS Med. Chem. Lett. 7 (2016) 929-932.
- O.M. Moradei, T.C. Mallais, S. Frechette, I. Paquin, P.E. Tessier, S.M. Leit, M. Fournel, C. Bonfils, M-C. Trachy-Bourget, J. Liu, T.P. Yan, A-H. Lu, J. Rahil, J. Wang, S. Lefebvre, Z. Li, A.F. Vaisburg, J.M. Besterman, Novel aminophenyl

benzamide-type histone deacetylase inhibitors with enhanced potency and selectivity. J. Med. Chem. 50 (2007) 5543-5546.

- P. Angibaud, K. Van Emelen, L. Decrane, S. van Brandt, P. ten Holte, I. Pilatte, B. Roux, V. Poncelet, D. Speybrouck, L. Queguiner, S. Gaurrand, A. Mariën , W. Floren, L. Janssen, M. Verdonck, J. van Dun, J. van Gompel, R. Gilissen, C. Mackie, M.D. Jardin, J. Peeters, M. Noppe, L. Van Hijfte, E. Freyne, M. Page, M. Janicot, J. Arts, Identification of a series of substituted 2-piperazinyl-5-pyrimidylhydroxamic acids as potent histone deacetylase inhibitors. Bioorg. Med. Chem. Lett. 20 (2010) 294-298.
- P. Bertrand, Inside HDAC with HDAC inhibitors. Eur. J. Med. Chem. 45 (2010) 2095-2116.
- P. Mandi, C. Nantasenamat, K. Srungboonmee, C. Isarankura-Na-Ayudhya, V. Prachayasittikul, QSAR study of anti-prion activity of 2-aminothiazoles. EXCLI J. 11 (2012) 453-467.
- P. Prathipati, N.L. Ma, T.H. Keller, Global bayesian models for the prioritization of antitubercular agents. J. Chem. Inf. Model. 48 (2008) 2362–2370.
- P. Trivedi, N. Adhikari, S.A. Amin, T. Jha, B. Ghosh, Design, synthesis and biological screening of 2-aminobenzamides as selective HDAC3 inhibitors with promising anticancer effects. Eur. J. Pharm. Sci. 124 (2018) 165-181.
- P.M. Lombardi, K.E. Cole, D.P. Dowling, D.W. Christianson, Structure, mechanism, and inhibition of histone deacetylases and related metalloenzymes. Curr Opin Struct Biol. 21 (2011) 735-743.
- Q.H. Sodji, J.R. Kornacki, J.F. McDonald, M. Mrksich, A.K. Oyelere, Design and structure activity relationship of tumor-homing histone deacetylase inhibitors conjugated to folic and pteroic acids. Eur. J. Med. Chem. 96 (2015) 340-359.
- R. Cincinelli, L. Musso, G. Giannini, V. Zuco, M.D. Cesare, F. Zunino, S. Dallavalle, Influence of the adamantyl moiety on the activity of biphenylacrylohydroxamic acid-based HDAC inhibitors. Eur. J. Med. Chem. 79 (2014) 251-259.
- R. David, H. Mathew, Extended-connectivity fingerprints. J. Chem. Inf. Model. 50 (2010) 742–754.

References

- R. De Vreese, N. Van Steen, T. Verhaeghe, T. Desmet, N. Bougarne, K. De Bosscher, V. Benoy, W. Haeck, L. Van Den Bosch, M. D'hooghe, Synthesis of benzothiophene-based hydroxamic acids as potent and selective HDAC6 inhibitors. Chem. Commun. 51 (2015) 9868-9871.
- R. Furumai, A. Matsuyama, N. Kobashi, K.H. Lee, M. Nishiyama, H. Nakajima, A. Tanaka, Y. Komatsu, N. Nishino, M. Yoshida, S. Horinouchi, FK228 (depsipeptide) as a natural prodrug that inhibits class I histone deacetylases. Cancer Res. 62 (2002) 4916-4921.
- R. Gaikwad, S.A. Amin, N. Adhikari, S. Ghorai, T. Jha, S. Gayen, Identification of molecular fingerprints of phenylindole derivatives as cytotoxic agents: a multi-QSAR approach, Str.Chem. 29 (2017) 1095-1107.
- R. He, Y. Chen, Y. Chen, A.V. Ougolkov, J-S. Zhang, D.N. Savoy, D.D. Billadeau, A.P. Kozikowski, Synthesis and biological evaluation of triazol-4-ylphenyl-bearing histone deacetylase inhibitors as anticancer agents. J. Med. Chem. 53 (2010) 1347-1356.
- R. Muthyala, W.S. Shin, J. Xie, Y.Y. Sham, Discovery of 1-hydroxypyridine-2-thiones as selective histone deacetylase inhibitors and their potential application for treating leukemia. Bioorg. Med. Chem. Lett. 25 (2015) 4320-4324.
- R. Neelarapu, D.L. Holzle, S. Velaparthi, H. Bai, M. Brunsteiner, S.Y. Blond, P.A. Petukhov, Design, synthesis, docking, and biological evaluation of novel diazide-containing isoxazole and pyrazole-based histone deacetylase probes. J. Med. Chem. 54 (2011) 4350-4364.
- S. Balasubramanian, J. Ramos, W. Luo, M. Sirisawad, E. Verner, J.J. Buggy, A novel histone deacetylase 8 (HDAC8)-specific inhibitor PCI-34051 induces apoptosis in T-cell lymphomas. Leukemia 22 (2008) 1026-1034.
- S. Banerjee, N. Adhikari, S.A. Amin, T. Jha, Histone deacetylase 8 (HDAC8) and its inhibitors with selectivity to other isoforms: An overview. Eur. J. Med. Chem. 164 (2019a) 214-240.
- S. Banerjee, N. Adhikari, S.A. Amin, T. Jha, Structural exploration of tetrahydroisoquinoline derivatives as HDAC8 inhibitors through multi-QSAR modeling study. J. Biomol. Struct. Dyn. (2019b) (In Press).

References

- S. Debnath, P. Nath, R.K. Nath, Identification of novel HDAC8 inhibitors using pharmacophore based virtual screening, 3D QSAR and molecular docking approach, Am. J. Pharmtech. Res. 4 (2014) 253-267.
- S. Kim, Y. Lee, S. Kim, S.J. Lee, P.K. Heo, S. Kim, Y.J. Kwon, K.W. Lee, Identification of Novel Human HDAC8 Inhibitors by Pharmacophore-based Virtual Screening and Density Functional Theory Approaches. Bull. Korean Chem. Soc. 39 (2018) 197-206.
- S. Oh, J-C. Jungb, M.A. Avery, Synthesis of new β-lactam analogs and evaluation of their histone deacetylase (HDAC) activity. Z. Naturforsch 62b (2007) 1459-1464.
- S. Praseetha, S. Bandaru, M. Yadav, A. Nayarisseri, S.S. kumar, Common SAR derived from multiple QSAR models on vorinostat derivatives targeting HDACs in tumor treatment. Curr. Pharm. Des. 22 (2016) 5072-5078.
- S. Shen, V. Benoy, J.A. Bergman, J.H. Kalin, M. Frojuello, G. Vistoli, W. Haeck, L. Van Den Bosch, A.P. Kozikowski, Bicyclic-capped histone deacetylase 6 inhibitors with improved activity in a model of axonal charcot−marie−tooth disease. ACS Chem. Neurosci. 7 (2016) 240-258.
- S. Terracciano, S. Di Micco, G. Bifulco, P. Gallinari, R. Riccio, I. Bruno, Synthesis and biological activity of cyclotetrapeptide analogues of the natural HDAC inhibitor FR235222. Bioorg. Med. Chem. 18 (2010) 3252-3260.
- S. Thangapandian, S. John, S. Sakkiah, K.W. Lee, Ligand and structure based pharmacophore modeling to facilitate novel histone deacetylase 8 inhibitor design. Euro. J. Med. Chem. 45 (2010) 4409-4417.
- S. Yu, J. Yuan, J. Shi, X. Ruan, T. Zhang, Y. Wang, Y. Du, HQSAR and topomer CoMFA for predicting melanocortin-4 receptor binding affinities of trans-4-(4-chlorophenyl) pyrrolidine-3-carboxamides. Chemometr. Intell. Lab. Syst. 146 (2015) 34-41.
- S. Zhang, W. Huang, X. Li, Z. Yang, B. Feng, Synthesis, biological evaluation, and computer-aided drug designing of new derivatives of hyperactive suberoylanilide hydroxamic acid histone deacetylase inhibitors. Chem. Biol. Drug. Des. 86 (2015) 795-804.

References

- S.A. Amin, N. Adhikari, T. Jha, Structure–activity relationships of hydroxamate-based histone deacetylase-8 inhibitors: reality behind anticancer drug discovery. Future Med. Chem. 9 (2017a) 2211-2237.
- S.A. Amin, N. Adhikari, T. Jha, Is dual inhibition of metalloenzymes HDAC-8 and MMP-2 a potential pharmacological target to combat hematological malignancies?. Pharmacol. Res. 122 (2017b) 8-19.
- S.A. Amin, N. Adhikari, S. Gayen, T. Jha, First report on the structural exploration and prediction of new BPTES analogs as glutaminase inhibitors. J. Mol. Structure, 1143 (2017c) 49-64.
- S.A. Amin, N. Adhikari, T. Jha, Diverse classes of HDAC8 inhibitors: In search of molecular fingerprints that regulate activity. Future Med. Chem 10 (2018a) 1589-1602.
- S.A. Amin, N. Adhikari, T. Jha, Structure-activity relationships of HDAC8 inhibitors: Non-hydroxamates as anticancer agents. Pharmacol. Res. 131 (2018b) 128–142.
- S.A. Amin, N. Adhikari, S.K. Baidya, S. Gayen, T. Jha, Structural refinement and prediction of potential CCR2 antagonists through validated multi-QSAR modeling studies. J. Biomol. Str. Dynamics. 37 (2019) 75-94.
- S.C. Mwakwari, W. Guerrant, V. Patil, S.I. Khan, B.L. Tekwani, Z.A. Gurard-Levin, M. Mrksich, A.K. Oyelere, Non-peptide macrocyclic histone deacetylase inhibitors derived from tricyclic ketolide skeleton. J. Med. Chem. 53 (2010) 6100-6111.
- S.M. Gantt, C. Decroos, M.S. Lee, L.E. Gullett, C.M. Bowman, D.W. Christianson, C.A. Fierke, General base–general acid catalysis in human histone deacetylase 8. Biochemistry 55 (2016) 820-832.
- S.M. Gao, C.Q. Chen, L.Y. Wang, L.L. Hong, J.B. Wu, P.H. Dong, F.J. Yu, Histone deacetylases inhibitor sodium butyrate inhibits JAK2/STAT signaling through upregulation of SOCS1 and SOCS3 mediated by HDAC8 inhibition in myeloproliferative neoplasms. Exp. Hematol. 41 (2013) 261-270.
- S.N. Ononye, M.D. VanHeyst, E.Z. Oblak, W. Zhou, M. Ammar, A.C. Anderson, D.L. Wright, Tropolones as lead-like natural products: The development of potent and selective histone deacetylase inhibitors. ACS Med. Chem. Lett. 4 (2013) 757-761.

References

- S.Y. Park, J.A. Jun, K.J. Jeong, H.J. Heo, J.S. Sohn, H.Y. Lee, C.G. Park, J. Kang, histone deacetylases 1, 6 and 8 are critical for invasion in breast cancer. Oncol. Rep. 25 (2011) 1677-1681.
- T. Higuchi, T. Nakayama, T. Arao, K. Nishio, O. Yoshie, SOX4 is a direct target gene of FRA-2 and induces expression of HDAC8 in adult T-cell leukemia/lymphoma. Blood 121(2013) 3640-3649.
- T. Suzuki, N. Muto, M. Bando, Y. Itoh, A. Masaki, M. Ri, Y. Ota, H. Nakagawa, S. Iida, K. Shirahige, N. Miyata, Design, synthesis, and biological activity of NCC149 derivatives as histone deacetylase 8-selective inhibitors. Chem. Med. Chem. 9 (2014) 657-664.
- T. Suzuki, Y. Ota, M. Ri, M. Bando, A. Gotoh, Y. Itoh, H. Tsumoto, P.R. Tatum, T. Mizukami, H. Nakagawa, S. Iida, R. Ueda, K. Shirahige, N. Miyata, Rapid discovery of highly potent and selective inhibitors of histone deacetylase 8 using click chemistry to generate candidate libraries. J. Med. Chem. 55 (2012) 9562-9575.
- T. Tashima, H. Murata, H. Kodama, Design and synthesis of novel and highly-active pan-histone deacetylase (pan-HDAC) inhibitors. Bioorg. Med. Chem. 22 (2014) 3720–3731.
- T.Y. Taha, S.M. Aboukhatwa, R.C. Knopp, N. Ikegaki, H. Abdelkarim, J. Neerasa, Y. Lu, R. Neelarapu, T.W. Hanigan , G.R.J. Thatcher, P.A. Petukhov, Design, synthesis, and biological evaluation of tetrahydroisoquinoline-based histone deacetylase 8 selective inhibitors. ACS Med. Chem. Lett. 8 (2017) 824-829.
- V. Andrianov , V. Gailite, D. Lola, E. Loza, V. Semenikhina, I. Kalvinsh, P. Finn, K.D. Petersen, J.W. Ritchie, N. Khan, A. Tumber, L.S. Collins, S.M. Vadlamudi, F. Björkling, M. Sehested, Novel amide derivatives as inhibitors of histone deacetylase: Design, synthesis and SAR. Eur. J. Med. Chem. 44 (2009) 1067-1085.
- V. Patil, Q.H. Sodji, J.R. Kornacki, M. Mrksich, A.K. Oyelere, 3‑hydroxypyridin-2-thione as novel zinc binding group for selective histone deacetylase inhibition. J. Med. Chem. 56 (2013) 3492-3506.
- V.K. Vyas, M. Ghate, N. Gupta, 3D QSAR and HQSAR analysis of protein kinase B (PKB/Akt) inhibitors using various alignment methods. Arab. J. Chem. 10 (2017) S2182-S2195.

References

- V.R. Pidugu, N.S. Yarla, S.R. Pedada, A.M.Kalle, A. KrishnaSatyab, Design and synthesis of novel HDAC8 inhibitory 2, 5-disubstituted-1, 3, 4-oxadiazoles containing glycine and alanine hybrids with anticancer activity. Bioorg. Med. Chem. 24 (2016) 5611-5617.
- W. Guerrant, V. Patil, J.C. Canzoneri, A.K. Oyelere, Dual targeting of histone deacetylase and topoisomerase II with novel bifunctional inhibitors. J. Med. Chem. 55 (2012) 1465-1477.
- W. Tang, T. Luo, E.F. Greenberg, J.E. Bradner, S.L. Schreiber, Discovery of histone deacetylase 8 selective inhibitors. Bioorg. Med. Chem. Lett. 21 (2011) 2601-2605.
- W.J. Huang, C.C. Chen, S.W. Chao, C.C. Yu, C.Y. Yang, J.H. Guh, Y.C. Lin, C.I. Kuo, P.Yang, C.I. Chang, Synthesis and evaluation of aliphatic-chain hydroxamates capped with osthole derivatives as histone deacetylase inhibitors. Eur. J. Med. Chem. 46 (2011) 4042-4049.
- W.S. Xu, R.B. Parmigiani, P.A. Marks, Histone deacetylase inhibitors: Molecular mechanisms of action. Oncogene 26 (2007) 5541-5552.
- X. Lin, W. Chen, Z. Qiu, L. Guo, W. Zhu, W. Li, Z. Wang, W. Zhang, Z. Zhang, Y. Rong, M. Zhang, L. Yu, S. Zhong, R. Zhao, X. Wu, J.C. Wong, G. Tang, Design and synthesis of orally bioavailable aminopyrrolidinone histone deacetylase 6 inhibitors. J. Med. Chem. 58 (2015) 2809-2820.
- X. Wang, X. Li, J. Li, J. Hou, Y. Qu, C. Yu, F. He, W. Xu, J. Wu, Design, synthesis, and preliminary bioactivity evaluation of N^1 -hydroxyterephthalamide derivatives with indole cap as novel histone deacetylase inhibitors. Chem. Biol. Drug Des. 89 (2017) 38-46.
- X. Zhao, M. Chen, B. Huang, H. Ji, M. Yuan, Comparative molecular field analysis (CoMFA) and comparative molecular similarity indices analysis (CoMSIA) studies on α 1A-adrenergic receptor antagonists based on pharmacophore molecular alignment. Int. J. Mol. Sci. 12 (2011) 7022-7037.
- X.Y. Xia, E.G. Maliski, P. Gallant, D. Rogers, Classification of kinase inhibitors using a bayesian model. J. Med. Chem. 47 (2004)4463–4470.
- Y. Chen, M. Lopez-Sanchez, D.N. Savoy, D.D. Billadeau, G.S. Dow, A.P. Kozikowski, A series of potent and selective, triazolylphenyl-based histone

deacetylases inhibitors with activity against pancreatic cancer cells and Plasmodium falciparum, J. Med. Chem. 51 (2008) 3437-3448.

- Y. Yamauchi, H. Boukari, I. Banerjee, I.F. Sbalzarini, P. Horvath, A. Helenius, Histone deacetylase 8 is required for centrosome cohesion and influenza A virus entry. PLoS Pathog. 7 (2011) e1002316.
- Y. Zhang, H. Fang, J. Feng, Y. Jia, X. Wang, W. Xu Discovery of a tetrahydroisoquinoline-based hydroxamic acid derivative (ZYJ-34c) as histone deacetylase inhibitor with potent oral antitumor activities. J. Med. Chem. 54 (2011b) 5532-5539.
- Y. Zhang, J. Feng, C. Liu, L. Zhang, J. Jiao, H. Fang, L. Su, X. Zhang, J. Zhang, M. Li, B. Wang, W. Xu, Design, synthesis and preliminary activity assay of 1, 2, 3, 4-tetrahydroisoquinoline-3-carboxylic acid derivatives as novel Histone deacetylases (HDACs) inhibitors. Bioorg. Med. Chem. 18 (2010) 1761-1772.
- Y. Zhang, J. Feng, Y. Jia, X. Wang, L. Zhang, C. Liu, H. Fang, W. Xu, Development of tetrahydroisoquinoline-based hydroxamic acid derivatives: potent histone deacetylase inhibitors with marked in vitro and in vivo antitumor activities. J. Med. Chem. 54 (2011a) 2823-2838.
- Y. Zhang, J. Feng, Y. Jia, Y. Xu, C. Liu, H. Fang, W. Xu, Design, synthesis and primary activity assay of tripeptidomimetics as histone deacetylase inhibitors with linear linker and branched cap group. Eur. J. Med. Chem. 46 (2011c) 5387-5397.
- Z. Li, W-G. Zhu, Targeting histone deacetylases for cancer therapy: from molecular mechanisms to clinical implications. Int. J. Biol. Sci. 10 (2014) 757-770.
- Z. Noor, N. Afzal, S. Rashid, Exploration of novel inhibitors for class I histone deacetylase isoforms by QSAR modeling and molecular dynamics simulation assays. PLoS One. 10 (2015) e0139588.
- Z.A. Gurard-Levin, J. Kim, M. Mrksich, Combining mass spectrometry and peptide arrays to profile the specificities of histone deacetylases. Chem. Bio. Chem. 10 (2009) 2159-2161.

Reprints

European Journal of Medicinal Chemistry 164 (2019) 214–240

Contents lists available at ScienceDirect

European Journal of Medicinal Chemistry

journal homepage: http://www.elsevier.com/locate/ejmech

Review article

Histone deacetylase 8 (HDAC8) and its inhibitors with selectivity to other isoforms: An overview

Suvankar Banerjee, Nilanjan Adhikari [1], Sk Abdul Amin, Tarun Jha [*]

Natural Science Laboratory, Division of Medicinal and Pharmaceutical Chemistry, Department of Pharmaceutical Technology, P. O. Box 17020, Jadavpur University, Kolkata, 700032, West Bengal, India

ARTICLE INFO

Article history:
Received 22 September 2018
Received in revised form
4 December 2018
Accepted 16 December 2018
Available online 19 December 2018

Keywords:
Histone deacetylase
HDAC8
Cancer
HDAC8 inhibitor
Structure-activity relationship (SAR)
Quantitative structure-activity relationship (QSAR)

ABSTRACT

The histone deacetylases (HDACs) enzymes provided crucial role in transcriptional regulation of cells through deacetylation of nuclear histone proteins. Discoveries related to the HDAC8 enzyme activity signified the importance of HDAC8 isoform in cell proliferation, tumorigenesis, cancer, neuronal disorders, parasitic/viral infections and other epigenetic regulations. The pan-HDAC inhibitors can confront these conditions but have chances to affect epigenetic functions of other HDAC isoforms. Designing of selective HDAC8 inhibitors is a key feature to combat the pathophysiological and diseased conditions involving the HDAC8 activity. This review is concerned about the structural and positional aspects of HDAC8 in the HDAC family. It also covers the contributions of HDAC8 in the pathophysiological conditions, a preliminary discussion about the recent scenario of HDAC8 inhibitors. This review might help to deliver the structural, functional and computational information in order to identify and design potent and selective HDAC8 inhibitors for target specific treatment of diseases involving HDAC8 enzymatic activity.

Contents

* Corresponding author.
E-mail address: tjupharm@yahoo.com (T. Jha).
[1] Present Address: School of Pharmaceutical Technology, ADAMAS University, Barasat-Barrackpore Road, P. O. Jagannathpur, Kolkata – 700126, West Bengal, India.

https://doi.org/10.1016/j.ejmech.2018.12.039
0223-5234/

Journal of Molecular Structure 1185 (2019) 128–142

Contents lists available at ScienceDirect

Journal of Molecular Structure

journal homepage: http://www.elsevier.com/locate/molstruc

Structural exploration of arylsulfonamide-based ADAM17 inhibitors through validated comparative multi-QSAR modelling studies

Sandip Kumar Baidya [1], Sk. Abdul Amin [1], Suvankar Banerjee, Nilanjan Adhikari [2], Tarun Jha*

Natural Science Laboratory, Division of Medicinal and Pharmaceutical Chemistry, Department of Pharmaceutical Technology, Jadavpur University, P. O. Box 17020, Kolkata, 700032, West Bengal, India

ARTICLE INFO

Article history:
Received 11 December 2018
Received in revised form
19 February 2019
Accepted 21 February 2019
Available online 26 February 2019

Keywords:
ADAM17
2D-QSAR
HQSAR
Bayesian classification
Pharmacophore mapping
Molecular docking

ABSTRACT

Zinc-dependent ADAM17 takes part in a number of life-threatening conditions such as inflammatory diseases, cancer, Alzheimer's disease and rheumatoid arthritis. Therefore, ADAM17 may be a valuable target to design specific inhibitors for combating these diseases. In this scenario, it is a challenging task to design specific ADAM17 inhibitors as none of the earlier investigated compounds has come into the market as a potential drug candidate. Here, molecular modelling including 2D-QSAR, HQSAR, Bayesian classification, pharmacophore mapping and molecular docking studies of arylsulfonamides were performed to explore the structural and pharmacophoric requirements for exerting higher ADAM17 inhibitory activity. All these molecular modelling approaches were validated individually and these were statistically significant and reliable. The bulky steric and hydrophobic P1′ substituents at the *para* position of the arylsulfonamido moiety favoured ADAM17 inhibition that supported and validated by molecular docking study. These crucial observations of arylsulfonamides may be considered for designing higher effective ADAM17 inhibitors in future.

1. Introduction

A disintegrin and metalloproteinase 17 (ADAM17), a zinc-dependant metalloenzyme, is a type I proteolytic enzyme adhered to the cell membrane. It belongs to the adamlysin family of protease enzymes under M12 subfamily of the subclan M under metalloproteinase clan MA [1–3]. ADAM17 is found to be involved in the shedding of several cytokines. The structural characterization of ADAM17, also known as Tumour necrosis factor-α converting enzyme (TACE), provides information about the large extracellular region comprising a number of domains. The cystine switch motif belongs to the prodomain regulates the activation and inactivation of the enzyme through coordination with the catalytic Zn^{2+} ion of the catalytic or metalloproteinase domain. The catalytic domain of the enzyme consists of the catalytic zinc ion which is responsible for the proteolysis. The catalytic domain also provides the specific characteristics for the identification of the enzyme for being a member of the metalloproteinase family. The presence of the disintegrin domain next to the catalytic domain is known as the ectodomain having a C-shaped structure to increase the stiffness of the ectodomain. The membrane proximal domain (MPD) adjacent to the disintegrin domain supervises the enzymatic activity and substrate binding [4,5]. The Conserved Adam Seventeen Dynamic Interaction Sequence (CANDIS), a small amphiphilic helical region, is observed between the MPD and the transmembrane region. The CANDIS region assists the substrate recognition and substrate-enzyme interaction [6]. A transmembrane region helps the protein to remain attached to the cell surface where the cytosolic region is located inside the cell cytosol [4,5,7]. This structural feature of ADAM17 ectodomain resembles the structural characteristics of some other metalloenzymes such as snake venom metalloproteinases (SVMs), ADAM-thrombospondin motifs (ADAM-TS), membrane-type matrix metalloproteinases (MT-MMPs) and matrix metalloproteinases (MMPs) [5]. Structures of ADAM17 and ADAM10 ectodomains are almost identical to each other whereas the metalloproteinase domain of ADAM17 resembles with SVM, MT-MMP, MMPs and ADAM-TS that might explain the inhibition of

* Corresponding author.
E-mail address: tjupharm@yahoo.com (T. Jha).
[1] Authors have equal contribution.
[2] Present Address: School of Pharmaceutical Technology, ADAMAS University, Barasat-Barrackpore Road, P. O. Jagannathpur, Kolkata – 700126, West Bengal, India.

https://doi.org/10.1016/j.molstruc.2019.02.081
0022-2860/

JOURNAL OF BIOMOLECULAR STRUCTURE AND DYNAMICS
https://doi.org/10.1080/07391102.2019.1617782

Structural exploration of tetrahydroisoquinoline derivatives as HDAC8 inhibitors through multi-QSAR modeling study

Suvankar Banerjee[a], Nilanjan Adhikari[a,b], Sk. Abdul Amin[a] and Tarun Jha[a]

[a]Natural Science Laboratory, Division of Medicinal and Pharmaceutical Chemistry, Department of Pharmaceutical Technology, Jadavpur University, Kolkata, West Bengal, India; [b]School of Pharmaceutical Technology, ADAMAS University, Kolkata, West Bengal, India

Communicated by Ramaswamy H. Sarma

ABSTRACT

Histone deacetylase 8 (HDAC8) is one of the crucial HDACs responsible for influencing the epigenetic functions of the body. Overexpression of HDAC8 is found to be involved in numerous disease conditions such as tumorigenesis, cell proliferation, cancer, viral infections, neuronal disorders and other epigenetic diseases. Therefore, inhibition of HDAC8 is a primary method to combat these diseases. In this article, a multi-QSAR modeling study on tetrahydroisoquinoline derivatives was conducted to identify important contributions of the structural features of these compounds toward HDAC8 inhibition. All these QSAR modeling techniques were individually validated and justified the observations of each other. The results implied that the tetrahydroisoquinoline moiety may be effective as a cap group than as a linker moiety for HDAC8 inhibition. Different substitutions at the tetrahydroisoquinoline scaffold were also found to be crucial in modulating HDAC8 inhibition.

ARTICLE HISTORY
Received 17 October 2018
Accepted 24 April 2019

KEYWORDS
HDAC8; tetrahydroisoquinoline; 2D QSAR; Bayesian classification; CoMFA; HQSAR

1. Introduction

The enzyme-mediated elimination of the lysine *N*-terminal acetyl group from the nuclear histone proteins is known as the deacetylation of histone proteins (Amin, Adhikari, & Jha, 2017a; Banerjee, Adhikari, Amin & Jha, 2019; Chakrabarti et al., 2015; Zhang et al., 2010). Histone deacetylases (HDACs) cause deacetylation of the histone proteins and are either Zn^{2+} or NAD^{+}-dependent deacetylases in nature (Amin et al., 2017a; Banerjee et al., 2019; Bertrand, 2010). These are found to regulate the DNA transcription process (Amin et al., 2017a; Yuan et al., 2018; Zhang et al., 2010). Apart from that, these HDACs are also associated with a number of cell-signaling pathways and are connected to the pathophysiological conditions and diseases (Amin et al., 2017a, Chakrabarti et al., 2015). HDACs are sub-grouped into four classes namely class I (HDAC1, 2, 3 and 8), class II (HDAC4–7, 9 and 10), class III (SIRT1-7) and class IV (HDAC11). Among four classes of HDAC family, only enzymes of class III (SIRT1-7) are NAD^{+}-dependent enzymes, whereas other classes of HDACs are Zn^{2+}-dependent metalloenzymes (Amin et al., 2017a; Bertrand, 2010; Chakrabarti et al., 2015, 2016; Gregoretti, Lee & Goodson, 2004; Seto & Yoshida, 2014).

HDAC8, one of the crucial class I HDACs, has been established as a lucrative therapeutic target for the design and discovery of small-molecule anticancer agents (Amin et al., 2017a; Amin Adhikari, & Jha, 2018a, 2018b; Chakrabarti et al., 2015, 2016). Overexpression of HDAC8 was related to a number of diseases such as childhood neuroblastoma, leukemia, tumor progression and cancers of lung, colon and pancreas (Amin et al., 2017a; Nakagawa et al., 2007; Oehme et al., 2009). Moreover, the RNAi-mediated HDAC8 knockdown has evidenced in the inhibition of human lung, cervical and colonal cellular proliferation (Chakrabarti et al., 2016; Nakagawa et al., 2007; Wu et al., 2013). Not only that the role of HDAC8 has been highly implicated in case of different hematological cancers or leukemias (Amin, Adhikari, & Jha, 2017b; Durst, Lutterbach, Kummalue, Friedman, & Hiebert, 2003; Higuchi, Nakayama, Arao, Nishio, & Yoshie, 2013; Lutterbach & Hiebert, 2000). HDAC8 is also a significant factor of p53 mutation and tumors containing p53 mutation (Wu et al., 2013). An influence of HDAC8 in the expression of gelatinase enzymes (MMP-2 and MMP-9) affects cell invasion and migration. Overexpression of HDACs including HDAC8 promotes the expression of MMP-9 and invasion in MCF-7 breast cancer cell lines (Amin et al., 2017 b; Park et al., 2011).

Apart from cancer, the involvement of HDAC8 in Uukuniemi virus and Influenza-A infections and in schistosomiasis has also been observed (Chakrabarti et al., 2015; 2016; Marek et al., 2013; Yamauchi et al., 2011). Though a number of HDAC inhibitors have been developed, only six pan-HDAC inhibitors have been approved by the United States Food and Drug Administration (USFDA) and the Chinese Food and Drug Administration (CFDA). Moreover, the lack of potent and selective HDAC8 inhibitors might be one of the major challenges for the treatment of cancer

CONTACT Tarun Jha tjupharm@yahoo.com; tjjupharm@yahoo.com Natural Science Laboratory, Division of Medicinal and Pharmaceutical Chemistry, Department of Pharmaceutical Technology, Jadavpur University, Kolkata, India

Supplemental data for this article is available online at https://doi.org/10.1080/07391102.2019.1617782